UNIVERSITÄTSKLINIKUM HAMBURG-EPPENDORF

Zentrum für Molekulare Neurobiologie Hamburg

Institute for Synaptic Physiology

Prof. Dr. Thomas G. Oertner

Optogenetic manipulation of intracellular cyclic nucleotides in hippocampal neurons

Dissertation

zur Erlangung des Doktorgrades Dr. rer. biol. hum. / PhD

an der Medizinischen Fakultät der Universität Hamburg

vorgelegt von

Oana M. Constantin

aus Iași, Romania

Hamburg 2021

Angenommen von der Medizinischen Fakultät am: 23.03.2022
Veröffentlicht mit Genehmigung der Medizinischen Fakultät der Universität Hamburg.

Prüfungsausschuss, der/die Vorsitzende: Prof. Dr. Thomas Oertner
Prüfungsausschuss, 2. Gutachter/in: Prof. Dr. Viacheslav Nikolaev

Table of contents

1. Introduction

1.1 Cyclic AMP as a signaling molecule

1.1.1 History, importance and general working mechanism

In 1945, Earl Sutherland and his collaborators embarked on a decade-long endeavor studying the mechanism of hormone-induced glycogen breakdown in the liver. On this Nobel prize-winning journey, they identified cyclic adenosine monophosphate (cAMP) (Figure 1.1), one of the most ubiquitous second messenger molecules. The experiments that lead to this discovery were performed in cell-free liver homogenates where they firstly separated the particulate fraction (containing cell membranes) from the supernatant (cell contents). The critical element that allowed them to discover cAMP was the separation of the cellular membranes from the contents. They were then able to independently observe the two steps involved in second messenger signaling: exposure to extracellular molecules and intracellular relay of signals. They observed that the hormones epinephrine and glucagon generated a "heat stable factor" (HSF) when they were added to the particulate fraction. This HSF was then able to stimulate liver phosphorylase, initiating the degradation of glycogen. If the hormones were added to the supernatant directly, glycogen was not degraded. It was thus clear that epinephrine and glucagon do not act directly on liver phosphorylase but they are able to generate an HSF at the cell membrane that triggers intracellular liver phosphorylase activity (Berthet et al., 1957).

After further work, cAMP was isolated and its structure determined (Berthet et al., 1957; Cook et al., 1957). Soon after, the enzymes that synthesize cAMP from ATP (adenylyl cyclases) were identified, as well as phosphodiesterases, enzymes which degrade cAMP to biologically inactive 5' AMP (Sutherland et al., 1962; Sutherland & Rall, 1958). Further research unraveled the fact that a multitude of hormones and neurotransmitters elicited intracellular effects by stimulating cAMP production and that cAMP itself triggers or modulates an impressive range of cellular functions. Sutherland was also the one to propose the name "second messenger", where the "first messenger" (i.e. hormone, neurotransmitter) binds to a receptor located in the plasma

membrane, stimulating adenylyl cyclases to produce cAMP from ATP. The change in intracellular cAMP concentration then regulates the rates of other intracellular processes (Blumenthal, 2012).

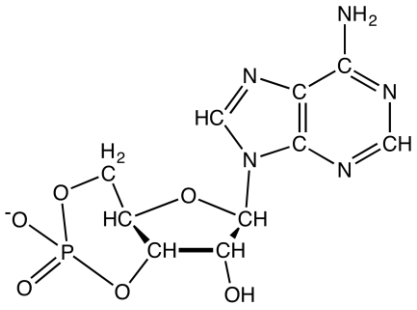

Figure 1.1 Cyclic adenosine monophosphate (cAMP) structure. Biochemically, cAMP (3',5'-cyclic adenosine monophosphate) is a small, diffusible, hydrophilic cyclic nucleotide composed of an adenine, a ribose and a phosphate group. In comparison to AMP, it occurs in cyclic structure as a 3'-5'-cyclic ester of AMP.

The discovery of cAMP triggered the subsequent identification and characterisation of the multiple components that make up the cAMP signaling cascade. Adding to Sutherland's own prize in 1971, an impressive number of Nobel prizes have been awarded to scientists working on cAMP and cyclic nucleotide-related phenomena, such as protein phosphorylation by PKA (1992, Fischer and Krebs), discovery of G proteins and their role in signal transduction (1994, Gilman and Rodbell), discovery of cGMP as a second messenger (1998, Furchgott, Ignarro and Murrad), uncovering signal transduction in the nervous system and cAMP-dependent CREB activation (2000, Calrsson, Greengard and Kandel), discovery of cAMP-dependent odorant receptors (2005, Buck and Axel) and the most recently for studies of G protein-coupled receptors (2012, Lefkowitz and Kobilka).

It would be almost impossible to list all the cellular processes or intracellular phenomena that are modulated or affected in one way or another by subtly changing levels of cAMP. This second messenger is an ancient molecule that holds a wide variety of roles in living organisms from virtually all kingdoms, from bacteria to prokaryotes, plants, fungi and of course, animals.

1.1.2 Molecules upstream of cAMP

Figure 1.2 is a summary of the ubiquitous cAMP signaling pathways. In this subchapter I will briefly introduce the molecules upstream of cAMP in the signaling pathway that are common to all cell types from all kingdoms.

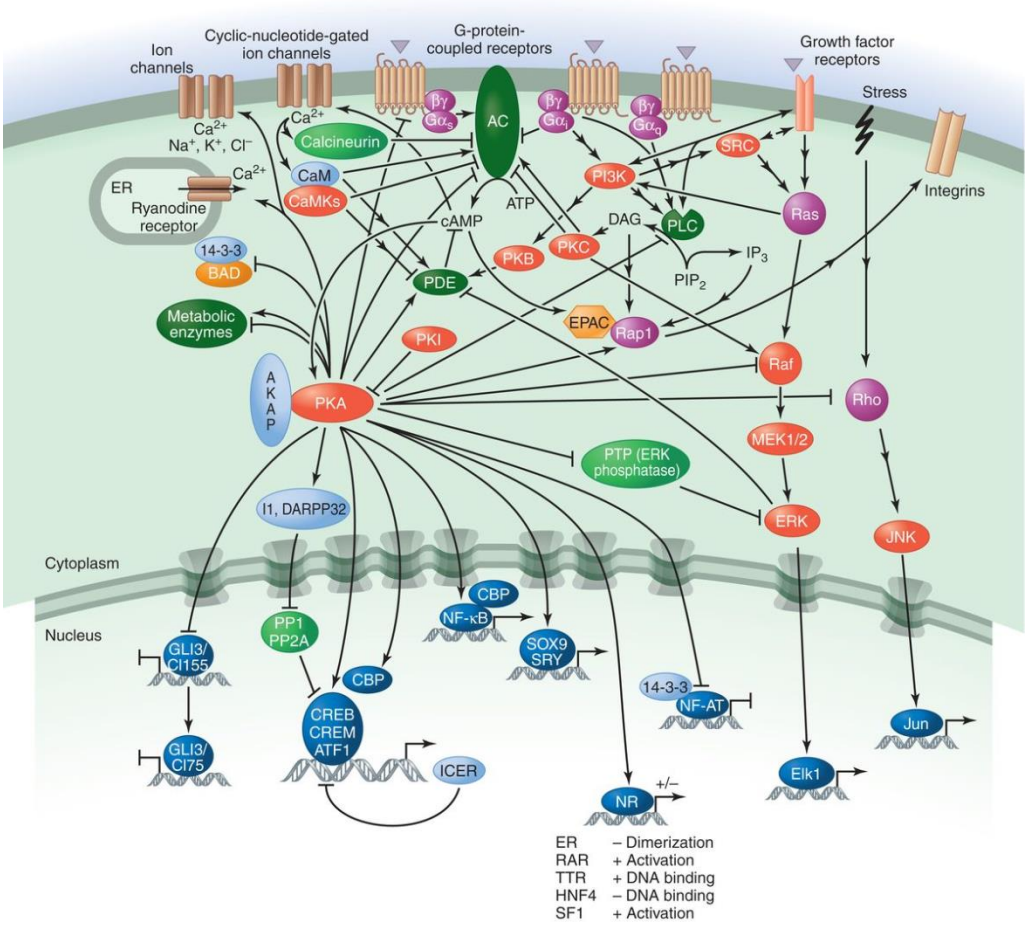

Figure 1.2 The cAMP-PKA signaling pathway and its interaction with other intracellular signaling pathways. Figure from (Sassone-Corsi, 2012).

G protein-coupled receptors

G protein-coupled receptors (GPCRs) are seven-transmembrane receptors that couple to intracellular G proteins (made out of α, β, γ subunits). Whenever an extracellular first-messenger (e.g. hormone, neurotransmitter, peptides) binds to a GPCR, they act as transducers of the extracellular signal to the intracellular space. Upon binding of the ligand, conformational changes trigger the exchange of a bound GDP to a GTP in the associated G protein α subunit. This allows the α subunit to dissociate from the G protein complex and interact with adenylyl cyclases. For instance, $G_{\alpha s}$ stimulates transmembrane adenylyl cyclases, raising cAMP whereas $G_{\alpha i}$ inhibits adenylyl cyclases lowering cAMP. Some general ligands that bind to GPCR and exert their

function via GPCR stimulation or inhibition of ACs are: epinephrine, norepinephrine, histamine, serotonin, dopamine, and certain chemokines (more information about GPCR ligands and their effects in the hippocampus are presented in chapter 1.2.4).

Adenylyl cyclases

Cyclic AMP is synthesised by adenylyl cyclases, enzymes that catalyse the conversion of ATP into cAMP and pyrophosphate. Currently, ten mammalian types of adenylyl cyclase have been identified, each with unique regulatory properties and cellular expression. From the ten isoforms of adenylyl cyclase, nine are membrane-spanning proteins (AC1-9), while AC10 is a soluble adenylyl cyclase (Dessauer et al., 2017).

Table 1.1 Regulation and distribution of adenylyl cyclase isoforms.

Isoform		Response to							Expression in hippocampus	Subcellular location
		Ca^{2+}	$G_{\alpha s}$	$G_{\alpha i}$	$G_{\beta\gamma}$	FSK	PKA	PKC		
I	AC1	↑	↑	↓	↓	↑		↑	++	lipid raft
	AC3	↑	↑	↓	↓	↑		↑	+++	lipid raft
	AC8	↑	↑	↓	↓	↑	↓		+	lipid raft
II	AC2	-	↑	-	↑	↑		↑	++	non-lipid raft
	AC4	-	↑	-	↑	↑			/	non-lipid raft
	AC7	-	↑	-	-	↑		↑	/ mouse + rat	non-lipid raft
III	AC5	↓	↑	↓	↑	↑	↓	↑	+	lipid raft
	AC6	↓	↑	↓	↑	↑	↓	↓	+	lipid raft
IV	AC9	-	↑	↓	-	-			+++	non-lipid raft
sAC		-	-	-	-	-				cytosol

Legend: (↑) stimulation, (↓) inhibition, (-) not sensitive, (+++) high level, (++) medium level, (+) low density, (/) not expressed. (data from (Dessauer et al., 2017; Sanabra & Mengod, 2011; Willoughby & Cooper, 2007)

Transmembrane adenylyl cyclases are divided into groups I-IV, based on their response to different modulators such as $G_{\alpha s}$, $G_{\alpha i}$, $G_{\beta\gamma}$, calcium, forskolin (FSK) and protein kinases (Table 1.1). Activity of all adenylyl cyclases can be modulated by the GPCR-activated Gs protein, with the exception of AC10 (soluble AC), which is activated by bicarbonate and other ions. Group I includes

isoforms AC1, 3 and 8 and their activity can be stimulated by calcium ions. Group II includes AC2, 4 and 7 and is characterised by being insensitive to calcium and stimulated by $G_{\beta\gamma}$. Group III (AC5 and 6) are inhibited not only by calcium, but also by $G_{\alpha i}$ and protein kinase A (PKA). Finally, group IV is AC9 which is the only tmAC resistant to forskolin, a potent AC stimulator which has been used extensively in cAMP signaling research (Cooper & Crossthwaite, 2006; Johnstone et al., 2018).

Interestingly, the calcium-sensitive adenylyl cyclases (groups I and III) also localize in lipid rafts, patches of membrane rich in cholesterol and sphingolipids, as well as other multiprotein signaling complexes. This specific expression profile could contribute to the differential cAMP signaling effects that can be induced by different GPCR ligands which activate the same GPCR-Gs pathway (Willoughby & Cooper, 2007).

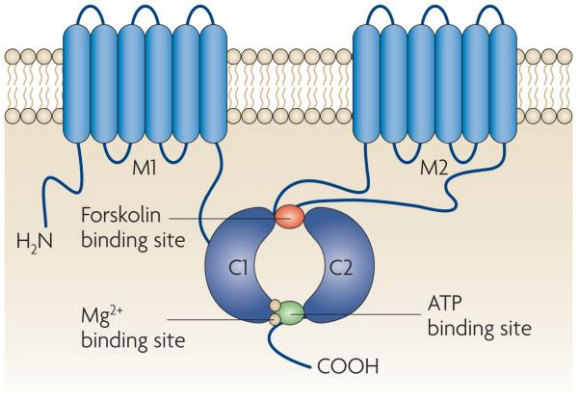

Figure 1.3 Transmembrane adenylyl cyclase structure: two transmembrane domains (M1 and M2) linked by two cytosolic domains (C1 and C2) that form the catalytically active site. Image from (Pierre et al., 2009).

Structurally, the transmembrane adenylyl cyclases (tmAC) contain two six-transmembrane domains that span the plasma membrane and two catalytic subunits (C1 and C2) that dimerize in order to form a catalytically-active core (Figure 1.3) The tertiary structure of a tmAC is that of a pseudo symmetrical enzyme, where residues from C1 and C2 contribute to form the active site. The substrate, ATP, binds in a pocket created at one of the interfaces between C1 and C2. Substrate specificity is achieved through the residues that bind the adenine section of the ATP molecule (Figure 1.4). Catalytic activity is initiated by the correct association of the two catalytic domains, a process that can be aided by either forskolin or $G_{\alpha s}$ binding in the symmetrically opposed site to that of ATP binding. Interestingly, $G_{\alpha i}$ inhibits AC activation by binding to the C1 domain interfering with the structural changes necessary for activation. Under basal conditions, the enzymatic activity is blocked by a regulatory loop within the enzyme which restricts access to the substrate binding pocket. In calcium-sensitive isoforms, Ca^{2+}/calmodulin binds to the regulatory residues, opening the pocket for ATP binding (Halls & Cooper, 2017; Willoughby &

Cooper, 2007).

Soluble adenylyl cyclases (AC10, or most commonly known as sAC) do not get activated by the typical GPCR activity, but their activity is rather regulated by bicarbonate and ATP. They are distributed throughout the cytoplasm and in specific cell compartments such as mitochondria, nuclei or centrioles (Steegborn, 2014; Tresguerres et al., 2011).

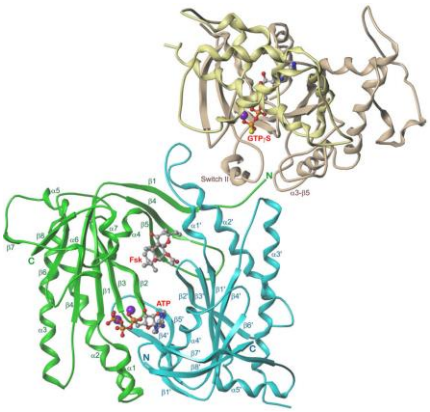

Figure 1.4 Structure of the catalytic domains of an adenylyl cyclase. Catalytic domains of adenylyl cyclase C1 (green) and C2 (cyan) in complex with forskolin, ATP, $G_{\alpha s}$. Image from (Dessauer et al., 2017).

1.1.3 Effector molecules

Four main molecules are located downstream of cAMP: (1) protein kinase A (PKA), (2) exchange protein directly activated by cAMP (EPAC), (3) cyclic nucleotide-regulated channels, (4) phosphodiesterases (PDEs). In this section I will describe these molecules, as well as other key players indirectly affected by cAMP.

Protein kinase A (PKA)

From all cAMP effectors, protein kinase A has been the most extensively studied starting with its discovery more than 50 years ago (Walsh et al., 1968). The structure of the PKA catalytic subunit was the first protein kinase structure to be solved and its study has yielded an immense body of knowledge about the working mechanism of similar enzymes (Knighton et al., 1991). Alongside other protein kinases, PKA plays an important role in virtually every aspect of cellular physiology, as PKA is able to phosphorylate other proteins (enzymes, channels, receptors, transcription factors), either enhancing or reducing their function. Phosphorylation mediated by PKA is tightly balanced by the dephosphorylation activity of protein phosphatases (PP), thus

ensuring a precise regulation of intracellular processes.

Structurally, PKA is a tetramer made out of two regulatory subunits (PKA-R) and two catalytic subunits (PKA-C) that are catalytically inactive in the absence of cAMP. When cAMP binds to the PKA-R (two molecules of cAMP per subunit), the inhibitory hold on the PKA-C is released, allowing the catalytic subunits to dissociate and phosphorylate Ser and Thr residues on PKA target substrates (Roskoski, 2015) (Figure 1.5). PKA activity is limited by a protein kinase inhibitor (PKI), an endogenous peptide that is present in all cell types. PKI inhibits PKA activity by binding to PKA catalytic subunits in a manner similar to the PKA regulatory subunits, making them enzymatically inactive (Liu et al., 2020). The activity of PKA is also tightly counterbalanced by protein phosphatases (PP1 and PP2A), which dephosphorylate PKA substrates. PKA is able to negatively regulate the activity of PPs by activating PP inhibitors (i.e. DARPP32), but it can also enhance the activity of PP2A by direct phosphorylation (Søberg & Skålhegg, 2018).

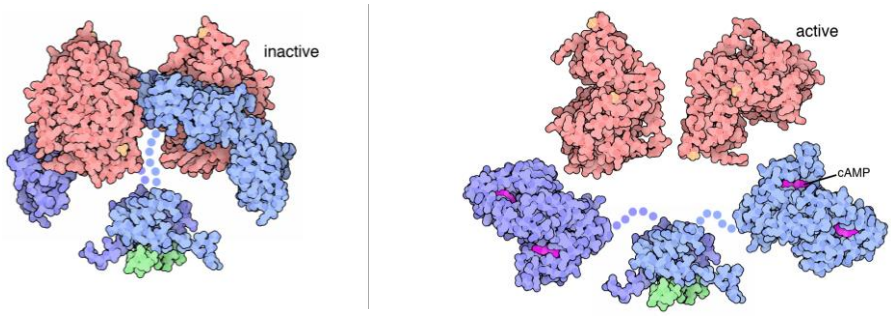

Figure 1.5 Structure of protein kinase A. Inactive (left) and active (right) conformations of PKA. Catalytic domains are red, regulatory domains are blue. Bound cyclic AMP is marked with magenta. Image from Protein Data Bank (entries 3tnp , 1j3h and 2h9r).

Besides binding and inhibiting the catalytic subunits, the regulatory subunits have the role of anchoring PKA to AKAP proteins. A-kinase anchoring proteins (AKAP) are a family of scaffolding proteins that bind and restrict the localisation of PKA, PDEs and even ACs to specific subcellular locations, creating distinct signaling microdomains by coupling cAMP synthesis, degradation and function (Kapiloff et al., 2014) (Figure 1.6). There are numerous AKAP isoforms (>70), and they bind with different affinities to PDEs or ACs, some downstream effectors like EPAC and PKA, but also non-cAMP pathway molecules (PKC, calcineurin, MAPK). By associating to anchoring proteins (AKAPs), PKA is readily available close to its target substrates in specific cellular compartments. Within the AKAP scaffold complexes, PKA can be found anchored to adenylyl cyclases or phosphodiesterases, ensuring a tight regulation of cAMP signaling (Dessauer, 2009).

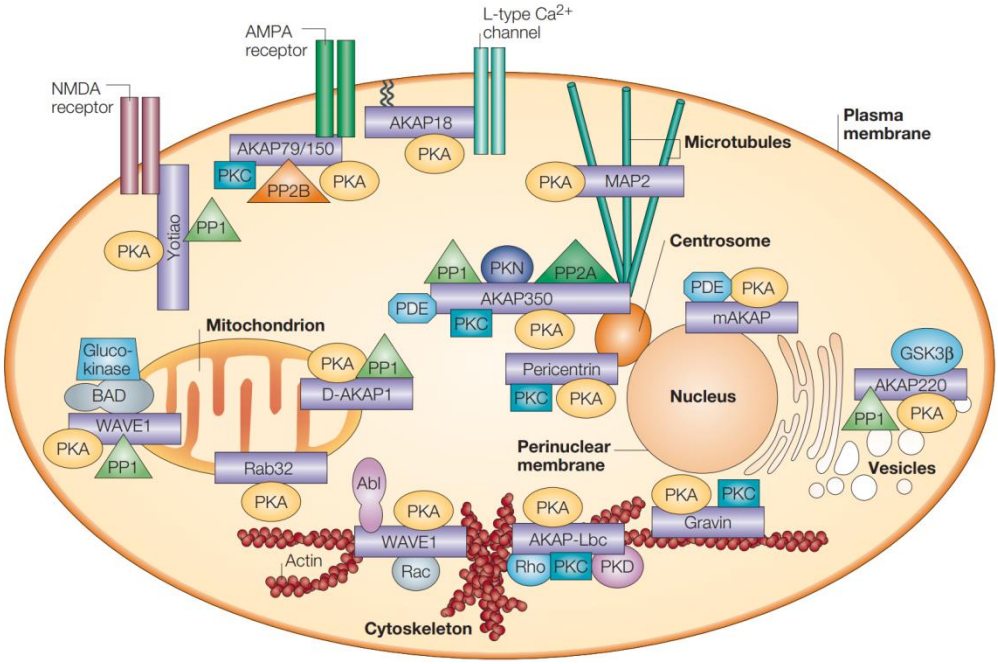

Figure 1.6 AKAP signaling complexes. A-kinase anchoring proteins (AKAP) create signaling complexes by binding and restricting the localisation of PKA and other proteins. Figure from (Wong & Scott, 2004).

There are a large number of intracellular proteins that get phosphorylated by PKA, having their function either enhanced or blocked. Such targets of PKA phosphorylation are NMDA and AMPA receptors, adrenergic receptors, calcium channels, other kinases like ERK and PKG, actin and other cytoskeletal proteins and even AC and PDEs (Howe, 2004; Joiner et al., 2010; Komagiri & Kitamura, 2007; Murphy et al., 2014; Murphy & Dell'Acqua, 2014; Nam et al., 2021; Qian et al., 2012). One of the most investigated interactions of PKA is that with the transcription factor CREB. Upon cAMP binding, catalytically active PKA-C translocates to the nucleus, where it will directly phosphorylate the transcription factor CREB at Ser133 (Gonzalez & Montminy, 1989; Hagiwara et al., 1993). CREB then binds to cAMP-responsive element (CRE), an eight base pair sequence that is part of different gene promoters, initiating transcription of new genes for *de novo* protein synthesis (Figure 1.7). A large number of genes contain CREs in their promoter and encode proteins with various functions, including metabolism, transcription (cFos, Jun), neuropeptides (enkephalin, VIP, somatostatin, vasopressin), cell cycle proteins (cyclins), growth factors (insulin, BDNF) and proteins involved in immune regulation (Mayr & Montminy, 2001). Besides being activated by PKA, CREB can be stimulated by other factors such as calcium and CaMKII/IV, insulin-like growth factor that acts via p38/Ras pathway and others (Bonni, 1999; Riccio, 1999).

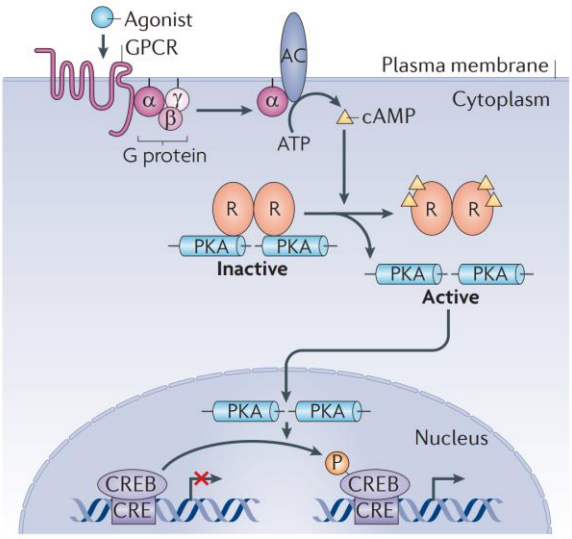

Figure 1.7 Simplified diagram of the cAMP-PKA-CREB signaling pathway. An intracellular increase in cAMP will activate PKA, leading to the dissociation of catalytically active PKA-C subunits. PKA-C subunits translocate to the nucleus where they will phosphorylate CREB, promoting the expression of genes containing cAMP-response elements (CRE). Figure from (Altarejos & Montminy, 2011).

Exchange protein directly activated by cAMP (EPAC)

In comparison to PKA, EPAC is a recent discovery that revitalised the cAMP signaling field, as PKA-independent effects have been previously reported (Pedarzani & Storm, 1995; Renström et al., 1997; Shintani & Marunaka, 1996; Wolfgang et al., 1996). Two EPAC isoforms exist, each with distinct tissue distribution: EPAC1 is ubiquitously expressed, whereas EPAC2 is present in the central nervous system, pancreas and adrenal glands (Kawasaki et al., 1998). Upon cAMP binding to the cyclic nucleotide-binding domain of the protein, EPAC becomes catalytically active. Subsequently, EPACs activate their main downstream effector, the Ras superfamily of small GTPases via a guanine nucleotide exchange (Figure 1.8). The Ras superfamily includes Rap1 and Rap2, which are proteins that control numerous basic cell functions like cell adhesion, exocytosis, cell differentiation, as well as the activity of other proteins (integrins, PLC, actin, RIM, ERK1/2) (Roscioni et al., 2008).

The existence of two intracellular cAMP downstream effectors with overlapping tissue distribution and mechanism of activation could enable a more precise control of cAMP signaling, even within the same cellular compartment. Cyclic AMP activation of EPAC alongside that of PKA provides a mechanism for differential intracellular biological responses starting from the same hormone or neurotransmitter. Multiple studies have shown that within the same cell, the PKA and EPAC pathways can elicit similar or opposing effects, demonstrating that the two pathways display synergistic cross-talk as well as independent signaling actions (Cheng et al., 2008).

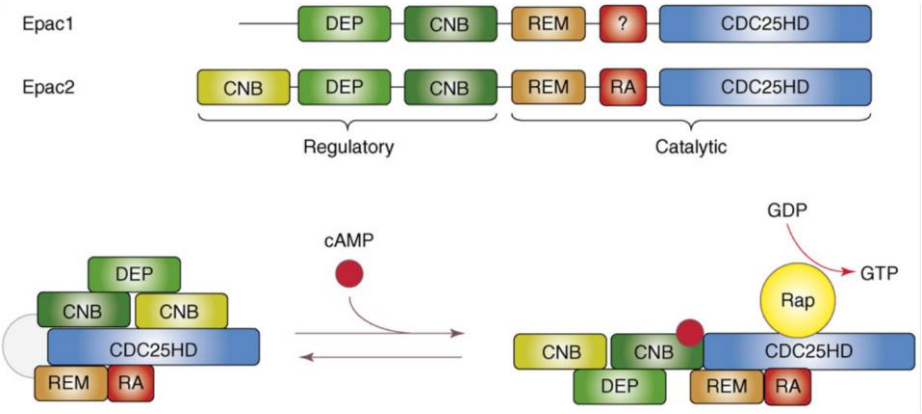

Figure 1.8 Structure and activation mechanism of Epacs. (top) Structurally, Epacs are composed of a regulatory region (with one or two cyclic nucleotide-binding domains) and a catalytic region. (bottom) Binding of cAMP to the regulatory domain opens up the protein and enables the interaction with the substrate (Rap) and catalytic activity (stimulating the release of GDP to allow binding of GTP). Image from (Bos, 2006).

Cyclic nucleotide-regulated cation channels

Cyclic nucleotide-regulated channels are a particular type of cAMP effector as they represent the only non-enzymatic proteins directly modulated by cAMP binding. Cyclic nucleotide-regulated channels are cation channels whose activation is directly regulated by binding of cAMP or cGMP and leads to ion influx and membrane depolarisation. These channels are represented by two different classes from the same superfamily: CNG (Cyclic Nucleotide-Gated) and HCN (Hyperpolarization-activated, Cyclic Nucleotide-gated) (Figure 1.9). Structurally, both CNG and HCN channels are tetrameric complexes, with each subunit consisting of a transmembrane channel domain and a cytosolic cyclic nucleotide-binding domain on the C terminus. The transmembrane domains are made up of six α helices and the channel's pore is formed between helix 5-6 and the pore loop. In the case of HCN channels, helix 4 has the role of voltage sensor, with positively charged residues moving according to the electric field. This movement will result in conformational changes within the channel protein, opening the pore and allowing ion flow (Hofmann et al., 2005; Kaupp et al., 2002). In terms of ion selectivity, both CNG and HCN channels pass monovalent cations like Na^+ and K^+. CNG channels are also permeable to divalent Ca^{2+} ions, whereas HCN channels' permeability to calcium is very low. It was shown that at physiological extracellular Ca^{2+} (2.5 mM), HCN channel's calcium currents are ~0.5%, while for CNG channels calcium accounts for 10-80% of ionic flow (Yu et al., 2007).

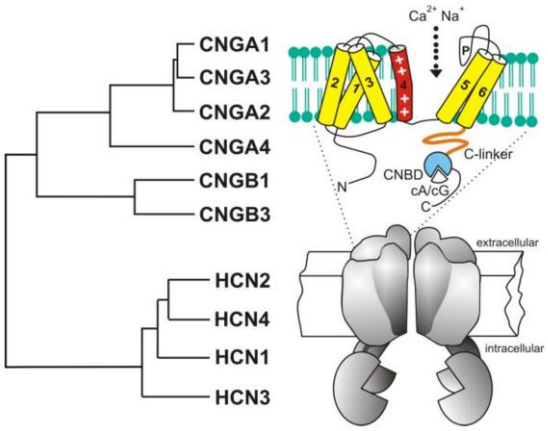

Figure 1.9 Cyclic nucleotide-regulated cation channels. Left: Phylogenetic tree of the cyclic nucleotide-regulated channel family. Right: Domain topology of CNG/HCN channels. Image from (Biel, 2009).

The intracellular domains have a highly conserved cyclic nucleotide-binding domain. Due to differences in a few key residues of the CNBD, the two types of channels have distinct cyclic nucleotide selectivity. While HCN channels have a higher affinity for cAMP over cGMP, CNG channels are highly selective for cGMP. In the case of CNG channels, binding of cyclic nucleotides to the CNBD generates conformational changes that lead to pore opening. While CNG channels only open upon cyclic AMP binding, HCN channels get activated at hyperpolarized voltages and cAMP binding shifts the voltage dependence of the channel's activation. In the case of HCN channels, the CNBD acts as an inhibitory domain in the absence of cAMP by interacting with the channel's pore. Cyclic AMP binding is not necessary for the channel's activation but when cAMP binds, CNBD's inhibitory effects are relieved, shifting the activation voltage of the HCN channel to more positive values (Biel et al., 2009).

CNG channels are mainly expressed in retinal photoreceptors and in olfactory sensory neurons, where their principal function is that of sensory transduction (Biel & Michalakis, 2007). In more recent years, a widespread distribution of CNG channels in the brain (cortex, amygdala, hippocampus) has been uncovered (Podda & Grassi, 2014). In the hippocampus, significant levels of CNG channels (CNG1-4) have been identified in pyramidal excitatory neurons (Bradley et al., 1997; Ding et al., 1997; Kingston et al., 1996; Strijbos et al., 1999). Due to the difficulty of electrophysiologically isolating the contribution of CNG channels, transgenic CNG-deficient animals have been used to evaluate the role of CNG conductance to long term potentiation of synapses (LTP) Interestingly, knocking out CNGA1 led to attenuated LTP after theta burst stimulation (TBS) of hippocampal Schaffer collateral synapses, while CNGA3-deficient mice presented an increased LTP at the same synapse but no difference to wild type animals in terms

of spatial memory (Michalakis et al., 2011; Parent et al., 1998).

HCN channels come in 4 different isoforms that differ in speed of activation and cAMP sensitivity. While HCN2 and HCN4 voltage dependency is highly modulated by cAMP, HCN1 and HCN3 display little cAMP regulation (Kaupp et al., 2001). HCN channels are expressed in cardiac cells and neurons, where they are responsible for a slow cation current (If (funny) or Ih (hyperpolarization)) that is generated by membrane hyperpolarization. In the heart, HCN channels control heart beating in sinoatrial node cells. All four isoforms have been detected in different brain regions, with HCN1 and HCN2 being the most expressed isoforms in the hippocampus (Seo et al., 2015). The specific roles of HCN in hippocampal learning and memory have been mostly investigated using HCN channel isoform-deficient transgenic mice. $HCN1^{-/-}$ mice show performance increase in hippocampal-dependent learning and memory in the Morris water maze. Interestingly, HCN1-deficient mice show enhancement of electrically-induced LTP at the synapse between the entorhinal cortex and CA1, but not at the Schaffer collateral synapse. This synapse-specific difference is thought to be due to the expression levels of HCN1 on CA1 dendrites, as HCN1 expression is higher in more distal dendrites (corresponding to the site of entorhinal cortex synapses) than on proximal segments where CA3 axons synapse (Nolan et al., 2004). In HCN2-deficient mice, perforant path to CA1 LTP was enhanced but only in a global deletion model, not when HCN2 was knocked out only from pyramidal neurons. In contrast to HCN1, HCN2 channels do not modulate dendritic integration in pyramidal neurons, but set the activity of inhibitory interneurons which will affect synaptic plasticity. Similarly to the HCN1 model, LTP was unaffected at the Schaffer collateral synapse (Matt et al., 2011).

Phosphodiesterases (PDEs)

The intracellular concentration of cAMP is highly dependent on the balance between its synthesis by ACs and its degradation by phosphodiesterases (PDEs). There are 11 known PDE isoforms (and over 50 splice variants) that are differently expressed in distinct cell types and that have different affinities to cAMP or cGMP. The affinity range for cAMP varies from 10-100 nM (PDE3 and PDE8) to more than 10 μM (PDE1 and PDE2) (Bender & Beavo, 2006; Conti & Beavo, 2007; Manganiello et al., 1995). Some isoforms prefer to hydrolyze only cAMP (PDE4, PDE7, PDE8) or cGMP (PDE5, PDE6, PDE9), while others hydrolyse both (PDE1, PDE2, PDE3, PDE10, PDE11) (Table 1.2).

Within the same cell, multiple isoforms are expressed allowing the degradation of a wide range of intracellular cAMP concentrations. Due to their relatively fast k_{cat}, PDEs limit cAMP diffusion thereby contributing to cAMP gradients. This compartmentalisation of cAMP allows for more specific cAMP signaling in terms of the spatio-temporal resolution. Furthermore, intracellular cAMP gradients allow for differential activation of downstream pathways, based on cAMP concentration in those compartments. PDE activity can also be directly inhibited by PKA (Sette & Conti, 1996), as both PDEs and PKA localise within the same AKAP scaffold complex (Dodge-Kafka et al., 2006). Additionally, distinct GPCR types can differentially activate specific PDEs (e.g. in myocytes β1AR activates PDE4D8 whereas β2AR activates PDE4D5 (Richter et al., 2008)). Similarly to cAMP and PKA, PDEs are not uniformly distributed within a cell. Their subcellular localisation depends on PDE's interaction with AKAP scaffolds, as well as direct interaction with organelles or the plasma membrane (Houslay, 2010).

Table 1.2 Substrate specificity and distribution of phosphodiesterase families.

Isoform family	Substrate specificity	Expression in hippocampus
PDE1	cAMP / cGMP	+
PDE2	cAMP > cGMP	+
PDE3	cAMP > cGMP	+
PDE4	cAMP	+ (except 4C)
PDE5	cGMP	+
PDE6	cGMP	no expression
PDE7	cAMP	+
PDE8	cAMP	+ (except 8A)
PDE9	cGMP	+
PDE10	cAMP > cGMP	+
PDE11	cAMP / cGMP	+

1.2 Cyclic AMP signaling in the hippocampus

1.2.1 The hippocampal structure

The hippocampus is a brain structure embedded deep in the temporal lobe. It received its name when the 16th century anatomist Arantius compared its shape to that of a sea-horse. The subsequent nomenclature "*Cornu Ammonis*" (due its resemblance to the horns of the Greek/Egyptian god Amun) is currently used to name the different regions of the hippocampus (CA1, CA2, CA3). While being 100 times smaller in volume compared to the cerebral cortex (Gilbert & Brushfield, 2009), studying the hippocampal formation has had a pivotal role in how we understand complex cognitive processes such as learning and memory. In part due to its surprisingly simple structure, the hippocampus continues to be an ideal model system for neurobiological research. Throughout the years, different roles have been attributed to the hippocampus, ranging from olfaction to reason, emotion and motor function. Although it was first reported as early as 1889 (Brown & Sharpey-Schäfer, 1889), memory didn't become a clear function of the hippocampus until the late 1950's due to the now-famous patient Henry Molaison, who was unable to form new memories after having the hippocampi surgically removed (Scoville & Milner, 1957).

The hippocampus is an unique brain area and distinctive from other cortical structures due to its cytoarchitecture and circuitry (Figure 1.10). It is also one of the few brain regions that receives highly processed inputs from a multitude of sources. Anatomically, it is composed of several subdivisions: the *hippocampus proper* (which includes areas CA1, CA2, CA3, CA4), and the dentate gyrus (Andersen et al., 2006). Hippocampal circuitry is remarkable in its architecture, as complex memory-related processes are computed through just a few synaptic connections. The main afferent input to the hippocampus is received from the cortex, via axons of the entorhinal cortex that project to the dentate gyrus (the perforant pathway). In terms of efferent pathways, the main output of the hippocampus are the connections between area CA1 and the subiculum, which in turn will project to other non-hippocampal regions such as the entorhinal cortex, amygdala, and other brain areas.

Within the hippocampus, the intrinsic circuitry is relatively simple, with the key features of

unidirectionality and orderliness of its connections. Simply put, neurons of the dentate gyrus send mossy fibers to CA3 area neurons that do not project back to the dentate gyrus. From here, part of CA3 neurons project to the opposite side of the hippocampus via the *corpus callosum*, while the rest connect unidirectionally to neurons in area CA1 via the Schaffer collaterals. From area CA1 projections leave the hippocampus, connecting to subiculum cells.

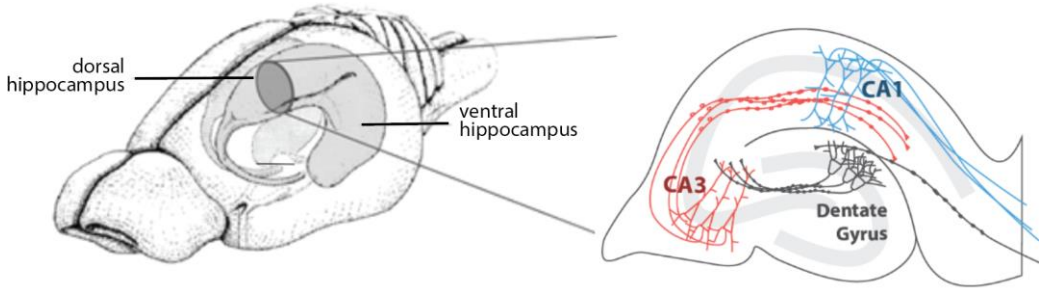

Figure 1.10 The hippocampus. (Left) Rat hippocampal formation; modified from (Burwell et al., 1995). (Right) Neuronal projections within the hippocampus: input reaches the hippocampus through the entorhinal cortex (EC) whose cells give rise to projections to the dentate gyrus (DG). DG projects to the CA3 region, which in turn provides the major unidirectional input to the CA1 neurons. The processing loop is closed in area CA1, whose neurons project not only to the EC, but also to the subiculum.

Most hippocampal substructures are characterised by a laminar cytoarchitectonic organisation. The dentate gyrus is divided into three layers, namely a molecular layer, a granule cell layer and a polymorphic layer. The principal excitatory neurons of the dentate gyrus, the dentate granule cells, are tightly packed together within the granule cell layer. Areas of the *hippocampus proper* are distinguished from the dentate gyrus by their multiple layer organisation. Going from deep and towards the superficial layers one can find the *alveus*, *stratum oriens*, *stratum pyramidale*, *stratum radiatum* and *stratum lacunosum-moleculare*. Additionally, areas CA3 and CA2 have a *stratum lucidum* between *str. pyramidale* and *str. radiatum* (Amaral et al., 2007). The only excitatory neurons in areas CA1-CA2-CA3 are the pyramidal neurons, with their cell bodies tightly packed within the *str. pyramidale*. Their basal dendrites occupy most of *str. oriens*, while their apical dendrites stretch across *str. radiatum* and *str. lacunosum-moleculare*. Dentate granule cells project onto CA3 and CA2 dendrites within *str. lucidum*, CA3 collaterals connect to CA2 and CA1 dendrites mainly in *str. radiatum*, CA2 axons connect to CA1 pyramidal neuron in *str. oriens*, while CA1 sends its axons to subiculum through *str. oriens* (Dudek et al., 2016).

1.2.2 Synapses and hippocampal synaptic plasticity

The synapse: unit of information transfer

An excitatory synapse is composed of a presynaptic component (bouton), a postsynaptic component (dendritic spine) and a surrounding astrocyte. Simply put, if the synaptic inputs generate a change in the membrane potential at the presynaptic neuron's hillock region that is large enough, an action potential will be generated. It will travel along the axon via the voltage-gated sodium channels until it reaches the axon terminals or synaptic boutons. Here, the depolarisation will lead to calcium influx through the opening of voltage-gated calcium channels. In a calcium-dependent process, synaptic vesicles filled with the neurotransmitter glutamate will fuse to the active zone of the presynaptic bouton, releasing the neurotransmitter molecules into the synaptic cleft, the ~20 nm space between the presynaptic and the postsynaptic membrane compartments. Glutamate will diffuse across the synaptic cleft and bind to specialized postsynaptic receptors. The most relevant to the process of fast excitatory synaptic transmission are the AMPA receptors, ionotropic glutamate receptors that open upon glutamate binding, leading to an influx of positively charged ions into the postsynaptic dendritic spine. The depolarisation mediated by AMPA receptors, together with that of NMDA receptors (will be described in detail below), represents the excitatory postsynaptic potential (EPSP) that integrates with EPSPs from other synaptic sites in the dendritic tree. If their summation surpasses the firing threshold at the axon hillock, the process starts all over again (Figure 1.11).

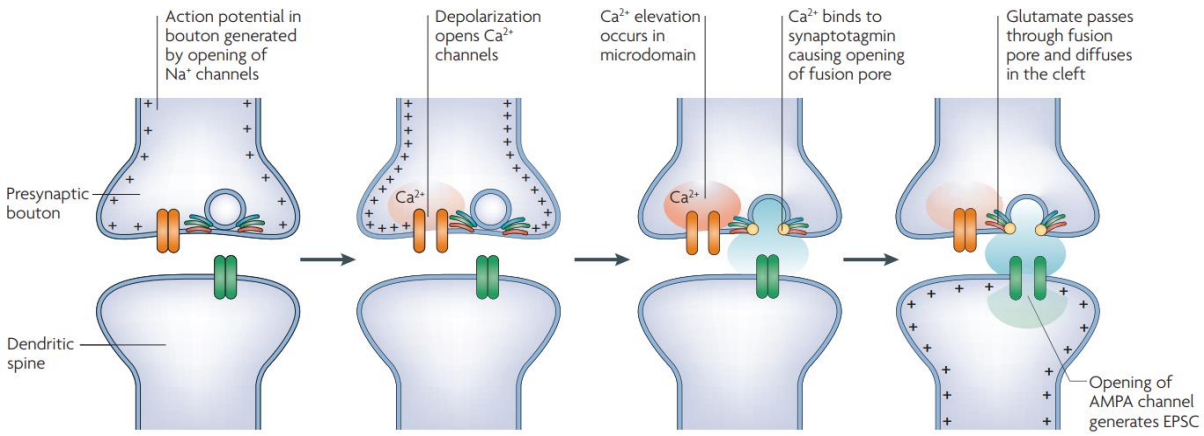

Figure 1.11 Simplified working mechanism of chemical synaptic transmission. Image from (Lisman et al., 2007).

Synaptic plasticity

Starting with patient Henry Molaison, the role of the hippocampus has been closely associated with that of learning and creation of memories, as after the removal of both his hippocampi, Henry Molaison suffered not only from amnesia, but he was unable to form new memories (Scoville & Milner, 1957). Multiple mechanisms of learning and memory have been proposed over the years, starting with Ramon y Cajal who proposed that memories are encoded in synaptic connections (Ramón y Cajal, 1909). The concept of potentiation was named and proposed by Jerzy Konorski in 1948 (Konorski, 1948) and formulated by Donald Hebb in 1949 with his now famous quote *"When an axon of cell A is near enough to excite cell B and repeatedly or persistently takes part in firing it, some growth process or metabolic change takes place in one or both cells such that A's efficiency, as one of the cells firing B, is increased"* (Hebb, 2005). The first experimental evidence of long-lasting changes in the strength of synapses in mammals came only in 1973, when Bliss and Lomo observed that a brief high-frequency stimulation of the perforant pathway inputs to the dentate gyrus results in a sustained enhancement of synaptic transmission (Bliss & Lomo, 1973) (Figure 1.12). Nowadays, it is generally accepted that the synapse represents the location of memory storage and that synaptic plasticity is the molecular mechanism that allows for memories to be stored in the brain.

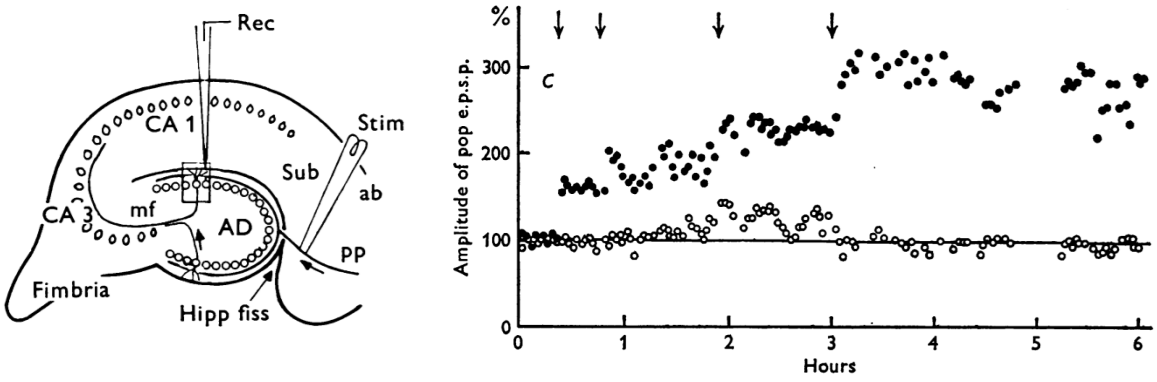

Figure 1.12 First experimental evidence of long-term potentiation in mammals. Left: placement of stimulation and recording electrodes in the hippocampus of an anaesthetized rabbit. Right: high-frequency stimulation of the perforant pathway induces an increase in the responses recorded in the dentate granule cell layer. Image taken from (Bliss & Lomo, 1973).

The process of long term potentiation (LTP) modifies the way information flows through neuronal circuits. It represents an activity-dependent persistent change in the synaptic strength between two neurons, altering the way in which information is encoded. Information processing

relies on efficient communication between different brain regions but for learning additional associations need to be created. This is thought to be done through connectivity changes that shape the output of circuits (Basu & Siegelbaum, 2015; Lüscher & Malenka, 2012). Since its discovery in the hippocampus, LTP has been observed in multiple other brain areas and it is thought to represent the fundamental mechanism of learning and memory in the brain (Bliss et al., 2018).

General molecular mechanism of LTP in the hippocampus

Hippocampal long term potentiation has been the most studied and characterised form of plasticity, partly due to the properties of hippocampal circuitry and the possibility of making and recording from acute slices with conserved intrinsic hippocampal connectivity. Long term potentiation is characterised by an early stage (< 3 hours), where pre-existing proteins are modified, and a late stage (> 3 hours), in which new proteins must be synthesized in order to sustain the structural changes necessary for the prolonged enhancement of synaptic transmission (Kandel, 2001; Sweatt, 1999). Long term potentiation is also defined by three distinct mechanisms in terms of its *induction, expression* and *maintenance* (Malenka & Bear, 2004).

The most studied and understood type of hippocampal LTP is NMDAR-dependent LTP, a plasticity mechanism that defines entorhinal cortex-dentate gyrus synapses, as well as CA3-CA1 synapses. It is defined by cooperativity, associativity and input specificity (Lüscher & Malenka, 2012) (Figure 1.13). An exception to this typical Hebbian LTP is the dentate gyrus to CA3 synapse, where postsynaptic activity is not required for potentiation. Here, LTP is induced by presynaptic activity and modulation of transmitter release.

At the forefront of hippocampal Hebbian LTP is the NMDA receptor, a glutamate receptor subtype with unique properties (Morris, 2013). In contrast to AMPA receptors, NMDA receptors do not get activated when glutamate binds, unless the membrane is depolarised enough to eliminate their Mg^{2+} block. Additionally, they are highly permeable to calcium and display slower kinetics than AMPA receptors upon glutamate binding. Upon a strong enough stimulus, the depolarisation triggered by AMPA receptors is sufficient to open the NMDA receptors, increase intracellular calcium concentration and *induce* LTP of that particular connection (input specificity). NMDA receptors act as coincidence detectors, as their activation requires strong presynaptic activity as well as sustained postsynaptic depolarisation. A sufficient amount of inputs need to be

activated in order for LTP to be induced (cooperativity), which might be a mechanism used to filter relevant information-containing stimuli. Additionally, weak stimuli that would not be sufficient to trigger LTP on their own can be enabled by stronger stimuli, as long as their timing coincides (associativity) (Citri & Malenka, 2008).

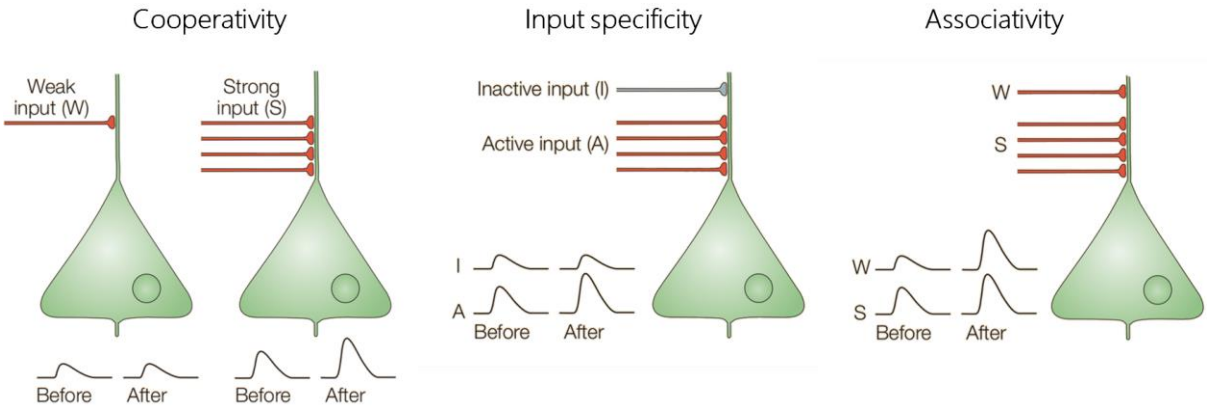

Figure 1.13 Basic properties of long-term potentiation. Image from (Malenka, 2003).

Due to the multiple molecular components of LTP, as well as ways to induce and investigate it, there is no clear consensus about the molecular mechanism of *expression* (Kerchner & Nicoll, 2008; Lisman, 2009). However, experimental evidence suggests that expression mechanisms affect the probability of neurotransmitter release (presynaptic expression locus) or the ion conductance and the number of AMPA receptors (postsynaptic LTP expression) (Bliss & Collingridge, 2013) (Figure 1.14). The expression of NMDA-dependent LTP depends on the calcium ions that flood the dendritic spine upon NMDA receptor activation (Bliss & Collingridge, 1993). Calcium will bind to calmodulin and the Ca^{2+}/calmodulin (Ca^{2+}/CaM) complex will act as a second messenger by activating numerous proteins, including CamKII, PKC and adenylyl cyclases (Lisman et al., 2002; Malenka & Nicoll, 1999; Sweatt, 2004; Thomas & Huganir, 2004; Yasuda et al., 2003). The activity of these enzymes is critical for the early phase of LTP, as AMPA and NMDA receptors get phosphorylated resulting in an increase in conductance and open probability. Furthermore, new AMPA receptors get trafficked to the postsynaptic density (Bredt & Nicoll, 2003; Song & Huganir, 2002). Presynaptic changes that enhance synaptic vesicle exocytosis might also contribute to the expression of LTP (Emptage et al., 2003). Since the induction is a postsynaptic event, retrograde messengers like NO, BDNF or adhesion proteins need to communicate from the postsynaptic cell to the presynaptic terminals (Castillo, 2012; Zakharenko et al., 2003).

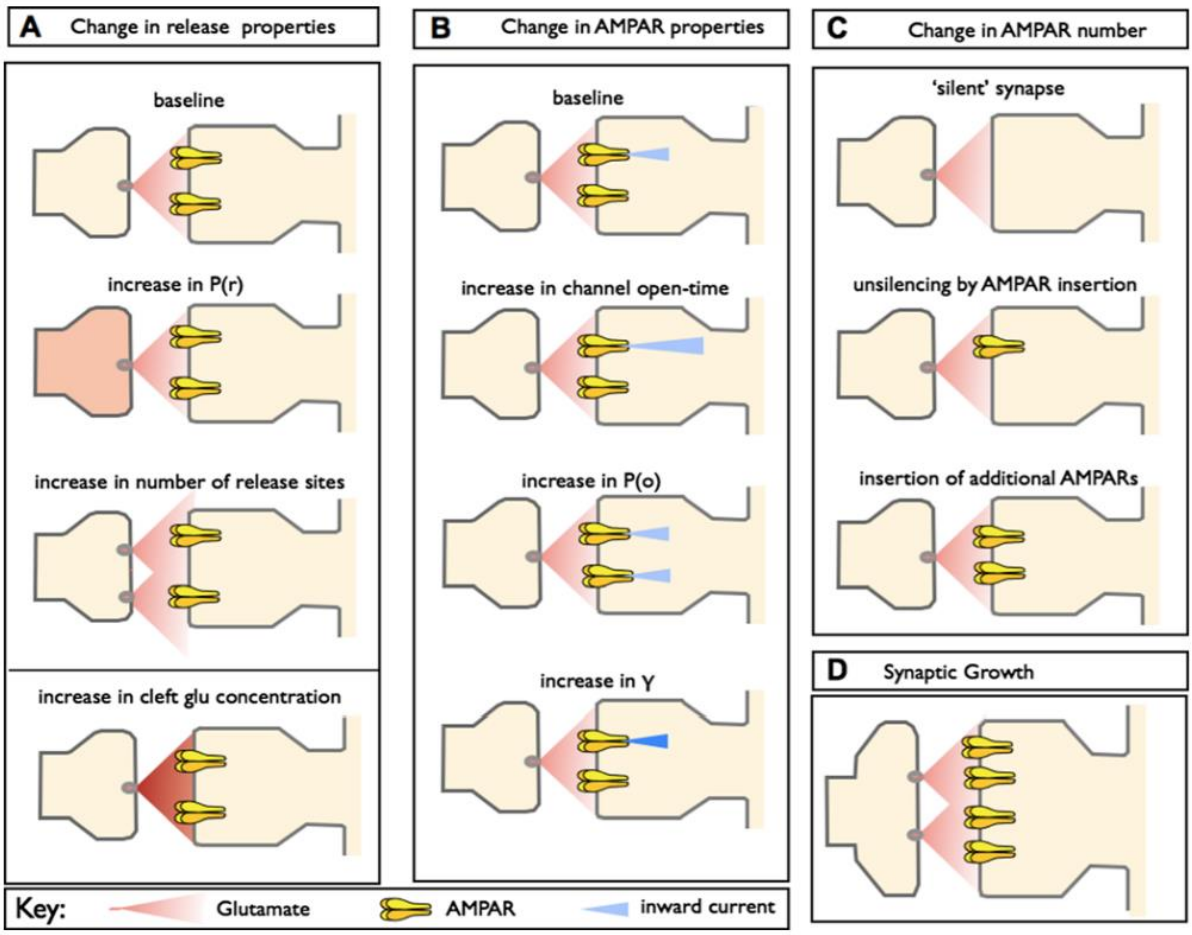

Figure 1.14 Potential expression mechanisms for LTP. Image from (Bliss & Collingridge, 2013).

The transition between the early and the late phase of LTP is done through kinase-dependent (PKA, ERK) activation of transcription factors (e.g. CREB) and initiation of protein synthesis, enabling the creation of new proteins necessary for the *maintenance* of LTP (Abraham & Williams, 2003; Matsuzaki et al., 2004; Silva et al., 1998; Yuste & Bonhoeffer, 2001). Interestingly, multiple other studies have shown that the late phase of LTP does not require the synthesis of new proteins, in contrast to the classical rules of LTP induction and maintenance (Rudy, 2008; Villers et al., 2012).

Almost 50 years since the "discovery" of LTP by Bliss and Lomo, there are still unanswered questions about its precise molecular mechanisms. There have been hundreds of molecules identified as having a role in LTP, but it is unclear if they mediate LTP or are merely modulators (Sanes & Lichtman, 1999) (Figure 1.15). However, multiple expression mechanisms for LTP have been shown to exist indicating that multiple intracellular pathways might be involved in the

induction of LTP (Lisman et al., 2003). The debate regarding the locus of expression in NMDA-dependent LTP also remains unsettled, as retrograde signaling could allow for a postsynaptic induction but presynaptic expression mechanisms that influence transmitter release. However, most retrograde molecules that could sustain the presynaptic expression hypothesis have not been successfully demonstrated in experimental settings (Castillo, 2012; Pigott & Garthwaite, 2016; Pigott, 2012).

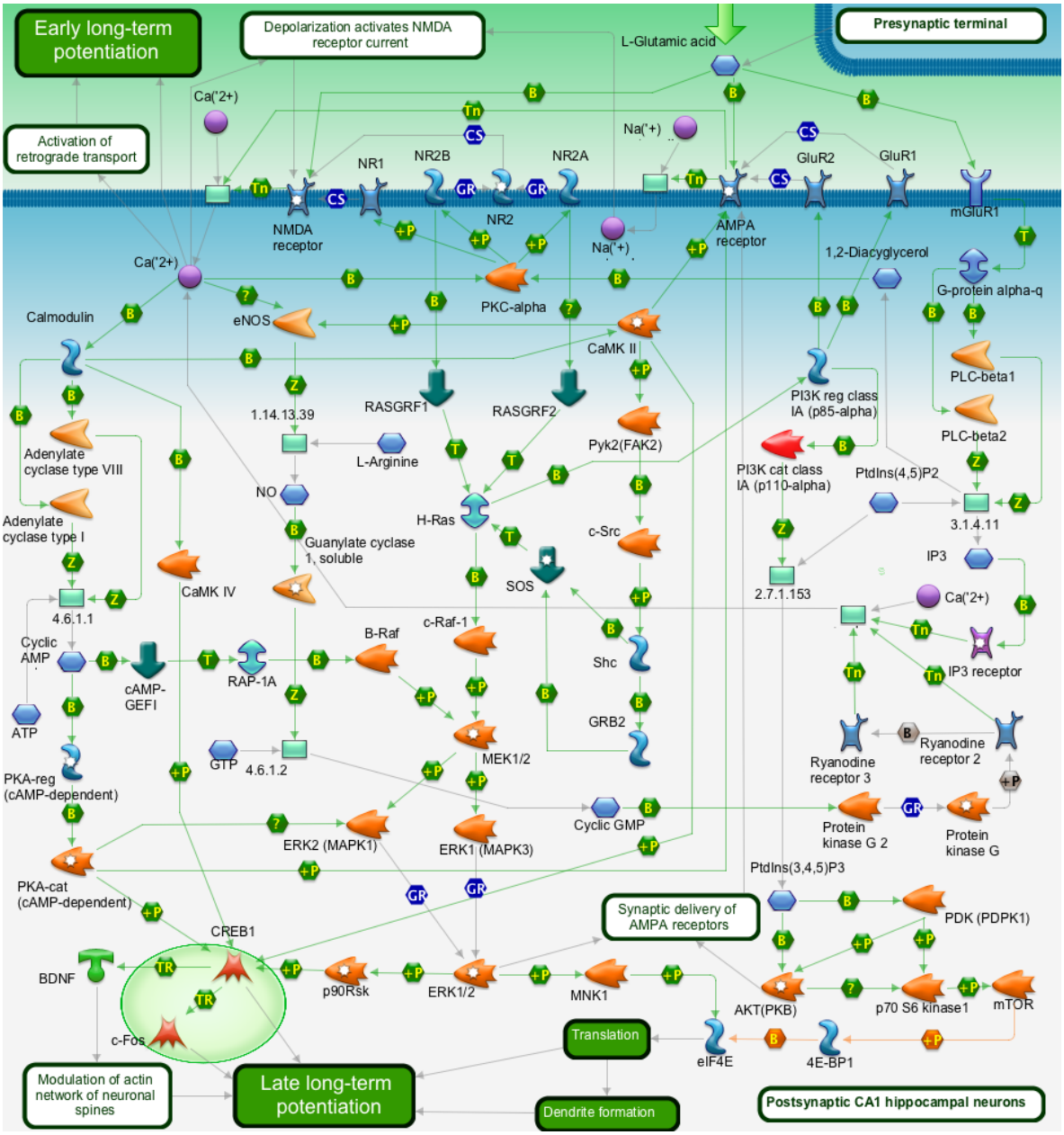

Figure 1.15 Molecular pathways involved in NMDA-dependent postsynaptic long-term potentiation in CA1 hippocampal neurons. Image from BioRad.

1.2.3 Synaptic changes mediated by cAMP

Presynaptic cAMP-mediated changes in LTP

Perhaps the best-characterised form of presynaptic potentiation is found at the synapse between dentate gyrus granule cells and hippocampal CA3 pyramidal neurons. Here, LTP is NMDA receptor-independent, relies on presynaptic cAMP and PKA signaling and results in changes in release machinery (Bliss & Collingridge, 2013; Castillo, 2012; Nicoll & Schmitz, 2005; Yang & Calakos, 2013) (Figure 1.16).

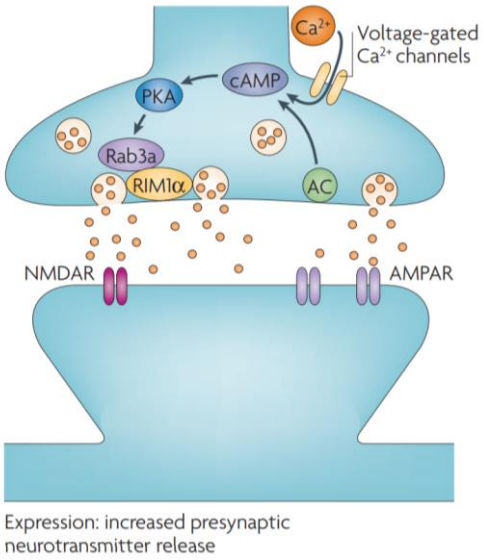

Figure 1.16 Simplified diagram of the induction and expression of presynaptic LTP. Image from (Kauer & Malenka, 2007).

The activation of adenylyl cyclases with the diterpene forskolin increases synaptic transmission at the mossy fiber synapse and occludes electrically induced LTP (Weisskopf et al., 1994). Furthermore, inhibiting the activity of PKA regulatory or catalytic subunits blocked the induction of electrically stimulated LTP (Weisskopf et al., 1994). A reduction in the paired-pulse facilitation during the forskolin-stimulated enhancement of transmission argues for a presynaptic locus of expression. Additionally, the requirement for cAMP signaling in presynaptic mossy fiber LTP has been reconfirmed in studies using transgenic mice. While Schaffer collateral LTP is unchanged in adenylyl cyclase 1-deficient mice, mossy fiber electrically-induced LTP is impaired, but can be partially recovered using forskolin to stimulate the cAMP synthesis by other adenylyl cyclase isoforms (Villacres et al., 1998; Weisskopf et al., 1994). Furthermore, mossy fiber LTP is impaired in PKA-deficient mice and synaptic transmission cannot be enhanced with the

application of forskolin (Huang et al., 1995). This shows that cAMP-PKA signaling is necessary and sufficient to enhance synaptic transmission at the mossy fiber synapse through presynaptic mechanisms.

Mechanistically, presynaptic Ca^{2+} activates the production of cAMP at the terminals via Ca^{2+}/CaM-sensitive adenylyl cyclases. This increase in cAMP will activate PKA which will phosphorylate presynaptic proteins, leading to an enhanced glutamate release (Nicoll & Schmitz, 2005). The expression mechanism of cAMP-dependent presynaptic LTP has been linked to changes in release machinery and size of the active zone rather than to changes in the probability of release (Orlando et al., 2021). From all presynaptic proteins involved in synaptic vesicle exocytosis that get phosphorylated by PKA, the active zone protein RIM1α has emerged as a key player in the expression of presynaptic LTP (Castillo et al., 2002). RIM1α is a scaffold protein located in the presynaptic active zone that interacts with other proteins that regulate vesicle exocytosis, including Rab3A and synaptotagmin-12 (Castillo et al., 1997; Kaeser-Woo et al., 2013; Monday et al., 2018). It has been shown that an increase of PKA-dependent phosphorylation of RIM1α leads to LTP in the cerebellum and amygdala (Chevaleyre et al., 2007; Fourcaudot et al., 2008; Lonart et al., 2003). In the hippocampus, while baseline synaptic transmission is unaltered in RIM1α-deficient mice, mossy fiber LTP cannot be induced (Castillo et al., 2002). However, there have been studies which show that PKA-dependent RIM1α phosphorylation might not actually be necessary for mossy fiber LTP (Kaeser et al., 2008).

The main constraints in identifying the exact molecular players in presynaptic LTP are the small size of the boutons and inaccessibility for chemical or electrophysiological manipulations. Additionally, neurotransmitter release is a complex process that requires multiple molecules and thus, there are many possible points of regulation (Castillo, 2012).

Postsynaptic cAMP-mediated changes in LTP

NMDA-dependent LTP at Schaffer collateral synapse is perhaps one of the most studied molecular processes in the brain. While the detailed molecular signaling cascades are not completely understood, since the early 1990s a large body of work has focused on elucidating cAMP's contribution to long-term potentiation at Schaffer collateral synapse. The first studies linked key processes in NMDA-dependent potentiation with PKA activity. Patching cultured hippocampal neurons with PKA catalytic subunit in the pipette increased AMPA currents when

glutamate was delivered, effect which could be replicated with the cAMP analogue Sp-cAMPS or with forskolin, a stimulator of endogenous adenylyl cyclases. Additionally, inhibiting PKA reversed this enhancement (Greengard et al., 1991; Wang et al., 1991). Soon after, PKA was uncovered as a component of the molecular mechanisms that generate the late stage of LTP. By pre-incubating the slice with inhibitors of PKA, the late phase of LTP was completely blocked, as field excitatory postsynaptic potentials decayed to baseline with a time course similar to when protein synthesis blockers are used (Frey et al., 1993; Huang & Kandel, 1994). More evidence linking cAMP mediation of late LTP came when it was shown that perfusing cAMP analogues or forskolin (to stimulate cyclase activity) was sufficient to induce potentiation and that this effect was blocked when inhibitors of protein synthesis were pre-incubated (Frey et al., 1993). Since these early findings, numerous studies have demonstrated the critical role cyclic AMP and its signaling pathway have in plasticity related processes (Figure 1.17). These studies have been carried out mostly by the use of pharmacology, either stimulating the production of cAMP or blocking elements of its pathway. Investigations using transgenic animals and more recently, optogenetic tools, have offered a more nuanced and precise manipulation. Subchapter 1.3 of the Introduction will present the most popular strategies for manipulating cAMP and controlling elements of its signaling pathway.

At the present moment, the general consensus is that cAMP signaling mediates the early phase of potentiation and gates its conversion to late LTP. Upon sustained presynaptic stimulation, the rise in postsynaptic calcium activates CaMKII and some subtypes of adenylyl cyclases, triggering cAMP production. Cyclic AMP will activate PKA which together with CaMKII will be responsible for most cellular changes involved in the acute enhancement of postsynaptic responses. To promote the expression of early LTP, PKA phosphorylates AMPA receptors, increasing their conductance (Park et al., 2021; Renner et al., 2017), as well as stimulates AMPA receptor insertion into the synapse (Diering et al., 2016; Esteban et al., 2003; Purkey & Dell'Acqua, 2020). An additional mechanism supposes that the activation of PKA inhibits protein phosphatases via protein phosphatase inhibitors, augmenting the activity of other kinases (Woolfrey & Dell'Acqua, 2015).

Perhaps the most well known and accepted role of cAMP is that of gating the conversion of early LTP to late LTP. The early stages of long term potentiation, namely 1-3 hours after the induction, rely mostly on modifying the activity of pre-existing proteins. In contrast, the late stages of potentiation can last for hours, days, and even more, and are accompanied by structural changes that depend on gene transcription and *de novo* protein synthesis. The cAMP-PKA

signaling pathway is considered the critical link in developing long lasting potentiation. Once activated by cAMP, the catalytic subunits of PKA translocate to the nucleus where they directly phosphorylate the transcription factor CREB, effectively initiating the transcription of CRE-associated genes. A large number of genes encoding proteins involved in plasticity-related processes are regulated by CREB, including *cfos, jun, BDNF, zif268* (Barco et al., 2002; Deisseroth et al., 1996).

The role of cAMP signaling pathway role in the expression of NMDA LTP at Schaffer collateral synapse have come from experiments using a LTP induction protocol without high frequency electrical stimulation of the pathway, but chemical wash-in of cAMP elevating drugs, such as forskolin. Through this protocol, named "chemical LTP", one can directly induce the late stages of LTP, as protein synthesis inhibitors do not block its induction (Bolshakov et al., 1997; Duffy & Nguyen, 2003). Some experimenters reported the need of adding cAMP phosphodiesterase inhibitors to the pharmacological cocktail in order to observe sustained potentiation induction (Otmakhov et al., 2004). While the necessity of synaptic activity and postsynaptic calcium entry is an accepted mechanism of LTP induction, it has been found that chemical LTP can occur both in the absence or presence of stimulation (Bolshakov et al., 1997; Duffy & Nguyen, 2003; Frey et al., 1993; Lu & Gean, 1999; Otmakhov et al., 2004). Interestingly, while using forskolin to potentiate the Schaffer collateral synapses unto CA1, measurements of miniature spontaneous presynaptic release events revealed an increase in their frequency, hinting at a presynaptic locus of expression (Carroll et al., 1998; Chavez-Noriega & Stevens, 1994; Sokolova et al., 2006). However, the presynaptic locus idea was later challenged and the frequency increase explained as due to the recruitment of new AMPA receptors in "silent synapses", which due to their lack of AMPA receptors when chemically unstimulated, would not elicit measurable postsynaptic potentials (Kerchner & Nicoll, 2008; Sokolova et al., 2006). While classical experiments have revealed multiple molecules involved in cAMP-dependent synaptic transmission enhancement, the methodologies used lack spatial and temporal resolution. Chemical and electrical stimulation do not represent physiological stimulation patterns that happen *in vivo*. Additionally, an all-chemical approach disregards important spatial information, such as cell type (not only principal excitatory neurons are affected, but also inhibitory neurons, as well as glial cells), synaptic compartment (one cannot easily target the drug to the pre or postsynaptic neuron only), or subcellular compartments (pharmacology cannot differentially elicit its effects within the same cell). Furthermore, one cannot target a single cell, all findings being

derived from studies of cell populations. But perhaps the most concerning aspect is related to the multitude of non-specific effects of pharmacological agents used. Without proper controls, interpretation of the results is difficult to correctly formulate.

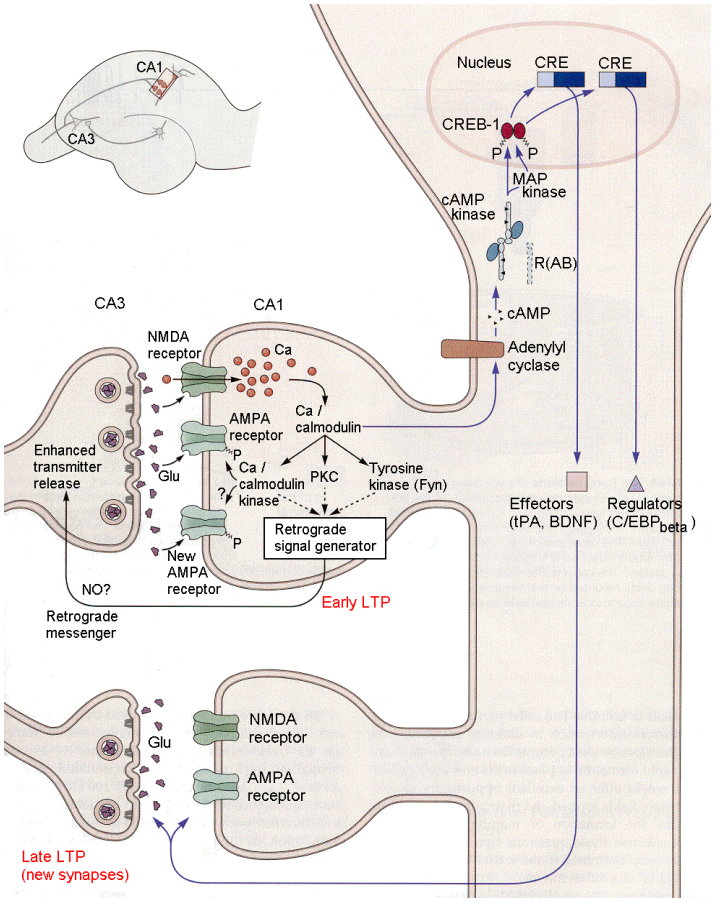

Figure 1.17 Simplified diagram of the main molecular pathways involved in NMDA-dependent LTP. Image from (Kandel, 2013).

1.2.4 Hippocampal neuromodulatory inputs that work via cAMP signaling

Properties of fast excitatory and inhibitory transmission can be altered by the release of neurotransmitters from long-range modulatory projections coming from extra-hippocampal sources. Activation of synaptic modulatory receptors on the presynaptic or postsynaptic side alters the way synaptic information is transmitted or processed. The hippocampus receives dense modulatory input from other brain regions, influencing a large range of functions, including cell

excitability, synaptic transmission, action potential firing, resting membrane potential, and synaptic input integration. All modulatory neurotransmitters act by binding to G protein-coupled receptors, triggering intracellular signaling cascades. Gs or Gi-coupled receptors will either lead to stimulation or inhibition of adenylyl cyclases, modulating intracellular cAMP levels. Some neurotransmitters whose receptors bind to Gs/Gi are acetylcholine, norepinephrine, dopamine, serotonin (Figure 1.18). Although the topic of my PhD work does not include extra hippocampal modulatory input stimulation, these inputs exist *in vivo* and affect synaptic transmission through cAMP signaling. In this subchapter I give a brief overview of four main modulatory inputs to the hippocampus that modulate neuronal activity in a cAMP-dependent manner.

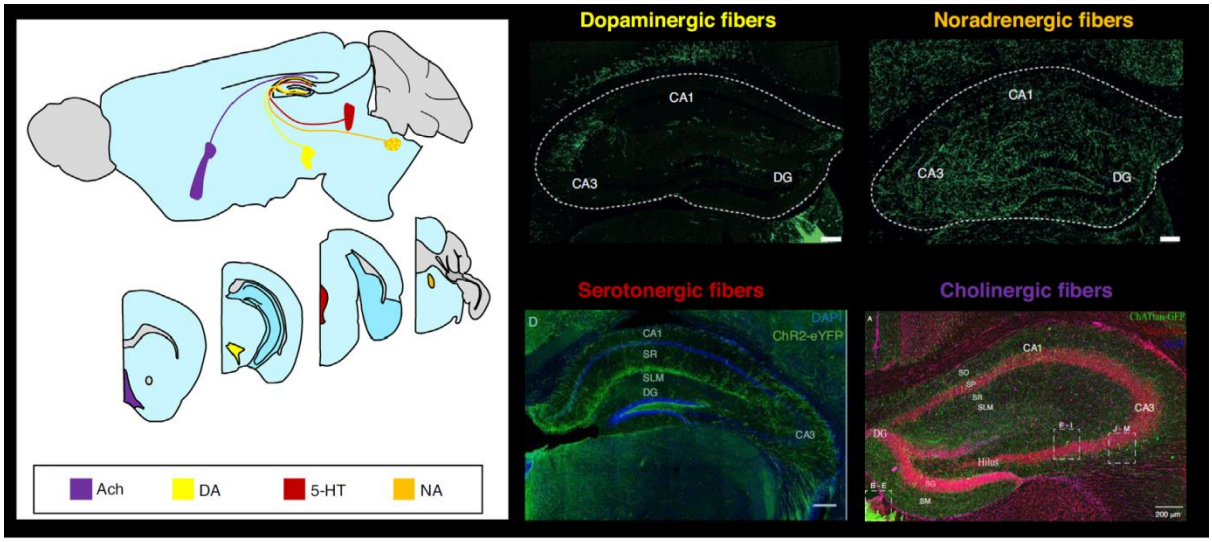

Figure 1.18 Neuromodulatory projections to the hippocampus. (Left) Location of nuclei containing the cell bodies that give rise to neuromodulator projections for Acetylcholine (Ach), Dopamine (DA), Serotonin (5-HT) and Noradrenaline (NA). Sagittal (top) and Coronal (bottom) sections. Data from Allen Brain Atlas for mouse brain. (Right) Images of neuromodulatory projection fibers within the hippocampus. Image from (Palacios-Filardo & Mellor, 2019).

Acetylcholine

Long thought to establish a diffuse, volumetric method of transmission (i.e. release from axon terminals into extracellular space rather than at synapses (Descarries et al., 1997; Takács et al., 2018), cholinergic fibers arise from the medial septum and diagonal band of Broca and release acetylcholine into the hippocampus, affecting multiple cells and cellular compartments. Acetylcholine (ACh) acts via nicotinic and muscarinic receptors, which are differentially expressed

in hippocampal principal cells and interneurons, as well as astrocytes (Dannenberg et al., 2017). While the nicotinic acetylcholine receptor is a non-selective, cationic ionotropic receptor (that enhances depolarization in neurons and release of D-serine in astrocytes, facilitating LTP induction (Kalappa et al., 2010; Papouin et al., 2017)), the muscarinic AChR is a metabotropic receptor, acting via G protein interaction.

From the five subtypes of muscarinic receptors, M1, M3 and M5 are coupled to Gq proteins, while M2 and M4 are coupled to Gi/o subtypes (Wess, 2003). Activation of M2 and M4 receptors leads to an inhibition of adenylyl cyclases and thus a reduction of intracellular cAMP production. In the hippocampus, 30-50% of all muscarinic receptors are M2 and M4 subtypes, with M2 being expressed only in interneurons (Levey et al., 1995). The Gi-coupled M4 subtype is preferentially expressed at glutamatergic terminals and it modulates presynaptic inhibition at Schaffer collaterals *in vitro* and *in vivo* (Dasari & Gulledge, 2011; Hasselmo & Giocomo, 2006; Shirey et al., 2008). Interestingly, muscarinic presynaptic inhibition affects only CA3 to CA1 synapses, not the synaptic connection between EC and CA1, suggesting that acetylcholine modulates a differential spread of activity within the hippocampus (Hasselmo & Giocomo, 2006).

Norepinephrine

Noradrenergic fibers arise mainly from Locus Coeruleus (LC), a small nucleus in the brainstem that gets activated by novelty or arousal stimuli. Noradrenergic fibers project almost ubiquitously throughout the brain, in both cortical and subcortical areas. Upon release, norepinephrine (NE) binds to the post- or pre-synaptically expressed noradrenergic receptors (α_1, α_2, β_1 and β_2) (AR). All four subtypes are expressed in the hippocampus and all couple to G proteins (Guo & Li, 2007). The α-adrenergic receptors signal via either Gq or Gi proteins, while β-adrenergic receptors couple to Gs-type of G proteins (Hussain et al., 2021; O'Dell et al., 2015). In the hippocampus, norepinephrine binding to β-ARs facilitates synaptic plasticity and memory consolidation (Izquierdo et al., 1998; Murchison et al., 2004; Qi et al., 2008). Furthermore, the activation of β-ARs by norepinephrine at excitatory synapses enhances LTP induction when using a single train of 100 Hz stimulation, theta burst stimulation or spike-time dependent plasticity induction protocols (Gelinas & Nguyen, 2005; Hansen, 2017; Makino et al., 2011; Nguyen & Connor, 2019; Nguyen & Gelinas, 2018; Qian et al., 2012). Thus, activation of β-ARs has the role of lowering the threshold for LTP of weak stimuli or patterns of activity.

The underlying molecular mechanisms of β-AR activation starts with cAMP production, which will phosphorylate a number of targets, including a suppressor of protein-phosphatase 1, thus facilitating kinase activity (Brown et al., 2000). Additionally, β-AR dependent PKA activation modulates NMDA receptor signaling, as their phosphorylation by PKA can increase the channel's open probability and permeability to Ca^{2+} (Murphy et al., 2014). Another mechanism suggests that β-AR signaling works by promoting AMPA receptor phosphorylation, as AMPA receptors have been found to form complexes with β_2-ARs, PKA and adenylyl cyclases (Joiner et al., 2010; Tenorio et al., 2010).

Dopamine

The hippocampus receives modulatory input from the brain stem also in the form of dopaminergic projections that arise from the ventral tegmental area and from *substantia nigra pars compacta* (Gasbarri et al., 1997; Scatton et al., 1980). While most hippocampal excitatory neurons express dopamine receptors, area CA1 receives the most dopaminergic projections. Pyramidal neurons in area CA1 express dopamine receptors more abundantly in *stratum lacunosum-moleculare* than in *stratum radiatum*, suggesting that these modulatory inputs are less important for Schaffer collateral-CA1 synapses but rather for entorhinal axons that synapse not only onto the dentate gyrus, but also onto CA1 neurons. Dopamine acts on metabotropic receptors that are positively or negatively coupled to adenylyl cyclases. Activation of receptors of the "D1-like" subtype (D1 and D5) have the net effect of stimulating adenylyl cyclases, while "D2-like" subtypes (D2, D3, D4) inhibit their activity. The distribution of dopamine receptor subtypes is heterogenous, with particular subtypes being present more often in specific hippocampal areas and dendritic compartments (e.g. D1/D5 receptors are more dense in CA1 than in other areas, but have different distributions in the basal and apical dendrites of CA1 neurons) (Edelmann & Lessmann, 2018).

The activation of dopamine receptors that upregulate intracellular cAMP has been linked with the induction of protein-synthesis dependent late stage of LTP in the hippocampus, more specifically in area CA1 (Lisman & Grace, 2005). Blocking dopamine receptors during strong tetanic stimulation blocks the consolidation of early LTP to late LTP (Frey et al., 1990; Huang et al., 1995; Matthies et al., 1997; but also Mockett et al., 2004), while activation of these receptors facilitate the conversion. Recent experiments using modern techniques have confirmed that

dopamine and activation of its receptors in the hippocampus promote memory storage during spatial learning (Espadas et al., 2021; McNamara et al., 2014). Furthermore, an optogenetic release of dopamine onto CA1 from the VTA results in opposing physiological effects that depend on the pattern/volume of dopamine being released (low levels depressing the Schaffer collateral-CA1 synapse, while high levels of release potentiating transmission) (Rosen et al., 2015). The effects of dopamine innervation of the hippocampus (particularly the CA1) are still not fully understood. Due to the lack of specific agonists and antagonists, the contributions of specific receptor subtypes could not be precisely determined until now. Furthermore, activation of dopamine receptors has been linked with non canonical, cAMP-independent signaling pathways (Beaulieu & Gainetdinov, 2011).

Serotonin

Another monoamine being released in the hippocampus from the brain stem is serotonin (5-HT), which originates from diffuse projections of the median raphe nucleus (Moore & Halaris, 1975). In the hippocampus, serotonergic axons are found predominantly in area CA3, with the lowest density in CA1. Serotonin elicits its effects on hippocampal cells by binding to serotonin receptors, that are either GPCRs (families $5\text{-HT}_{1, 2, 4\text{-}7}$) or ligand-gated ion channels (5-HT_3). Serotonin receptors couple to different G protein subtypes, with $5\text{-HT}_{1, 5}$ being coupled to Gi, thereby inhibiting adenylyl cyclases, and $5\text{-HT}_{4, 6, 7}$ to Gs, leading to an elevation of intracellular cAMP (Bockaert et al., 2006). The effects of 5-HT in the hippocampus are cell type and receptor subtype specific, as serotonin facilitates or attenuates LTP in CA1, is inhibitory at mossy fiber-CA3 synapses, while also activating interneurons (Corradetti et al., 1992; Otmakhova & Lisman, 2006; Staubli & Xu, 1995; Twarkowski et al., 2016; Varga et al., 2009; West et al., 2009).

1.3 Approaches to investigate cAMP signaling

1.3.1 Pharmacology

Concrete advances in drug development that are able to translate current knowledge about cAMP signaling into pharmacological agents have proven to be challenging. This is due to the complex nature of the cAMP signaling pathway, as intracellular cAMP concentration can be modulated directly and indirectly by a vast pool of molecules like ions (Ca^{2+}), neurotransmitters and modulators, G protein-coupled receptors, enzymes ($G_{\alpha s}/G_{\alpha i}$, AC, EPAC, PKA, PDE) (see subchapters 1.1.2 and 1.1.3). Pharmacological manipulation of cAMP signaling has focused on drugs that stimulate adenylyl cyclases to produce cAMP, inhibit its degradation by phosphodiesterase antagonists or that target its most studied effector, protein kinase A (Figure 1.19).

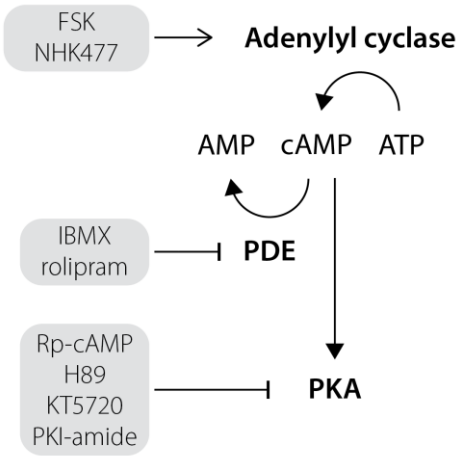

Figure 1.19 Most used pharmacological agents for perturbing cAMP signaling pathway.

Forskolin

The most widely used stimulator of endogenous adenylyl cyclases is the diterpene forskolin. It is extracted from the root of the plant *Coleus barbatus* (or *Coleus forskohlii*) and it has been used for centuries in Ayurvedic traditional medicine to treat a number of affections, including cardiovascular diseases, pain, asthma or weight gain (Alasbahi & Melzig, 2010a, 2010b).

Forskolin is an unselective activator of almost all adenylyl cyclase isoforms, except for AC9

and the soluble AC10 (sAC). The catalytically active site of any tmAC is created by the interaction between its cytosolic domains in the correct orientation. The binding of $G_{\alpha s}$ or forskolin to the interface between the two domains induces a catalytically active conformational change. The equivalent of the forskolin binding site in the case of sAC is a bicarbonate binding site, which is too small to accommodate forskolin, making sAC insensitive to forskolin (Alasbahi & Melzig, 2012; Dessauer et al., 2017; Halls & Cooper, 2017; Pierre et al., 2009; Pinto et al., 2008). The distinct feature of forskolin of directly activating adenylyl cyclases (in comparison to drugs that lead to intracellular cAMP elevation *via* indirect mechanisms like GPCR activation), as well as it being one of the few naturally-occurring AC stimulators, established forskolin as the most used pharmacologic agent in cyclic AMP signaling investigation.

Due to forskolin's low water solubility, derivatives with better aqueous solubility have been developed, such as NKH477 (Sengupta & Mehta, 2018). While this new water-soluble compound is more suitable for various *in vivo* treatments in comparison to DMSO-soluble forskolin, it cannot cross the blood-brain barrier and it appears to have different affinities to adenylyl cyclase subtypes than its predecessor (Alasbahi & Melzig, 2010b). NKH477 is found on the Japanese market as an approved drug for the treatment of acute heart failure and glaucoma.

Inhibitors of phosphodiesterase (PDEs)

Cyclic AMP is quickly degraded into adenosine monophosphate by phosphodiesterases, a hydrolysing process that tightly regulates the intracellular concentration of cAMP. Since phosphodiesterases directly control the amount of cAMP that is available intracellularly, agents that inhibit PDEs are the focus of drug development, as raising or lowering intracellular cAMP is interesting therapeutically. Due to the large number of PDE subtypes (and splicing variants), each with different affinities for cAMP and cGMP and different histological/cellular profiles, research in the development of PDE inhibitors has the potential of advancing current therapeutics and drug development. By blocking or activating specific PDE isoforms, one could be able to target specific cell types or to selectively control cAMP over cGMP or *vice versa*. In the brain, and particularly the hippocampus, almost all PDE isoforms are present, with the exception of PDE4C, PDE6(A-D) and PDE8A (Francis et al., 2011; Xu et al., 2011).

One of the most extensively studied and used PDE inhibitors is IBMX (3-isobutyl-1-methylxanthine), a non-specific inhibitor of PDEs with an IC_{50} ranging from 7 to 50

μM. From all PDE isoforms, only PDE8 and PDE9 are insensitive to IBMX. IBMX has the net effect of raising the intracellular concentration of cAMP and cGMP, indirectly leading to the activation of PKA and PKG. The most widely used PDE inhibitor in studies involving cAMP-dependent processes is rolipram, a selective cAMP-specific PDE4 inhibitor (Peng et al., 2020).

While PDEs represent an important target for pharmacological manipulation of cyclic AMP, considerations need to be taken regarding the disruption of spatio-temporal signaling patterns. Cyclic AMP is a molecule that exerts its effects in subcellular microdomains, thus local gradients are critical for its signaling. Disrupting its degradation with PDE inhibitors could lead to paradoxical effects where cAMP gradient-dependent processes are inhibited. Additionally, the accumulation of cyclic AMP intracellularly might trigger the activation of other, indirect signaling pathways that cross-talk with cAMP pathway (cGMP, Ca^{2+} or NF-κB pathways) (Yan et al., 2016).

Protein kinase A inhibitors

Protein kinase A (PKA) translates most of the signals from the extracellular space (in the form of intracellular cAMP elevation) into functional changes of intracellular processes, by catalysing the phosphorylation of a large number of proteins. Multiple types of synthetic PKA inhibitors have been developed, such as small-molecule chemical inhibitors of PKA or synthetic protein kinase inhibitor peptides.

The most used chemical inhibitors of PKA are Rp-cAMP compounds, H89 and KT5720. Rp-cAMP is a cAMP analogue that competitively binds to the regulatory unit of PKA, restraining further PKA activation. Due to the unwanted property of being hydrolyzed by PDEs, PDE-resistant variants have been developed, like Rp-8-Br-cAMP. However, due to the similarity to cAMP, Rp-cAMP compounds can bind to other downstream molecules such as cyclic nucleotide-gated channels or EPAC proteins (de Wit et al., 1984). The other two most used compounds used for PKA inhibition, H89 and KT5720, block PKA activity by targeting its catalytic subunits. The drugs act as competitive antagonists by binding in the ATP-binding cassette of the catalytic subunits of PKA. Both H89 and KT5720 have very high affinity for PKA, with a Ki of ~50 nM. However, they exhibit some non-specific binding to other protein kinases like PKG, PKB, ERK, as well as channels (β2-adrenergic receptors, Kv1.3 channels) (Davies et al., 2000; Limbutara et al., 2019; Murray, 2008).

Another strategy of inhibiting PKA activity involves the development of synthetic protein kinase inhibitor peptides. Protein kinase inhibitor (PKI) is an endogenous peptide that is present in

all types of tissue. It inhibits PKA activity by binding to PKA catalytic subunits in a manner similar to the PKA regulatory subunits, making them enzymatically inactive. Synthetic analogues of PKI have been developed and used in probing PKA's contribution to intracellular processes, such as PKI(6-22) amide (Dalton & Dewey, 2006; Liu et al., 2020). However, a recent kinase screening has shown that PKI compounds inhibit other kinases, such as CamKI and DAPKI, and even facilitate the activation of multiple PKC isoforms (Chen & Sabatini, 2021).

1.3.2 Transgenic approaches

In order to evaluate the role of cAMP synthesis in cellular processes, a large number of cAMP signaling studies in the late 1990s to mid-2000s used a transgenic approach by knocking out one or multiple isoforms of adenylyl cyclase. Studies using adenylyl cyclase-deficient animals have confirmed the necessity of calcium stimulation of adenylyl cyclases activity for long term plasticity. Type I adenylyl cyclases, which are calcium-activated, include the AC1, AC3 and AC8 isoforms.

In AC1 knockout animals, cerebellar LTP was completely blocked (Storm et al., 1998). Interestingly, in the hippocampus, knocking out AC1 only reduced tetanus-driven LTP (Villacres et al., 1998; Wu et al., 1995), the same being true for AC8 knock-out. However, when both AC1 and AC8 are knocked out, hippocampal LTP is abolished but can be restored by local injection with the adenylyl cyclase stimulator forskolin (Wang et al., 2003; Wieczorek et al., 2012; Wong et al., 1999). Moreover, transgenic mice that exhibited an overexpression of AC1 showed elevated LTP in comparison to wild-type animals, as well as increased memory performance for object recognition and slower rates of extinction for contextual memory (Wang et al., 2004; Zhang & Wang, 2013). These results suggest that the stimulation of Ca^{2+}-sensitive adenylyl cyclases isoforms present in the brain is required for late-phase LTP. Deficiency of AC1 and AC8 leads to memory defects that can only be restored by the chemical, non-physiological stimulation of other AC isoforms.

In more recent years, the role of AC3 in memory-related processes has been investigated, as AC3 is a Ca^{2+}-sensitive AC isoform that is expressed exclusively in the primary cilia of neurons. AC3-deficient mice show deficits in multiple hippocampal-dependent memory tasks, including

novel object recognition and contextual fear extinction, demonstrating the importance of differential, compartmentalised cAMP signals in distinct forms of memory (Wang et al., 2011).

1.3.3 Optogenetic strategies

The advent of optogenetics provided the scientific community with the great advantage of being able to selectively manipulate intracellular processes in individual cells with high spatio-temporal resolution. The available toolbox for signaling pathway manipulation is continuously expanding, with new tools adapted to precisely regulate the different steps in the signaling chain: light activation of membrane receptors (light-activated GPCRs), activation of transmembrane ACs (photo-activatable adenylyl cyclases), activation of cAMP-effector proteins (opto-PKA), and degradation of second messenger molecules (light-activated phosphodiesterases). In this subchapter, I will give a brief overview of the most established tools in each category as well as highlight the most promising new candidates. One major focus of this thesis work is the development and characterisation of new optogenetic tools, especially in the context of cyclic nucleotide manipulation.

Light-activated GPCRs

G protein-coupled receptors are activated by diverse extracellular stimuli and act through intracellular G proteins that control distinct intracellular signaling pathways, depending on the G protein's alpha subunit type: Gs and Gi control the activity of adenylyl cyclases, Gq activates PLC and G12 couples to guanine nucleotide exchange factor (GEF). In recent years there have been numerous attempts to engineer photo-activated GPCRs, from opto-chemically controlled GPCRs to chimeric proteins that combine an opsin's light switching mechanisms to an intracellular G protein binding domain (Abreu & Levitz, 2020; Kleinlogel, 2016; Spangler & Bruchas, 2017).

Photopharmacological approaches combine endogenous GPCRs with photo-activatable ligands that control their activity. The most used strategy includes caged ligands, where the ligand becomes biologically active and able to bind its receptor only after photolysis of the light-sensitive cage. To circumvent the obvious limitation of the irreversibility of uncaging, photo-switchable ligands have been developed where light is used as a switch between isomerisation states of the ligand that binds and unbinds endogenous GPCRs (Beharry & Woolley, 2011). Numerous such

compounds were developed, including agonists for opioid receptors (Schönberger & Trauner, 2014), muscarinic receptors (Agnetta et al., 2017) and cannabinoid receptors (Westphal et al., 2017).

Another approach of light stimulating G protein signaling pathways is through the use of naturally occurring opsins (photo-sensitive GPCRs) that are expressed in heterologous systems. An opsin identified in jellyfish and named JellyOp was expressed and characterised in mammalian cells where, upon light stimulation, intracellular cAMP concentration increased (Bailes et al., 2012). Similarly, the activation of chimeric GPCRs (opto-XRs) represents the most comparable signaling process to that of endogenous GPCRs. Opto-XRs are composed of a membrane-spanning, light-sensitive opsin with intracellular loops and the G protein binding domains of endogenous GPCRs. Using such strategy, different light-activated "analogues" of endogenous GPCR were engineered, including adrenergic receptors (Opto-α1AR and Opto-β2AR) (Airan et al., 2009; Kim et al., 2005; Siuda et al., 2015), adenosine receptors (Opto-A2R) (Li et al., 2015), opioid receptors (OMOR) (Siuda et al., 2015), metabotropic glutamate receptors (Opto-mGluR6) (van Wyk et al., 2015) and serotonin receptors (Oh et al., 2010; Spoida et al., 2014).

Some limitations to the use of chimeric optoXRs remain, such as the lack of GPCR-specific extracellular domains. These residues contribute to wild-type GPCR function as they enable the association with other receptors to form oligomers or they facilitate specific ligand-receptor interactions (Tichy et al., 2019).

Photo-activatable adenylyl cyclases

BLUF domain-based cyclases

The first naturally-occurring photo-activated cyclase (PAC) identified was EuPAC (Iseki et al., 2002; Ntefidou et al., 2003), a BLUF-based cyclase used by the flagellate *Euglena gracilis* as a sensor for phototaxis. Structurally, EuPAC is a tetramer with two PACα and two PACβ subunits, each subunit comprising two BLUF domains and two cyclase domains (Figure 1.20). The light-sensing domain, namely BLUF (Blue Light sensor Using FAD), is found in a family of photoreceptors that sense blue light and that use flavin as a light-absorbing chromophore. The energy carried by photons in the 400-520 nm range is sufficient to cause structural changes within the photoreceptor, triggering conformational changes in the cyclase domain and thus

rendering the whole complex enzymatically active (Iseki et al., 2002; Ito et al., 2005). Upon blue light stimulation, EuPAC increases its activity 80-fold. It has been successfully used to investigate cAMP-dependent processes in *Aplysia* neurons, *Xenopus* oocytes, *Drosophila* flies and mammalian cultured neurons (Nagahama et al., 2007; Schröder-Lang et al., 2007; Zhou et al., 2016). However, due to its large size (400 kDa, tetramer) and relatively high activity in the dark, EuPAC has not been extensively used.

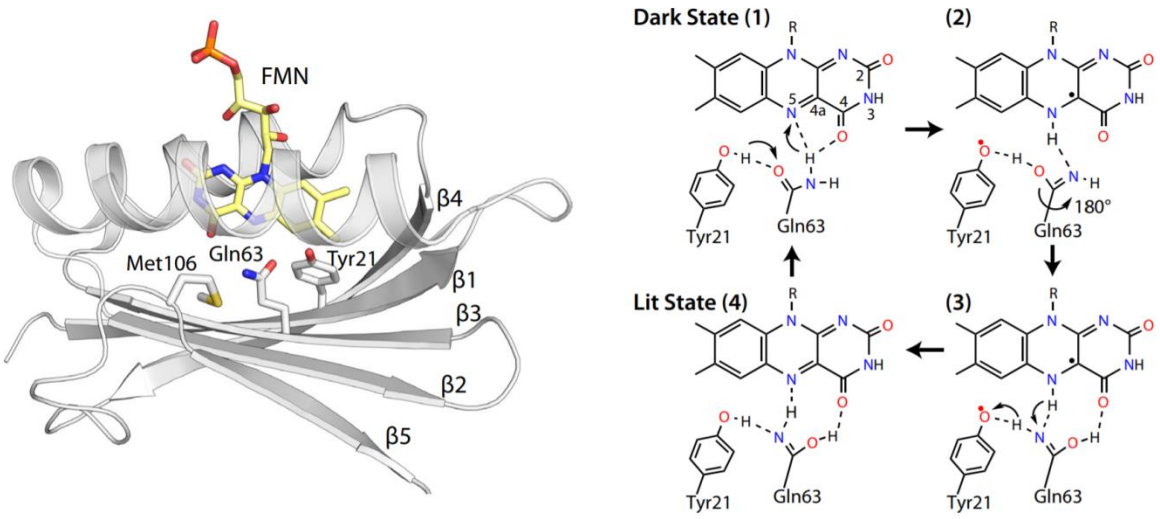

Figure 1.20 Structure and photocycle of the BLUF domain. Image from (Lindner, 2019).

Currently, the most widely used opto-cyclase in heterologous systems is bPAC, a photo-activated cyclase that was identified in the sulfur bacterium *Beggiatoa* sp. (Ryu et al., 2010; Stierl et al., 2011). What makes bPAC a more attractive tool for cAMP manipulation in comparison to EuPAC, are its smaller size (300 amino acids, EuPAC 1019 amino acids), its low cyclase activity in the dark, and its higher light/dark activity ratio (1600 bPAC, 180 EuPAC). The discovery of bPAC triggered the subsequent identification of similar light-dependent cyclases in other bacteria (Blain-Hartung et al., 2018; Fritz-Laylin et al., 2010; Ohki et al., 2016; Penzkofer et al., 2014; Penzkofer et al., 2015; Raffelberg et al., 2013; Tanwar et al., 2018; Yasukawa et al., 2013) (Figure 1.21). Furthermore, subcellular targeted variants of bPAC have been developed, including plasma membrane and endosomal targeted (Tsvetanova & von Zastrow, 2014) and synaptoPAC, a presynaptically targeted variant (Oldani et al., 2021).

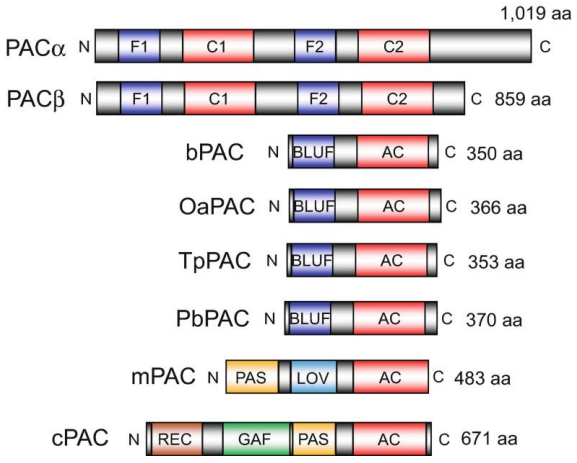

Figure 1.21 Domain organization of photoactivatable adenylyl cyclases from different organisms. Image from (Iseki & Park, 2021).

Rhodopsin-based cyclases

The recently discovered enzyme rhodopsins are a unique family of microbial rhodopsins, composed of a membrane-spanning rhodopsin domain which is linked to a cytoplasmic enzyme domain. In comparison to other rhodopsins, enzyme rhodopsins consist of an 8-transmembrane domain that harbours an *all-trans* retinal molecule as its chromophore (Figure 1.22).

The first rhodopsin cyclase discovered was BeRhGC, a light-activated guanylyl cyclase from the zoospore of the aquatic fungus *Blastocladiella emersonii* (Avelar et al., 2014b). Presenting a high light/dark activity ratio (5000), BeRhGC (also named Cyclop) has been tested in *Xenopus* oocytes, hippocampal neurons, and used for behavioural tests in *C. elegans*, where stimulation of the cyclase in muscle cells resulted in contractions while expression and activation in BAG neurons slowed down locomotion (Gao et al., 2015; Scheib et al., 2015). The photocycle of BeRhGC has a dark state, with a 525 nm maximum absorption, that upon photoexcitation forms an intermediate state which is thought to represent the catalytically active form of the protein (Kato, 2021). More recently, several mutants of BeRhGC with different properties were developed, such as blue and red-shifted variants, as well as a double mutant that changes the enzyme to an adenylyl cyclase (Trieu et al., 2017). Unfortunately, the modifications brought to the substrate-binding domain also increased the catalytic activity of the enzyme in the dark.

The ideal optogenetic tool for cAMP manipulation in mammalian systems should be able to meet the following requirements: fast onset of cyclase activity, small molecular size, insignificant activity in the absence of light, high light sensitivity, high light/dark ratio, narrow

activation spectra, no toxicity when expressed in mammalian cells. Until now, there is no photo-activated cyclase (natural or engineered) that can meet all of these criteria.

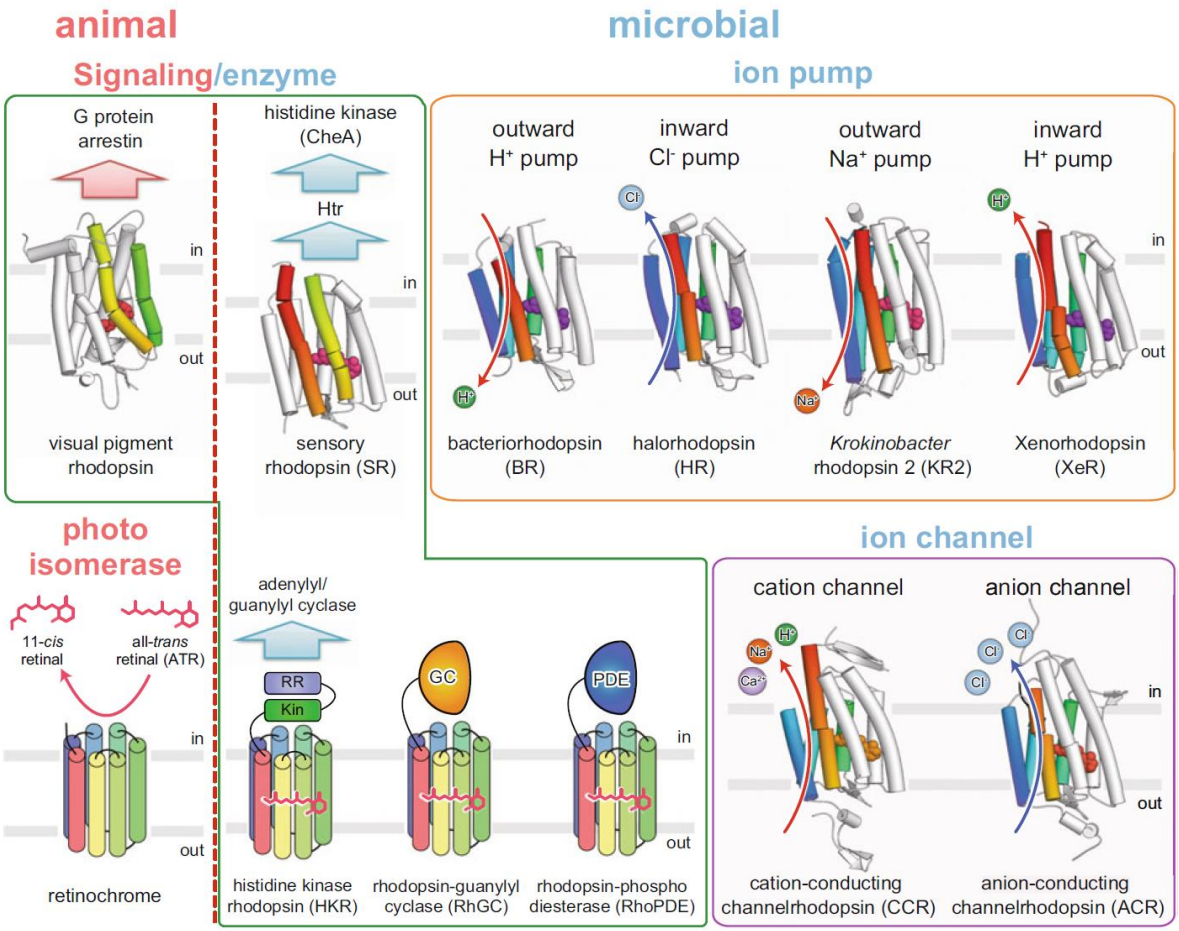

Figure 1.22 Classification of rhodopsin family proteins. Image from (Kato, 2021).

Light-activated phosphodiesterases (LAPD)

Phosphodiesterases control the action of intracellular cyclic nucleosides by mediating their breakdown to nucleoside monophosphate. All phosphodiesterase isoforms present a regulatory domain that binds the substrate and a catalytic domain that becomes enzymatically active upon activation of the regulatory domain. Engineering artificial light-activated phosphodiesterases takes advantage of this working mechanism by replacing the chemosensor of the regulatory domain with a structurally similar photosensor. The first LAPD to be developed

used a bacterial phytochrome to replace the PDE's photosensor, as they have very similar structural architecture (Gasser et al., 2014). Bacterial phytochromes are photo-receptors that use biliverdin as chromophore and that are regulated by red and far-red light. By shortening the linker between the two domains, a catalytically active, light-sensitive phosphodiesterase was generated. Based on this approach, a suite of constructs with better reversibility of activation and stronger hydrolysis activity was developed (Stabel et al., 2019).

The chimeric LAPD strategy gives a number of advantages, such as reversible light switching (allowing for a better temporal control) and the use of long wavelength light which penetrates tissue better and is compatible with other optogenetic tools. Furthermore, there is no need to supplement the exogenous factors, as biliverdin is available endogenously (Tian et al., 2020).

OptoPKA

Protein kinase A is one of the most important effectors downstream from cAMP as it controls a large variety of cellular processes. The possibility of specifically activating PKA (and not other cAMP effector molecules) with high spatio-temporal resolution could enable more complex experimental designs and thus, a more profound understanding of its intracellular actions. The first (and only) attempt to engineer a photo-activated protein kinase A came from the lab of David Lawrence with the generation of optoPKA (O'Banion et al., 2018).

The inherent enzymatic activity of light-activated proteins in the absence of light constitutes a challenge in their engineering. To circumvent this problem, optoPKA is designed as a cAMP-independent enzyme, by introducing mutations in the catalytic subunit which eliminate the repressive action of the regulatory subunits (normally, upon cAMP binding the regulatory subunits activate the catalytic subunits). Additionally, point mutations were introduced in key residues of the catalytic subunits that reduced the enzymatic activity to 1% of the wild-type enzyme. In order to establish light-control of the kinase's activity, optoPKA was coupled with the Cry2/Cib photo-dimerisation protein pair, where the Cib component was targeted to intracellular locations of interest, such as the outer mitochondrial membrane or the plasma membrane. What resulted was a two-component construct, with Cib targeted to a specific subcellular compartment and Cry2-PKA (with low catalytic activity) cytoplasmically diffuse. Light stimulation promoted the photodimerization of the two components, raising the local concentration of low catalytic activity

optoPKA and increasing the local phosphorylation activity. When coexpressed in the same compartment with a PKA reporter, 1 minute of blue-light illumination of optoPKA was sufficient to trigger phosphorylation of the reporter, an effect which was blocked by pretreatment with the PKA activity inhibitor H89.

While the generated optoPKA has clear limitations in terms of light dose needed and temporal resolution of its effects, this type of construct design could be used for the generation of other light-activatable enzymes, as the point mutations used in reducing enzymatic activity are equivalent in many other kinases.

2. Aim of the thesis and statement of contributions

Aim 1 - Development of photoactivated tools

The first aim of my project is the development and characterisation of new optogenetic tools in the context of cyclic nucleotide signaling. In comparison to other types of optogenetic tools, such as optical actuators or Ca^{2+} sensors, the toolbox available to manipulate intracellular cyclic nucleotides is not as diverse. Throughout my work, I sought to expand the existing palette of light-activated cyclases and to validate their functionality by characterising the tools in hippocampal neurons. To achieve this aim, I worked on three separate projects, from which a number of optogenetic tools were developed, including CaRhGC and CaRhAC (rhodopsin-based light-activated guanylyl and adenylyl cyclases), KPAC (the first functional light-activated potassium channel) and PACmn (membrane-targeted variant of the photo-activated adenylyl cyclase bPAC with no dark activity).

Project 1 - Development and characterisation of new light-activated guanylyl and adenylyl cyclases

Published in 2018 in *Nature Communications*, I am a co-author. I designed, conducted and analysed all of the experiments in hippocampal slice cultures. I also participated in writing of the manuscript, as well as creation/design of the figures representing the data I collected and analysed. My work is explicitly displayed in Figures: 2, 6, S3, S9, S10, S11, as well as in Table S3.

- Scheib U, Broser M, Constantin OM, Yang S, Gao S, Mukherjee S, Stehfest K, Nagel G, Gee CE, Hegemann P. Rhodopsin-cyclases for photocontrol of cGMP/cAMP and 2.3 Å structure of the adenylyl cyclase domain. *Nature Communications* 9(1): 2046 (2018) DOI 0.1038/s41467-018- 04428-w

Project 2 - Improved optogenetic cAMP control with *Beggiatoa*-derived light activated cyclases

Published in 2021 in *BMC Biology*, I am a shared first author. I designed, conducted and analysed

all of the experiments in hippocampal slice cultures. I also participated in writing of the manuscript, as well as creation/design of all the figures. My work is explicitly displayed in Figures: 1, 4-6 and S1.

- Yang S[#], **Constantin OM[#]**, Sachidanandan D[#], Hofmann H, Kunz TC, Kozjak-Pavlovic V, Oertner TG, Nagel G, Kittel RJ, Gee CE, Gao S. PACmn for improved optogenetic control of intracellular cAMP. *BMC Biology* 19:227 (2021). DOI 10.1186/s12915-021-01151-9; [#] equal contribution

Project 3 - Cyclic AMP-derived silencing optogenetic tools

Part 1 published in 2018 in *Frontiers in Neuroscience*. I am a co-author on this publication. I designed, conducted and analysed all of the experiments in hippocampal slice cultures. I also participated in writing of the manuscript, as well as creation/design of the figures representing the data I collected and analysed. My work is explicitly displayed in Figures: 2, 4 and S1.

- Beck S, Yu-Strzelczyk J, Pauls D, **Constantin OM**, Gee CE, Ehmann N, Kittel RJ, Nagel G and Gao S. Synthetic Light-Activated Ion Channels for Optogenetic Activation and Inhibition. *Frontiers in Neuroscience* 12:643 (2018). DOI 10.3389/fnins.2018.00643

Part 2 is unpublished but a manuscript is in the works. I will be the shared first author on this publication. I designed, conducted and analysed all of the experiments in hippocampal slice cultures. I created and designed the figures and wrote the manuscript together with co-authors. In the following Results chapter I will present the unpublished data regarding the improved KPAC construct.

Aim 2 - Assessment of cAMP modulation of hippocampal synaptic transmission

Starting with its discovery more than half a century ago, cAMP has emerged as a critically important molecule in an impressive number of cellular processes. Cyclic AMP signaling is crucial in all systems but in the brain (and particularly in the hippocampus) it contributes to all phases of

long-term potentiation. The aim of this project was to assess the role of cAMP signaling in synaptic transmission in the hippocampus through the use of photo-activated cyclases that allow more specific spatial and temporal manipulation of cAMP.

- This work is unpublished but a manuscript is in the works. I will be the first author on this publication. I helped conceptualise and design the experiments, conducted and analysed all of the hippocampal culture experiments in this publication. The *in vivo* injections and acute slice recordings were not performed by me but all other aspects of those experiments (design, analysis and interpretation) were done by me. I created and designed the figures and wrote the manuscript together with co-authors.

3. Materials and Methods

3.1 Materials

3.1.1 Media

Slicing solution

Slicing solution: 110 mM choline chloride, 25 mM $NaHCO_3$, 25 mM D-Glucose, 11.6 mM sodium-L-ascorbate, 7 mM $MgSO_4$, 1.25 mM NaH_2PO_4, 2.5 mM KCl, and 0.5 mM $CaCl_2$. pH 7.4, 320 mOsm/kg, saturated with 95% O_2 / 5% CO_2.

Slice culture medium

Slice culture medium: 79% MEM, 20% heat-inactivated horse serum, 13 mM D-glucose, 109 mM NaCl, 0.8 mM $MgSO_4$, 1.8 mM $CaCl_2$, 1 mM L-glutamine, 0.006 mM ascorbic acid, 0.01 mg/ml insulin. pH 7.28, 320 mOsm/kg.

Extracellular recording solutions

ACSF 4/4 (carbogenated): 119 mM NaCl, 26.2 mM $NaHCO_3$, 11 mM D-glucose, 2.5 mM KCl, 1 mM NaH_2PO_4, 4 mM $MgCl_2$, 4 mM $CaCl_2$. pH 7.4, 310 mOsm/kg, saturated with 95% O_2 / 5% CO_2.
ACSF 1/2.4 (carbogenated): 124 mM NaCl, 26.2 mM $NaHCO_3$, 11 mM D-glucose, 4 mM KCl, 1 mM NaH_2PO_4, 1 mM $MgSO_4$, 2.4 mM $CaCl_2$. pH 7.4, 310 mOsm/kg, saturated with 95% O_2 / 5% CO_2.
ACSF HEPES 1/2 : 145 mM NaCl, 10 mM HEPES, 12.5 mM D-glucose, 2.5 mM KCl, 1.25 mM NaH_2PO_4, 1 mM $MgCl_2$, 2 mM $CaCl_2$. pH 7.4, 310 mOsm/kg.

Intracellular recording solution

K^+-gluconate solution: 135 mM K-gluconate, 10 mM HEPES, 4 mM $MgCl_2$, 4 mM Na_2-ATP, 0.4 mM Na

GTP, 10 mM Na_2-phosphocreatine, 3 mM ascorbate. pH 7.2, 290-300 mOsm/kg.

3.1.2 Vectors

Plasmids

Hippocampal slice cultures were transfected using the following plasmids:

1. Cyclases:

BeRhGC: pAAV-syn-BeRhGC-2A-tDimer, Addgene plasmid #66779, internal plasmid #79

CaRhGC: pAAV-syn-CaRhGC-2A-tDimer, Addgene plasmid #101720, internal plasmid #162

YFP-CaRhGC: pAAV-syn-YFP-CaRhGC, internal plasmid #215

YFP-CaRhAC: pAAV-syn-YFP-CaRhAC, Addgene plasmid #101721, internal plasmid #163

KPAC: pAAV-syn-SthK(TV418_(T378V))_GolgiEx_Venus_bPAC_myc_EREx, internal plasmid E18-128

bPAC: pCI-syn-bPAC-myc, Addgene plasmid #28134, internal plasmid #DU5

PACmn: pAAV-syn-2xLyn-ERex-Venus-bPAC(F198Y), Addgene plasmid #165491, internal plasmid #205

PACmn_dV: pAAV-Syn-2xLyn-ERex-Venus(Y145W)-bPAC(F198Y), Addgene plasmid #165492, internal plasmid #288

2. Fluorescent proteins:

mTSapphire: pCI-syn-mTSapphire, internal plasmid number #26

mKate2: pCI-syn-mKate2, internal plasmid number #57

3. Cyclic nucleotide gated channels:

cGMP-sensitive CNGA2 channel: pCI-syn-CNGA2, internal plasmid #82

cAMP-sensitive CNGA2 channel: pCI-syn-CNGA2(C460W/E583M), internal plasmid #DU14

4. Sensors:

BoosterPKA: pCAGGS-4493NES, Addgene #138373, internal plasmid number AD79

Adeno-associated viruses (AAVs)

Adeno-associated viruses were prepared at the UKE vector facility. The following virus was used for transfection of hippocampal neurons either *in vivo* or in slice cultures: rAAV2/9-

CaMKII-PACmn_dV : PACmn under the control or CaMKII promoter with an additional a point mutation (Y145W) to make the fluorescent protein Venus non-fluorescent (Ganesan et al., 2006), thus making the tool compatible with orange/red imaging tools.

3.2 Methods

3.2.1 Hippocampal slices

Rat organotypic slice cultures

Organotypic hippocampal slice cultures were prepared from female or male Wistar rats at postnatal day 5-7 (Unilever Wistar HsdCpd:Wu, Envigo) and cultured in the absence of antibiotics as previously described (Gee et al., 2017).

Mouse acute slices

Adult (3.5-5 months old) C57BL/6J mice were housed and bred at the University Medical Center Hamburg-Eppendorf under a light/dark cycle of 12/12 h. Previously injected and non-injected mice were anesthetized with 80% CO2 / 20% O2 and decapitated. Their brains were quickly removed and each hemisphere was glued to the support of a Compresstome which was then filled with 42°C agarose. After cooling, coronal slices (350 µm) were cut in ice-cold slicing solution and excess agarose was removed. Slices were then left to recover at 33 °C for 15 min and then 45 min in 30°C in ACSF 1/2.4 (carbogenated).

3.2.2 Transfection

Single cell electroporation

Organotypic slice cultures (6-3 days *in vitro*) were transfected by single-cell electroporation or viral-vector transduction (Wiegert et al., 2017a, 2017b). Total time of expression of the constructs varied between experiments (5-14 days).

For characterisation of optogenetic tools (rhodopsin-based cyclases, PACs and KPACs),

neurons in area CA3 were co-electroporated with DNA encoding the optogenetic tool (10 ng/µl for bPAC-derived tools; concentrations used for rhodopsin-based tools varied and are specified in the figure legends) together with DNA encoding the far-red fluorescent protein mKate2 (20 ng/µl) (for bPAC-derived tools) or the green fluorescent protein mtSapphire (5 ng/µl) (for rhodopsin-based tools). Where specified, neurons were co-electroporated with the cGMP-sensitive CNGA2 channel ($K_{1/2}^{cAMP}$ = 36 µM, $K_{1/2}^{cGMP}$ = 1.3 µM) or the cAMP-sensitive CNGA2 channel (C460W/E583M) ($K_{1/2}^{cAMP}$ = 0.89 µM, $K_{1/2}^{cGMP}$ = 6.2 µM) (Rich et al., 2001). For FRET imaging experiments CA3 neurons were electroporated with DNA encoding the PKA FRET sensor Booster-PKA (25 ng/µl) alone or with DNA encoding a cyclase (25 ng/µl) (Watabe et al., 2020). For miniature EPSC and evoked EPSP recordings, as well as cFos induction experiments, CA1 neurons were co-electroporated with plasmids encoding either PACmn or bPAC (10 ng/µl) and mKate2 (20 ng/µl). Neurons were only electroporated with DNA encoding mKate2 for the control conditions of the cFos experiments.

Virus injection (slices/*in vivo*)

Viral transduction of rat hippocampal slices was done with a viral vector containing PACmn_dV under the control of CaMKII promoter (rAAV2/9-CaMKII-PACmn_dV). For expression in all regions of the hippocampus 1 µl drop of virus was carefully placed on top of the slice. For local expression, areas CA1 or CA3 were injected using a backfilled glass pipette coupled to a picospritzer. Low pressure puffs of viral vector were delivered into the area of interest.

In vivo AAV injections were performed using a stereotactic drill and injection robot. Mice were stereotactically fixed and injected under anesthesia (1.5% isoflurane in O_2). After the skin and connective tissue were removed, craniotomies were performed using an automated drill on the desired coordinates (1 per hemisphere for CA1 or CA3 conditions and 2 per hemisphere for PACmn everywhere condition). Using a glass pipette attached to a 5 ml Hamilton syringe, rAAV2/9-CaMKII-PACmn_dV (1x10^12 vg/ml) was injected bilaterally with a volume of 500-1000 nl per side. After the injections, the bone surface was cleaned with saline solution and the skin stitched.

3.2.3 Electrophysiology and optogenetic stimulation

Hippocampal culture electrophysiology setup

Whole-cell patch-clamp recordings were performed using an Axopatch 200B amplifier (Molecular Devices). National Instruments A/D boards and Ephus software running in Matlab,

were used to record and control the experiment (Suter, 2010). The microscope (Olympus BX61WI) was fitted with an LED (Mightex Systems), coupled through the camera port using a multimode fiber (1.0 mm) and collimator (Thorlabs). LED light used for photo-stimulation reached the slice through a 40 x water immersion objective (Plan-Apochromat, 40x 1.0 numerical aperture, Zeiss). The light intensity in the specimen plane was measured with a power meter fitted with a silicon detector (Newport 1936R, 818-ST2) and then divided by the illuminated field of the objective (0.244 mm^2). Recording temperature of all experiments was 30 ± 1 °C. The liquid junction potential was measured and compensated. Patch electrodes were made from thick-walled borosilicate glass and had resistances of 3-5 MΩ when filled. Series resistance during the recordings was less than 15 MΩ and was not compensated during voltage-clamp recordings. Slices were continuously perfused with extracellular solution while in the recording chamber.

Electrophysiological characterisation of optogenetic tools

Expressing CA3 neurons were whole-cell patch-clamped at -70 mV and light of different intensities, durations and wavelengths was applied. A mix of picrotoxin (100 µM), NBQX (10 µM) and CPPene (10 µM) (Tocris) was added to the extracellular solution (ACSF 4/4, carbogenated) to block fast synaptic responses. Where indicated, forskolin (FSK; 100 µM) and 3-isobutyl-1-methylxanthine (IBMX; 75 µM) (HelloBio) were added from concentrated stock solutions. Analysis of light evoked currents was performed using custom Matlab scripts.

Miniature EPSC recordings

Miniature EPSCs were recorded in postsynaptic CA1 neurons bathed in ACSF HEPES 1/2 (1 mM Mg^{2+} and 2 mM Ca^{2+}). A mix of bicuculline (20 µM, Sigma), CPPene (1 µM, Tocris) and TTX (1 µM, HelloBio) was added to the extracellular solution to block NMDA receptors, GABAA receptors, as well as action potential firing. Only one cell was recorded per slice. Expressing CA1 neurons were whole-cell patch-clamped at -70 mV. After 5 minutes of recording baseline events, either light (470 nm LED, 1 mW mm^{-2}, for transfected conditions) or forskolin (50 µM, for non-transfected condition) was applied/washed in for 5 minutes. Miniature events were recorded during the treatment, and 5-10 minutes after. Analysis of mEPSCs was performed using Clampfit's Threshold Event Detection after being high-pass filtered at 1 Hz. The event detection threshold was set at

around 5-8 pA.

Evoked EPSC recordings

Evoked EPSCs were recorded in carbogenated ACSF 1/2.4 (1 mM Mg^{2+} and 2.4 mM Ca^{2+}) and in the presence of D-Serine (30 µM, Tocris). A cut was made between areas CA3 and CA1 and the slice was left to rest in the bath for around 30-60 minutes before the start of the recording. A stimulation electrode (15 MΩ glass pipette filled with NaCl solution) was placed in *stratum radiatum* in CA1 and used to stimulate presynaptic axons once every 20 seconds (0.2 ms pulse length). Transfected or non-transfected CA1 cells were whole-cell patch-clamped at -70 mV. Evoked excitatory postsynaptic currents were measured as the peak inward currents 3-7 ms after stimulation. Maximum 15 minutes after establishing a stable baseline, either light (470 nm LED, 1 mW mm^{-2}, for transfected conditions) or forskolin (50 µM, for non-transfected condition) was applied/washed in for a duration of 10 minutes. Evoked EPSCs were recorded during the treatment, and up to 1 hour after. Analysis of evoked EPSCs was performed using custom Matlab scripts. The slope of the currents was calculated from 40 to 60% of the response amplitude.

Acute slice electrophysiology

Up to four acute slices were placed in the 4-chamber Synchroslice (Lohmann Research Equipment) recording chambers where they were submerged and perfused with carbogenated ACSF 1/2.4 (1 mM Mg^{2+} and 2.4 mM Ca^{2+}) at 30 °C. Two concentric stimulation electrodes were placed in CA1's *stratum radiatum*, while a bipolar recording electrode was placed in cell body layer, close to *stratum radiatum*. The position of the electrodes was adjusted to evoke maximum field excitatory postsynaptic potentials (fEPSPs). An input-output curve was generated and the stimulus intensity was adjusted to achieve 30% of maximum amplitude. Every 30 seconds a 200 µs stimulus was delivered through each stimulation electrode (with a 1 second delay between electrodes). For a selection of experiments, two 200 µs pulses were delivered through each electrode at 40 ms interval. At least 30 minutes after establishing a stable baseline, either light (470 nm, ~0.2 mW mm^{-2}, for PACmn injected conditions) or a cocktail of forskolin (50 µM, HelloBio) and IBMX (75 µM, HelloBio) (for wild-type condition) was applied/washed in for a duration of 10 minutes. Evoked fEPSPs were recorded during the treatment, and up to 2 hours after. Analysis of recorded potentials was performed using proprietary SynchroSlice software. The slope of the

currents was calculated from 30 to 70% of the response amplitude. Recordings were excluded from further analysis if the baseline was unstable.

3.2.4 PKA activity measurements FRET imaging

Five to seven days after electroporation, neurons expressing the PKA activity sensor Booster-PKA (alone or together with bPAC or PACmn) were imaged using a confocal laser scanning microscope (Olympus FLUOVIEW FV1000) at 32 °C while bathed with HEPES-buffered ACSF 1/2. A 559 nm laser line was used for excitation and donor/acceptor channels were set at 560-600 nm and 640-740 nm. All acquisition parameters were kept the same in all conditions and throughout all imaging sessions. Multiple Z-planes were acquired (step size 0.5 µm) every minute. After 5 minutes of baseline, the whole field of view was scanned for 2 seconds with the 488 nm laser line to activate the expressing cyclases or to measure the change in FRET generated by blue light illumination. The activation with the 488 nm laser started 3 seconds before the 559 nm sensor signal acquisition. Alternatively, forskolin (50 µM) was washed in to activate endogenous membrane bound adenylyl cyclases. One Z frame common to all time points was chosen for the analysis. Image analysis was done using ImageJ. After background removal, a translational alignment was applied using the StackReg plugin (Thevenaz et al., 1998) in order to align the time series in X and Y dimensions. Appropriate regions of interest were selected (soma or dendrites with spines) and the mean intensity of donor and acceptor channels were measured. Experiments in Figure 4.11A were done at a different Olympus FLUOVIEW FV1000 microscope at room temperature. A 559-nm laser line was used for excitation, and donor/acceptor channels were set at 560–600 nm and 640–740 nm. Multiple Z planes were acquired (step size 0.5 µm), and a maximum projection was used for analysis. After background removal, regions of interest were selected (somata) and the mean intensity of donor and acceptor channels were measured. For both experimental cases, the ratio reported was calculated from the individual donor and acceptor channel measurements. The ratio images were generated using the RatioPlus plugin.

3.2.5 cFos stimulation experiments

Hippocampal slice cultures with CA1 neurons expressing mKate2 and bPAC or PACmn-expressing neurons were stimulated with light in the incubator, through a LED-stimulation tower.

bPAC/PACmn was expressed either in CA1 with single cell electroporation (co-electroporated with mKate2) or by viral transfection (for PACmn; injected locally in CA1/CA3 or a virus drop being used to transfect all the regions). The 470 nm light from a high-power LED was collimated and controlled from outside the incubator. The light was shined for 10 minutes at 1 mW mm^{-2} (measured with a power meter fitted with a silicon detector Newport 1936R, 818-ST2). All slices were kept in the same stimulation incubator at the same time, the ones not being stimulated being protected from the light. If slices were chemically stimulated, a volume of 10 µl of slice culture feeding medium was dropped on the slice. The following chemicals were dissolved in the 10 µl treatment volume: forskolin (50 µM, HelloBio), 1,9-dideoxyforskolin (50 µM, Merck), NKH477 (25 µM, Sigma), DMSO (0.02%). The concentration specified is the final concentration in the 10 µl drop. In order to attempt blocking light or forskolin-driven cFos expression, slices were treated overnight with various blockers mixed into the culture medium (700 µl/slice). The treatment started 12 hours before light or acute chemical stimulation. The following chemicals were used: NBQX (10 µM, HelloBio), CPPene (1 µM, Tocris), Picrotoxin (100 µM, Tocris), TTX (1 µM, HelloBio), KT5720 (1 µM, HelloBio), ESI09 (30 µM, Tocris), U0126 (20 µM, HelloBio), ZD7288 (30 µM, HelloBio). The following combinations of chemicals were used: NBQX + CPPene + Picrotoxin; TTX; KT5720 + ESI09 + U0126; KT5720 + ESI09; U0126; ZD7288. All slices were kept in the incubator for 1 hour after the treatment before being fixed in PFA.

3.2.6 Immunohistochemistry and confocal imaging

Slices (acute or cultured) were fixed in 4% PFA in phosphate-buffered saline (PBS) for 30 minutes then washed three times with PBS. After incubation for two hours at room temperature in blocking buffer (0.3% TritonX, 5% goat serum in PBS), slices were placed in primary antibody solution overnight at 4 °C (0.3% TritonX, 5% goat serum, 1% BSA in PBS). After three 10-minute washes with PBS, slices were incubated for two hours at room temperature with secondary antibody solution (0.3% TritonX, 5% goat serum, 1% Bovine Serum Albumin in PBS). Prior to mounting, the slices were washed three times with PBS. The following primary antibodies were used: Rabbit Anti c-Fos 1:500 (Santa Cruz Inc. sc-52); Chicken Anti GFP 1:1000 (Invitrogen A10262, Lot 1972783). The following secondary antibodies were used: Anti-rabbit goat Alexa Fluor647 1:500 (Invitrogen A27040); Anti-chicken Alexa Fluor488 1:1000 (Life technologies; A11039).

Images of anti-cFos stained cultured slices were acquired with a confocal laser scanning

microscope (Olympus FLUOVIEW FV1000) using 20x oil immersion objective (UPLSAPO 20X NA: 0.85). A stack of multiple images (3 µm step at 1024 x 1024 pixel resolution) was acquired in CA1 using the 488 nm (Alexa488), 559 nm (mKate2) and 635 nm (Alexa647) laser lines (12.5 µs per pixel). In order to avoid spectral bleedthrough, acquisition was done sequentially. The settings of the cFos channel (laser power, gain, voltage, offset) were kept unchanged in all imaging sessions.

To validate the expression of PACmn virus in organotypic (initial testing of the construct) and acute slices (field recordings), images of anti-GFP stained slices were acquired with a confocal laser scanning microscope (Olympus FLUOVIEW FV1000 or Zeiss AiryScan 900). When using the Olympus, multiple stacks of images (3 µm step) were acquired using the 488 nm laser line and stitched together using ImageJ. Alternatively, when using the Zeiss to validate expression of PACmn virus in acute slices after field recordings, slices were imaged with a 488 nm laser line through an air objective. One focal plane was acquired, where the location of the electrodes was most clearly visible.

3.2.7 Data analysis

General data analysis and statistics

Electrophysiological data were analysed using Clampfit, Synchroslice software or custom Matlab scripts. Confocal data were analysed using FiJi (ImageJ). Graphs and statistical analyses were generated with GraphPad Prism 6.0. Bars and whiskers on graphs represent either mean and SEM or median and interquartile range, as specified in the figure legends.

Confocal image analysis

FiJi (ImageJ) software was used to identify cFos-positive nuclei and to measure their intensity. For each Z-stack, a maximum projection of acquired frames was performed. Based on the signal from the mKate2-positive cells, ROIs were drawn on top of each nucleus of electroporated cells and the average intensity or each ROI in the "cFos channel" was calculated. For display, the brightness of all cFos images was matched.

4. Results

4.1 Development of photoactivated tools

4.1.1 Development and characterisation of new light-activated guanylyl and adenylyl cyclases

Disclaimer: The results presented in this subchapter are part of the publication:

- Scheib U, Broser M, Constantin OM, Yang S, Gao S, Mukherjee S, Stehfest K, Nagel G, Gee CE, Hegemann P. Rhodopsin-cyclases for photocontrol of cGMP/cAMP and 2.3 Å structure of the adenylyl cyclase domain. *Nature Communications* 9(1): 2046 (2018) DOI 0.1038/s41467 -018-04428-w

A significant number of optogenetic tools are based on microbial rhodopsins, membrane spanning proteins (opsins) that are linked to a light sensing chromophore in the form of retinal. Recently, examining phototaxis of aquatic fungi species *Blastocladiella emersonii* and *Catenaria anguillulae* has uncovered gene fusions of rhodopsin and guanylyl cyclase domains (Avelar et al., 2014a). The photo-activatable guanylyl cyclase from *Blastocladiella emersonii* has been isolated and its cGMP producing capabilities demonstrated in *Xenopus* oocytes, *C. elegans* and hippocampal neurons (Gao et al., 2015; Scheib et al., 2015). This subchapter presents the characterisation and validation as a novel optogenetic tool of the guanylyl cyclase from *Catenaria anguillulae*, as well as attempts to generate rhodopsin adenylyl cyclases via mutations in the GTP binding site.

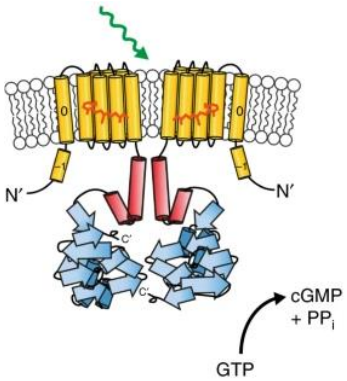

Figure 4.1. Model of the dimeric rhodopsin-guanylyl cyclases from *Catenaria anguillulae*. The photo-sensitive rhodopsin domain (yellow) is directly connected to the guanylyl cyclase domain (blue) via a coiled-coil stretch (red). Image from (Scheib et al., 2018).

CaRhGC is a dimeric rhodopsin guanylyl cyclase that contains a light-sensing rhodopsin domain directly connected to a guanylyl cyclase via a coiled-coil type linker (Figure 4.1). Unlike other type I rhodopsins that have a 7 transmembrane helix structure, CaRhGC's rhodopsin domain harbors 1-2 extra helices on the N terminus (Scheib et al., 2018). In order to visualise the distribution of the CaRhGC, the N terminus was labelled with the fluorescent protein YFP, which did not change the protein's enzymatic activity. Interestingly, adding the YFP to the cytosolic C terminus caused dark activity that increased cGMP levels 10 fold (Scheib et al., 2018). To test its cGMP producing capabilities, YFP-CaRhGC was co-electroporated together with cAMP or cGMP-sensitive cyclic nucleotide-gated channels in hippocampal neurons (cGMP-sensitive CNGA2 channel $K_{1/2}^{cAMP} = 36$ µM, $K_{1/2}^{cGMP} = 1.3$ µM; cAMP-sensitive CNGA2 channel (C460W/E583M) $K_{1/2}^{cAMP} = 0.89$ µM, $K_{1/2}^{cGMP} = 6.2$ µM (Rich et al., 2001)). Neurons expressing YFP-CaRhGC had normal morphology as observed from the fluorescence of co-expressed fluorescent protein mtSapphire (Figure 4.2 a).

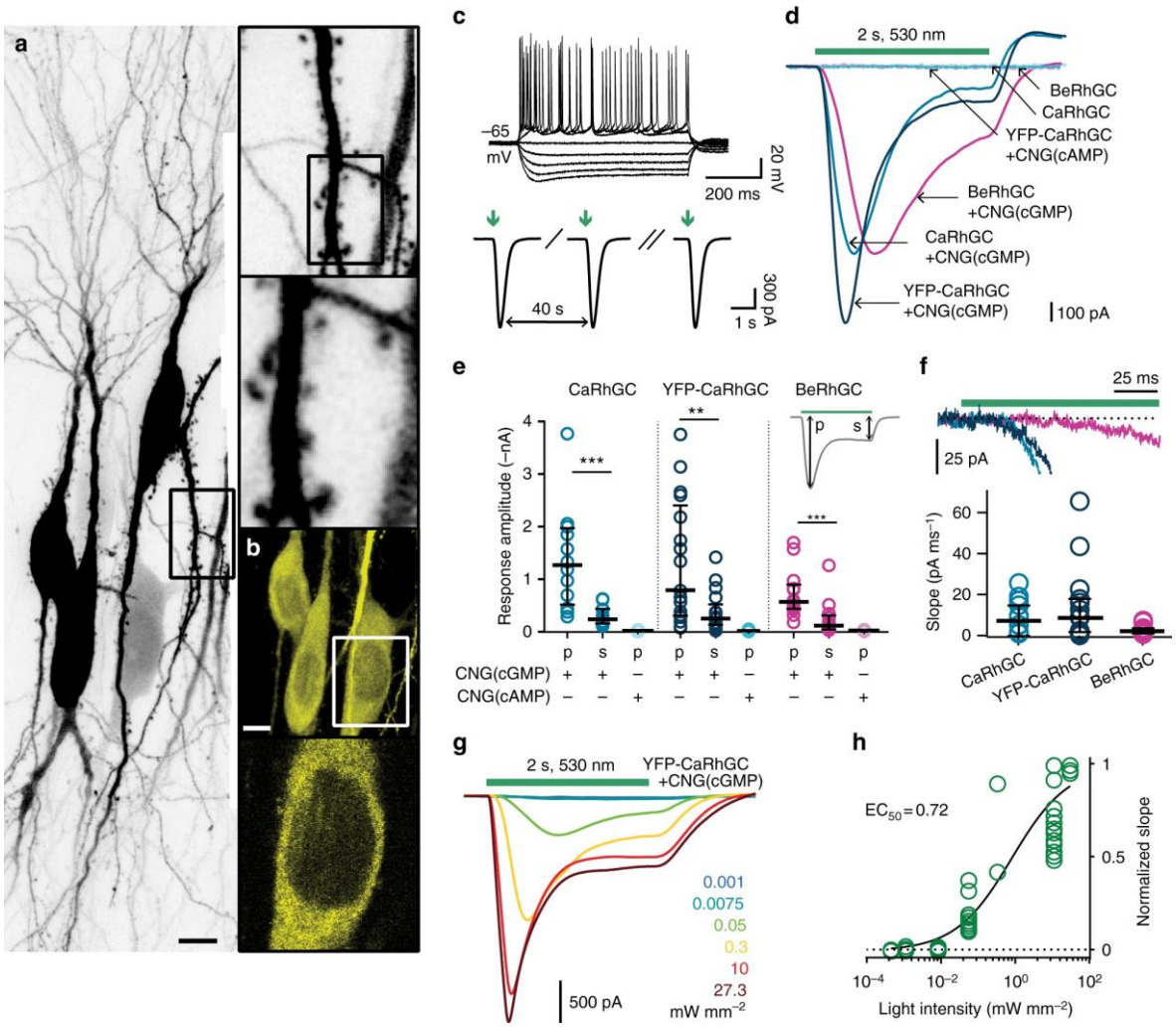

Figure 4.2 Characterisation of CaRhGC in hippocampal neurons. (a) and **(b)** Confocal images of neurons 8 days after electroporation with DNA encoding YFP-CaRhGC and mtSapphire (scale bars 10 µm). **(c)** Top: Whole-cell response to current injections from −400 pA to 400 pA in 100 pA steps. Bottom: The first, second and fifth currents evoked by repeated green light flashes (530 nm, 0.3 mW mm^{-2}, 100 ms, ISI 40 s). **(d)** Sample currents evoked by a 2 s green light pulse (530 nm, 27.3 mW mm^{-2}) in neurons expressing YFP-CaRhGC, CaRhGC or the guanylyl cyclase from Blastocladiella emersonii (BeRhGC) together with the cGMP or the cAMP-sensitive CNGA2 channels. **(e)** Peak photocurrents (p) and the sustained response (s) recorded from neurons expressing YFP-CaRhGC, CaRhGC, or BeRhGC and one of the CNG channels. ***p = 0.0001, p = 0.0006, **p = 0.009; Mann–Whitney test, peak vs sustained response of YFP-Ca/Ca/BeRhGC + CNG(cGMP). **(f)** Detail of photocurrent onset from neurons expressing YFP-CaRhGC, CaRhGC or BeRhGC, and CNG(cGMP). **(g)** Sample photo-currents recorded from a neuron expressing YFP-CaRhGC + CNG(cGMP) when stimulated with different intensities of 530 nm light. **(h)** Light intensity-response relationship for YFP-CaRhGC + CNG(cGMP) fitted with a quadratic equation. Photocurrents were normalized to the maximum current recorded for each neuron. Graphs show individual data points, median and 25–75% interquartile range. Figure and legend from (Scheib et al., 2018).

The distribution of the construct itself was uniform in the membrane, as evident from the fluorescence (Figure 4.2 b). Neurons expressing both the YFP-RhGC and the CNG channels had normal membrane properties (spiking threshold, resting membrane potential) (Figure 4.2 c). Inward currents were observed when patched expressing cells were illuminated with 2 seconds of green light. Light-activation of the YFP-RhGC produced cGMP that binds to the CNG channel, leading to opening of its pore and cation conductance (Figure 4.2 d). Currents were reversible and reproducible as multiple flashes of green light delivered at 40 seconds intervals elicited the same peak amplitude currents (Figure 4.2 c). Current amplitudes were very similar between YFP-CaRhGC, untagged CaRhGC, and BeRhGC. Interestingly, light stimulation of CaRhGC generated photo-currents in only 30% of transfected cells. When compared to the previously published BeRhGC, RhGCs derived from *Catenaria* were faster, with 4 times faster currents as evident from the slope calculation of recorded photocurrents (Figure 4.2 f). Currents were also light intensity dependent, with an EC_{50} value of around 0.7 mW mm^{-2}.

Since cAMP is an important signaling molecule in virtually all cellular systems, converting YFP-CaRhGC to an adenylyl cyclase would expand the toolbox for optogenetic manipulation of intracellular cAMP. In hippocampal neurons, I tested untagged adenylyl cyclase variants, as well as C or N-terminally tagged (Figure 4.4 and 4.5). The construct with an N terminal YFP tag, as well as E497K/C566D mutations proved superior, as it's activation mediated currents in all (100%) transfected neurons (BeRhAC 79%, CaRhAC 67%, CaRhAC-mycHis 40%). The mutated residues were chosen as they exist in the GTP binding domain of the cyclase and anchor the guanine base.

Mutations were made into aminoacids that naturally occur in adenylyl cyclases (E497 to K and C566 to D). I characterised this new construct electrophysiologically in hippocampal neurons where it had similar uniform membrane distribution as YFP-RhGC (Figure 4.3 a). Light pulses of green light evoked large, transient, inward currents through co-expressed cAMP-sensitive CNG channels (Figure 4.3 d-e). Neurons co-expressing the cGMP-sensitive variant of the CNG channel had little to no light-evoked currents, showing a successful conversion from a GC to an AC (Figure 4.3 e-f). As with YFP-RhGC, photo-currents were light intensity dependent, retaining a similar EC value (0.6 mW mm^{-2}) (Figure 4.3 g-h).

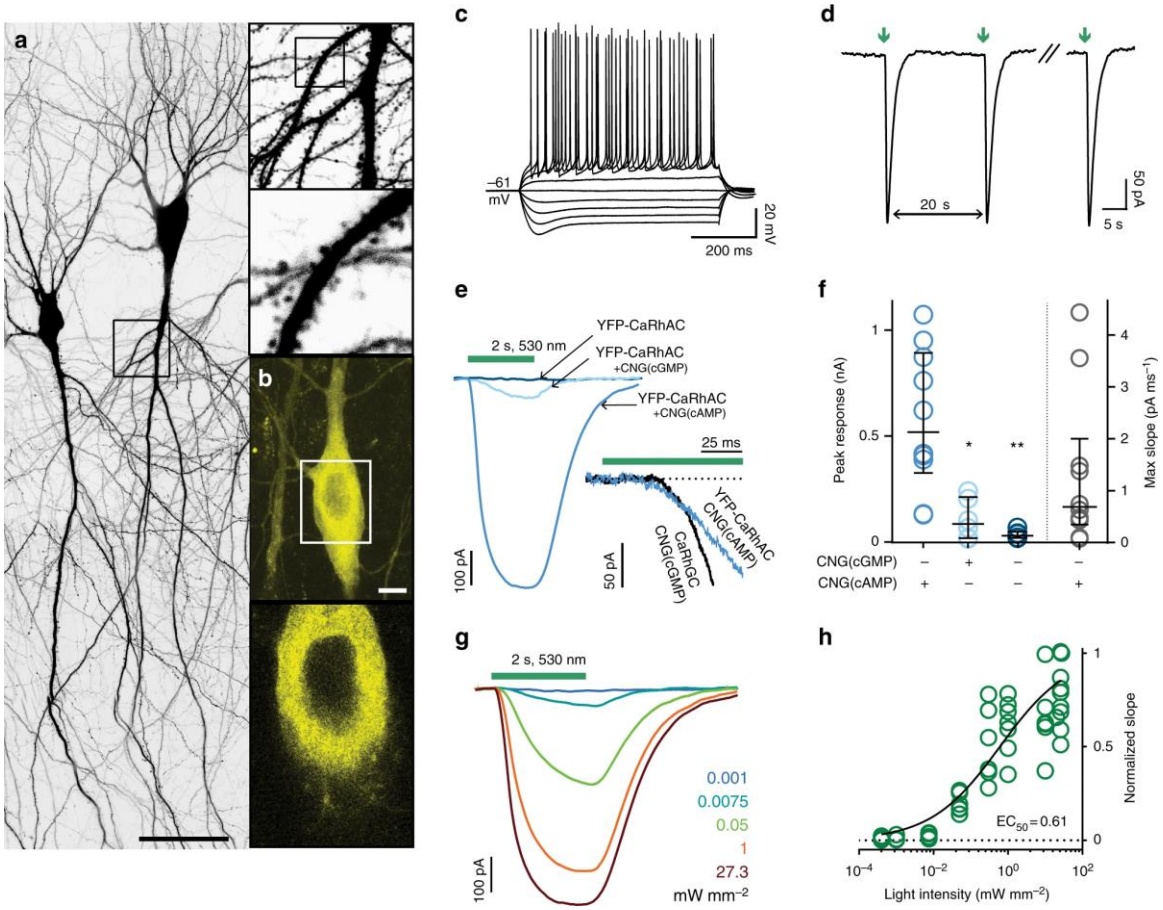

Figure 4.3 Generation and characterisation of YFP-CaRhAC. Two photon images neurons expressing YFP-CaRhAC alone **(b)** (scale bar 10 µm) or with mtSapphire **(a)** (scale bar 50 µm). **(c)** Whole-cell response to current injections (-400 to 400 pA) of a hippocampal neuron expressing YFP-CaRhAC plus the cAMP-sensitive CNGA2. **(d)** The first, second and fifth currents evoked by repeated green light flashes (530 nm, 0.3 mW mm^{-2}, 100 ms, ISI 20 s). **(e)** Sample currents evoked by green light (27.3 mW mm^{-2}) in neurons expressing YFP-CaRhAC together with CNG(cGMP), CNG(cAMP) or alone. Insert shows the onset and initial slope of the photocurrents. **(f)** Peak or slope of photocurrents recorded from neurons expressing YFP-CaRhAC and one of the CNG channels or by itself. *p = 0.023, **p = 0.0016, Kruskal–Wallis test vs YFP-CaRhAC + CNG(cAMP). **(g)** Sample currents from a neuron expressing YFP-CaRhAC + CNG(cAMP) when stimulated with green light of different intensity. **(h)** Light intensity-response

relationship of (g), fitted with a quadratic equation. Photocurrents were normalized to the maximum current recorded for each neuron. Graphs show individual data points, median and 25–75% interquartile range. Figure and legend from (Scheib et al., 2018).

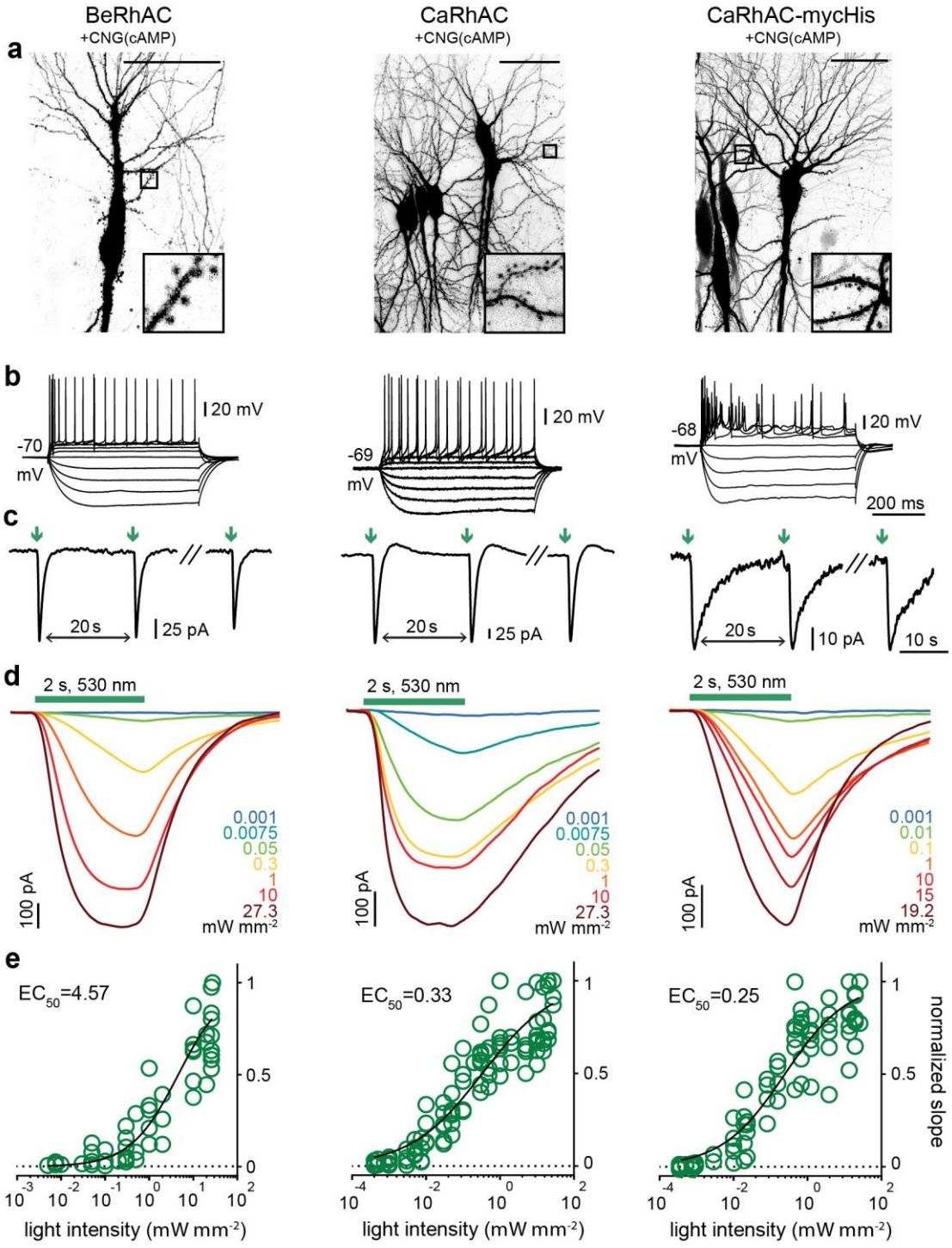

Figure 4.4 Characterization of adenylyl cyclases derived from RhGCs in hippocampal neurons. **(a)** Two photon images of mtSapphire fluorescence of hippocampal neurons 6-8 days after electroporation with: 25 ng µl^{-1} DNA encoding BeRhAC (left), 100 ng µl^{-1} DNA encoding CaRhAC (middle), 100 ng µl^{-1} DNA encoding CaRhAC-mycHis (right), plus 25 ng µl^{-1} DNA encoding CNG(cAMP) and 5 ng µl^{-1} DNA encoding

mtSapphire, scale bar 10 µm. **(b)** Whole-cell responses of hippocampal neurons (as above) to current injections of -400 pA to 400 pA. **(c)** Photocurrents evoked by 100 ms flashes of green light (530 nm) at 20 s intervals. Intensity (left to right): 27.3, 27.3, 0.019 mW mm^{-2}. **(d)** Representative currents recorded in response to 2 s green light flashes of different intensity. **(e)** Light intensity-response relationship fitted with a quadratic equation. n's = 8, 7, 6 (left to right). Figure and legend from (Scheib et al., 2018).

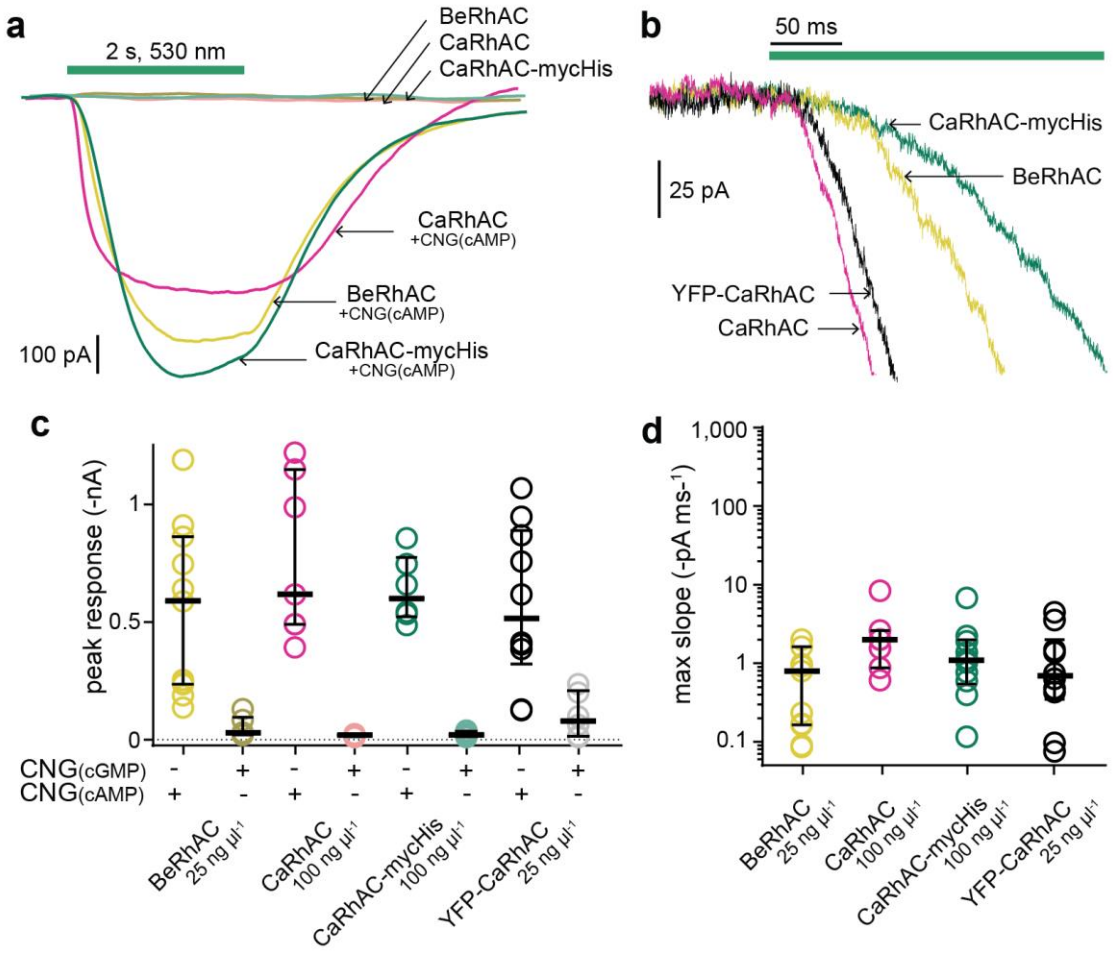

Figure 4.5 Comparison of photocurrents of adenylyl cyclases derived from RhGCs in hippocampal neurons. (a) Sample responses to 2 s green light (530 nm, 27.3 (CaRhAC, CaRhAC-mycHis) / 19.2 (BeRhAC) mW mm^{-2} of hippocampal neurons expressing the adenylyl cyclases together with CNG(cAMP) and CNG(cGMP) channels (both channels 25 ng µl^{-1}, BeRhAC 25 ng µl^{-1}, CaRhAC 100 ng µl^{-1}, CaRhAC-mycHis 100 ng µl^{-1} electroporation DNA). **(b)** The first 200 ms of the evoked responses shown in (a) in comparison to the response of YFP-CaRhAC. **(c-d)** Comparison of maximum peak (c) and slope (d) of currents evoked by green light (530 nm, 2 s, ≤ 27.3 mW mm-2) in hippocampal neurons expressing un-tagged, c-terminal myc-His tagged and n-terminal YFP tagged RhACs; numbers next to the construct name indicate the concentration of rhodopsin DNA electroporated (ng µl^{-1}). Channel DNA was always 25 ng µl^{-1}, mtSapphire 5 ng µl^{-1}. Note that comparable currents were evoked in neurons expressing rhodopsins with or without a c-terminal myc-His tag. Addition of an n-terminal YFP improved expression or surface localization of CaRhAC as comparable currents were obtained after electroporating 75% less DNA. n's = 11, 6, 7, 5, 6, 9, 10, 6, 11, 7, 10, 10 left to right. Bars show median and interquartile range. Figure and legend from (Scheib et al., 2018).

4.1.2 Improved optogenetic cAMP control with *Beggiatoa*-derived light activated cyclases

Disclaimer: The results presented in this subchapter are part of the publication:

- Yang S#, **Constantin OM#**, Sachidanandan D#, Hofmann H, Kunz TC, Kozjak-Pavlovic V, Oertner TG, Nagel G, Kittel RJ, Gee CE, Gao S. PACmn for improved optogenetic control of intracellular cAMP. *BMC Biology* 19:227 (2021). DOI 10.1186/s12915-021-01151-9; # equal contribution

The light-activated adenylyl cyclase bPAC is one of the first modulatory optogenetic tools discovered and used in complex experimental procedures. Some of its useful features are its high light sensitivity and compatibility of its excitation spectrum with other optogenetic tools. However, there are two main aspects limiting its usability. First, it has been reported that bPAC has a low but functionally significant activity in the dark (Stierl et al., 2011). This implies that even in the absence of light, bPAC-expressing cells have a higher resting level of cAMP due to the cyclase's activity. Second, bPAC is a soluble adenylyl cyclase. From all ten endogenous adenylyl cyclases, only AC10 is soluble, while AC1-AC9 are transmembrane proteins. Furthermore, the soluble endogenous ACs have functionally different roles as their signaling is regulated by bicarbonate and does not depend on GPCR activity or intracellular calcium. As cAMP is highly compartmentalised within the same cell, it would be ideal to have a powerful tool like bPAC targeted to the plasma membrane. Therefore, the aims of this project were to develop a bPAC variant with lower dark activity and to target it to the plasma membrane.

I started by evaluating the resting dark activity of bPAC in hippocampal neurons. Theoretically, there are a few ways one can look at resting cAMP levels in hippocampal neurons under the conditions we use in the lab (5-20 neurons electroporated/slice), such as using genetically-encoded cAMP Förster resonance energy transfer (FRET) sensors. Unfortunately, the toolbox available for monitoring cAMP is not as diverse as that for Ca^{2+}. From the few sensors available, most are incompatible with bPAC as they rely on cyan/yellow fluorescent protein pairs for FRET (bPAC would get activated by the light used to excite the sensor), or they express poorly in our cultures (Pink Flamindo, RFlincA (Harada et al., 2017; Ohta et al., 2018)). For these reasons, instead of looking at resting levels of cAMP, I evaluated the activation of PKA, one of the main downstream effectors of cAMP. I co-electroporated bPAC with Booster-PKA, an orange-red PKA

activity FRET sensor (Watabe et al., 2020). Booster-PKA sensor uses an orange fluorescent protein (mKOκ) as donor and a red fluorescent protein (mKate2) as acceptor, making it compatible with bPAC as the 559 nm light used to excite mKOκ will not activate the cyclase. Upon sensing the signal (PKA activity), the sensor domain changes its conformation and interacts with the ligand domain. This induces further conformational changes that will bring the donor and acceptor molecules closer together, enabling FRET between the two molecules (Figure 4.6 A). Thus, a change in the ratio between the donor and the acceptor molecule (or vice versa) would be an indicator of lower or higher PKA activity.

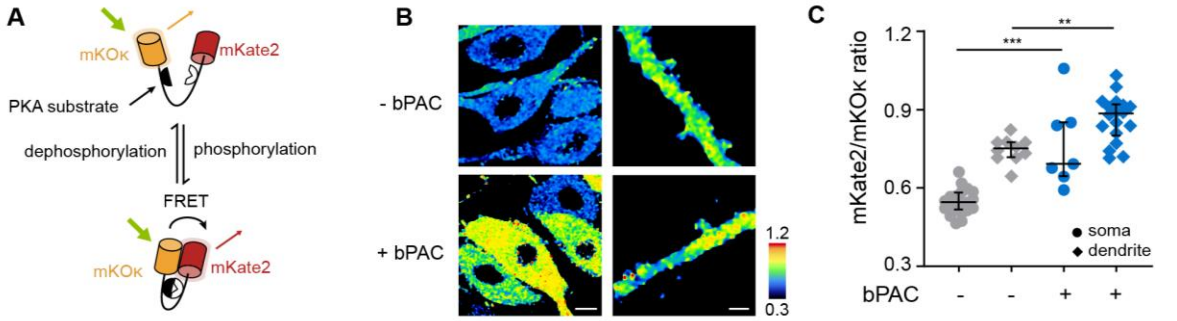

Figure 4.6 Low dark activity of bPAC is sufficient to induce PKA activity. (A) Working mechanism of the PKA activity FRET sensor Booster-PKA. **(B)** Representative ratio images (mKate2/mKoκ) of hippocampal neurons expressing BoosterPKA alone or together with bPAC (scale bar soma 10 µm, dendrite with spines 1 µm). **(C)** mKate2/mKoκ ratio values (bars show median and interquartile range). ***p < 0.0001, **p < 0.001, unpaired t-test soma bPAC(+) vs soma bPAC(-), unpaired t-test dendrite bPAC(+) vs dendrite bPAC(-). Image from (Yang et al., 2021).

In bPAC expressing cells, resting levels of PKA activity were increased, as the mKate2/mKOκ ratio was higher than in cells expressing only the sensor (Figure 4.6 B-C). This difference in PKA activation levels was apparent in both the cell bodies and in dendrites. The donor fluorescence was excited with 559 nm light, which does not get absorbed by the BLUF domain of bPAC (absorbance range between 350 and 520 nm) (Stierl et al., 2011). Thus, cross-activation of bPAC while stimulating donor fluorescence could not contribute to the higher resting FRET ratio, suggesting that bPAC raises cAMP in the absence of direct light stimulation when expressed in hippocampal neurons. This is sufficient to induce downstream signaling and activate PKA. This finding also indicates that the dark activity is quite significant, since intracellular PDEs are not able to quickly degrade all cAMP produced.

Structurally, bPAC is a dimer, each monomer comprised of an adenylyl cyclase (AC) domain connected by a coiled coil to a BLUF domain (Figure 4.7). Light absorption by BLUF

generates changes enabling catalytically-competent AC conformations. To reduce bPAC dark activity we introduced point mutations in either the BLUF domains, limiting their interaction (L123) or in substrate accommodating residues of the AC domains (K197, F198, H266, T267). Cyclic AMP measurement in oocytes (performed by our collaborators) (Yang et al., 2021) showed that the F198Y mutation in the substrate binding domain reduced dark activity to 4% of that of bPAC (dark turnover ≤ 0.0024 min^{-1}), while maintaining a relatively high light activity in comparison to the other variants tested (light-dark ratio >7000). Additionally, adding the fluorescent protein Venus/eYFP on the N or C terminus of bPAC further reduced its activity in dark conditions (cAMP concentration in the dark 24.7 µM bPAC, 9.7 µM for both Venus-bPAC and bPAC-eYFP).

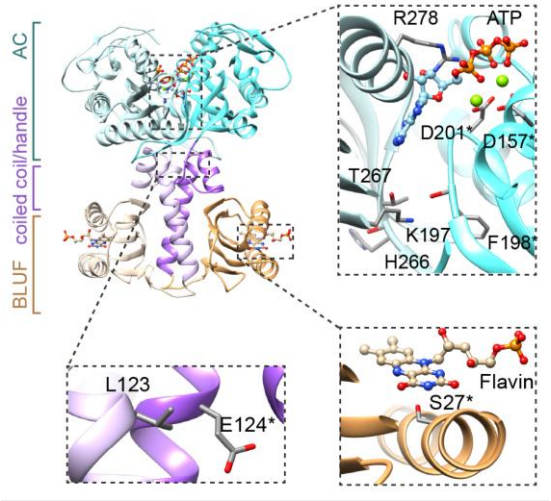

Figure 4.7 Model of bPAC structure. bPAC, (5MBK, 5M2A), a parallel homodimer (chain A and B colored in light and dark shades), marked with the "FAD" chromophore, ATP substrate and residues of interest. Asterisks indicate residues from the other chain of the dimer. Green spheres represent the two catalytic Mg^{2+} ions. Marked are the key residues that were screened (L123R, F198Y, F198W, H266W and T267Y, K197A, K197A/D201A and R278A). Image from (Yang et al., 2021).

Next, multiple strategies were used to target bPAC to the plasma membrane, such as fusing it to CD8, Gap43, CAAX peptide or a segment of the transmembrane protein Glycophorin. However, expression of these constructs was not optimal in hippocampal neurons (Yang et al., 2021). Successful targeting was achieved by adding on the N terminus two 11 amino acid long peptides from Lyn kinase, a tyrosine kinase from the Src family (Kasahara et al., 2004; Tsvetanova & von Zastrow, 2014). Together with the addition of Venus and the F198Y mutation in the bPAC segments, this construct was named PACmn and was electrophysiologically characterised in hippocampal neurons (Figure 4.8). PACmn-expressing pyramidal neurons had normal morphological and electrophysiological characteristics (Figure 4.9 A-D). Antibody staining against Venus revealed PACmn's uniform expression along the plasma membrane, as well as regions with high density of expression (Figure 4.9 A). This patchy appearance is most probably due to the peptide Lyn, as it is known to target Src family kinases to the plasma membrane, preferentially to lipid rafts (Sohn et al., 2008).

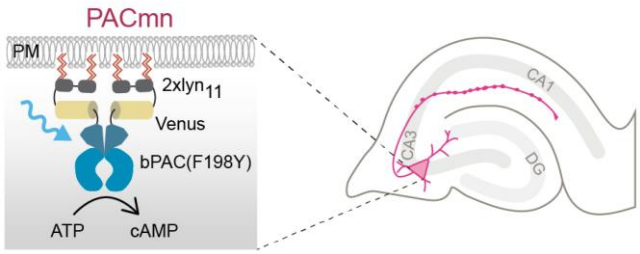

Figure 4.8 PACmn construct design. Membrane targeting of the construct was done via two lyn11 sequences, while the dark activity was reduced by introducing the F198Y mutation in the AC domain of bPAC, as well as adding a Venus fluorescent protein between lyn11 and bPAC domains.

In order to read-out of the levels of cAMP produced by light stimulation, PACmn was electroporated together with a cAMP-sensitive cyclic nucleotide-gated channel (CNGA2 C460W/E583M; $K_{1/2}^{cAMP}$ = 0.89 µM) (Rich et al., 2001). A brief pulse of blue light of low intensity generated cAMP and opened the co-expressed channel, generating inward currents (Figure 4.9 E). Currents were fully reversible (due to the degradation of the produced cAMP by PDEs) and repeatable. Photo-currents were light dose dependent. By changing the light intensity delivered but keeping the light pulse length the same, an EC_{50} of 4.1 mW mm^{-2} could be calculated (Figure 4.9 F). Similarly, by using a sub-EC_{50} light intensity, photo-currents were saturated with light flashes as short as 500 ms (Figure 4.9 G). The decay of the saturated photo-currents (500, 5000 and 15000 ms) varied with the pulse length, indicating that more cAMP was produced in the longer light pulse conditions even if the peak and slope of the currents saturated (probably due to channel saturation).

In comparison to bPAC-generated photocurrents, PACmn induced smaller inward currents in response to 50 ms light flashes of the same intensity (Figure 4.10 A). However, when the light intensity was increased 10 times, similar current amplitudes could be achieved (Figure 4.10 B-C). Similarly, by lengthening the light duration of PACmn activation light pulse resulted in similar photocurrents (–0.87 nA, 500 ms 1mW mm^{-2} from Figure 4.9 G) as when stimulating bPAC expressing cells with the same intensity light but 10 times shorter pulse (–1.21 nA, 50 ms 1 mW mm^{-2}, Figure 4.10 A, B). That shows that even with a lowered enzymatic activity, PACmn light activation can result in cAMP increases similar to that of bPAC by lengthening the light pulse duration or increasing the light intensity. PACmn photocurrents had similar kinetics as bPAC photocurrents, with current peaking within 1.7 s (PACmn) and 1.2 s (bPAC(wt)) from the start of illumination and decaying with a half-time of 6.4 s and 10 s, respectively (Figure 4.10 D). And similarly to bPAC (Stierl et al., 2011), PACmn photocurrents were larger than those generated by chemical stimulation of endogenous ACs and block of PDEs (Figure 4.10 E).

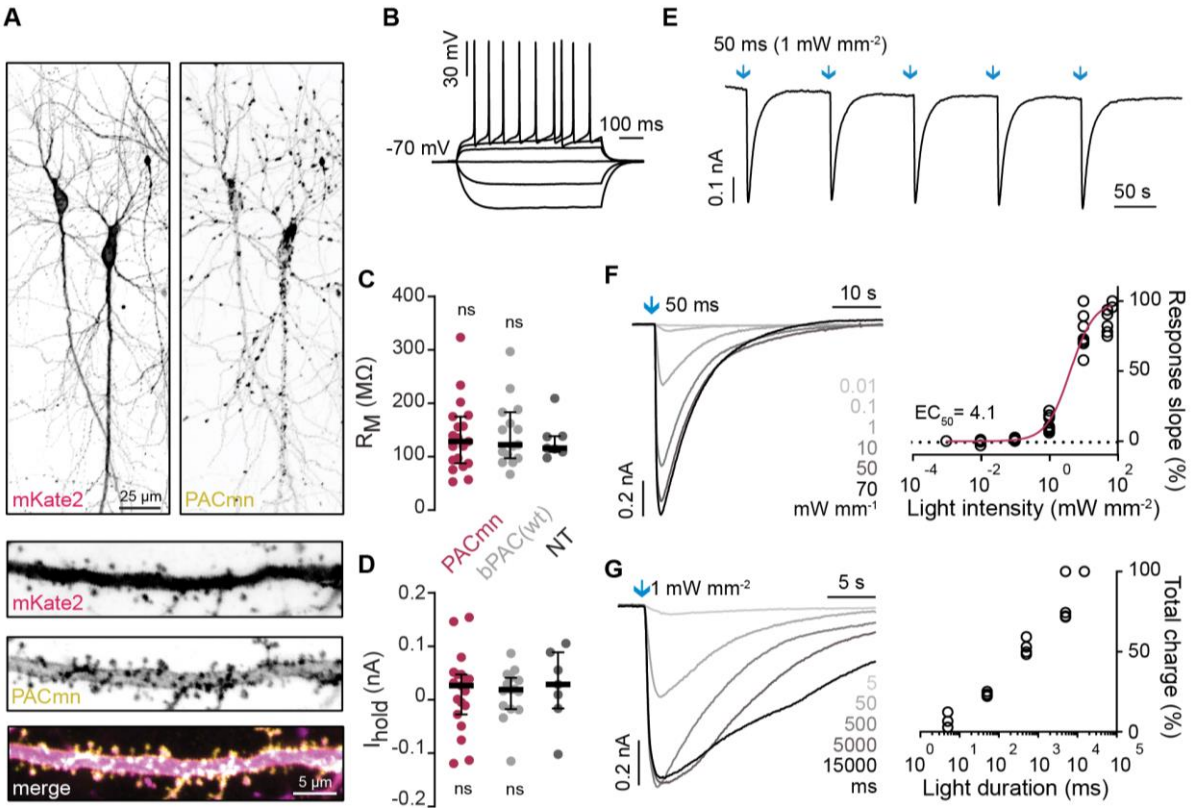

Figure 4.9 Characteristics of the light-evoked responses in expressing hippocampal neurons. (A) Confocal projection images of stained hippocampal neurons co-expressing PACmn (2xLyn-Venus-bPAC(F198Y)) and mKate2, together with close-up of an apical dendrite. Overview scale bar 25 µM, close up 10 µM. **(B)** Whole-cell responses to somatic current injections from -400 pA to 700 pA in a PACmn expressing neuron in the dark (resting membrane potential -70 mV). **(C-D)** Membrane resistance and holding current of non-transfected (NT) or PACmn/bPAC-expressing neurons when clamping the membrane voltage at -70 mV. **(E)** Photocurrents evoked by five consecutive light flashes (50 ms, 1 mW mm^{-2}, ISI 100 s) in a PACmn + mCNG-A2 expressing neuron. **(F)** Representative currents recorded from PACmn and mCNG-A2 expressing hippocampal neurons in response to 50 ms light pulse of varying intensity of 470 nm light together with the light intensity-response relationship fitted with a quadratic equation. Currents were normalized to the maximum current recorded for each neuron. **(G)** Representative currents recorded from PACmn and mCNG-A2 expressing hippocampal neurons in response to 1 mW mm^{-2} blue light pulses of varying duration (5 ms to 15 s) together with light duration-response relationship (total charge). The maximum charge from each neuron was set to 100%. Image from (Yang et al., 2021).

Having established the functionality of PACmn in cultured hippocampal neurons, resting PKA activity in PACmn expressing cells was evaluated by co-expressing it with Booster-PKA. Additionally, we compared resting PKA activity of PACmn with that of bPAC(wt) and other intermediate constructs we created: soluble bPAC with the F198Y mutation (Venus-bPAC(F198Y)) and membrane-targeted bPAC without the F198Y mutation (2xLyn11-Venus-bPAC). Remarkably,

expression of PACmn was the only condition tested in which basal PKA activity was not affected (Figure 4.11 A). We reconfirmed the dark activity of bPAC, as well as that of its plasma membrane-targeted version (without F198Y mutation).

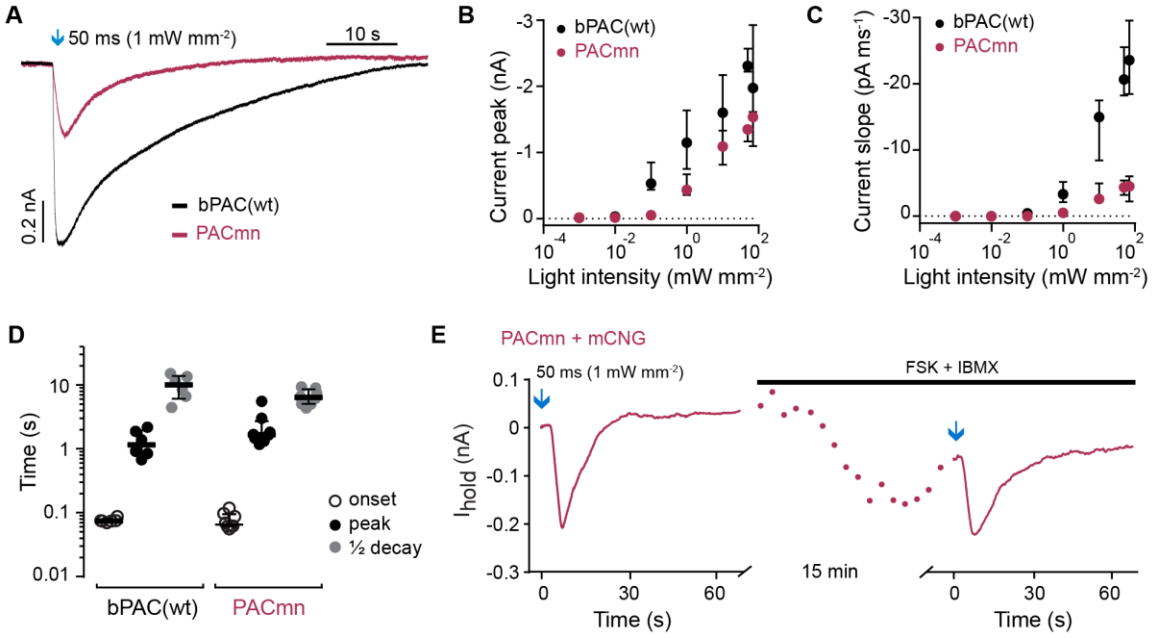

Figure 4.10 PACmn raises cAMP in hippocampal neurons. (A) Sample currents elicited by a 50 ms 470 nm light pulse (arrow) in neurons expressing either bPAC(wt) or PACmn together with mCNG. **(B)** Photocurrent amplitude and **(C)** slope recorded in neurons expressing PACmn or bPAC(wt) together with mCNG in response to 50 ms 470 nm light pulses of varying intensity. **(D)** Time from stimulation to onset, peak, and time from the peak to decay to ½ peak of responses to 50 ms, 1 mW mm^{-2} 470 nm light pulses. **(E)** Currents recorded from a neuron expressing PACmn together with mCNG in response to 50 ms, 1 mW mm^{-2} 470 nm light pulses (arrows), before and 15 min after wash-in of forskolin (FSK; 100 µM) and IBMX (75 µM). Plotted are median and interquartile range. Image and legend from (Yang et al., 2021).

Surprisingly, Venus-bPAC(F198Y) also increased PKA activity in hippocampal neurons, despite having no effect in the oocytes or on *Drosophila* behavior. In comparison to the slow and almost irreversible effects of forskolin, a brief 2 second activation of PACmn was able to rapidly increase PKA activity which decayed back to baseline in about 10 minutes (Figure 4.11 B-F). These results show the much lower dark activity of PACmn in comparison to bPAC and that PACmn is an appropriate optogenetic tool for fast and reversible manipulation of cAMP with high temporal and spatial resolution. These results show that in comparison to bPAC, PACmn has virtually no dark activity and that it can be used to activate cAMP-dependent intracellular signaling cascades in individual cells with high temporal and spatial resolution.

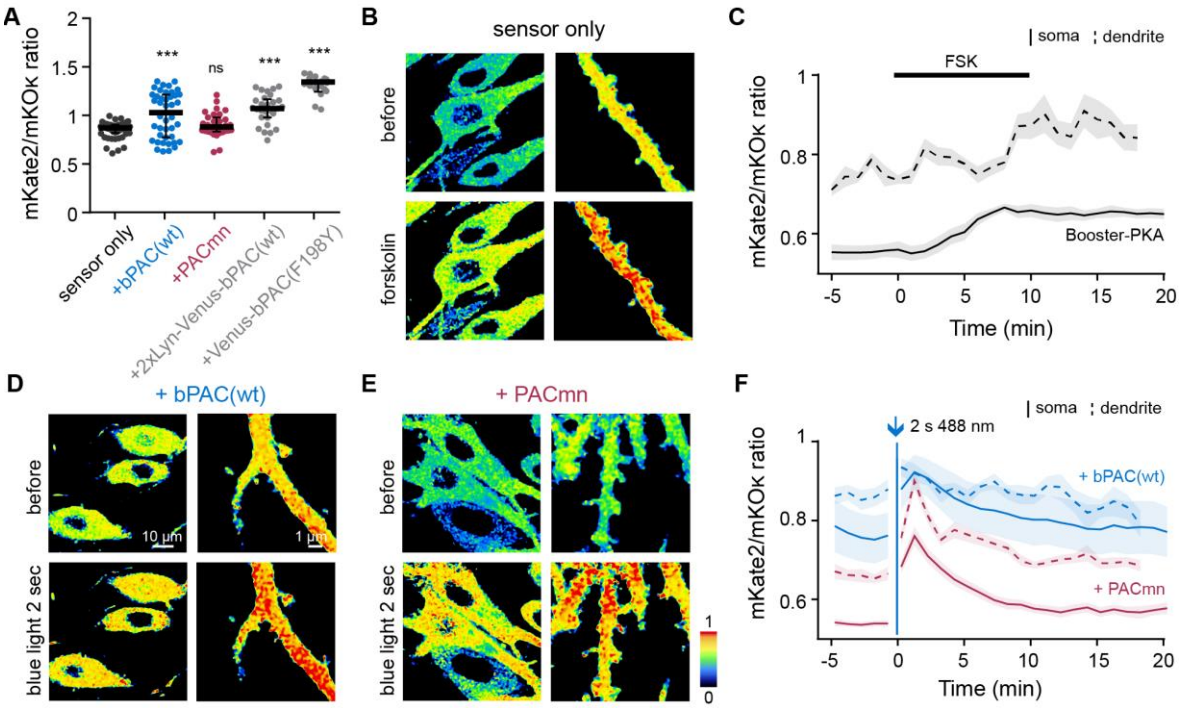

Figure 4.11 PACmn activates PKA when illuminated without altering basal activity in hippocampal neurons. (A) Resting FRET ratios (soma) in hippocampal neurons expressing Booster-PKA alone or together with bPAC variants. Note that only PACmn does not change resting PKA activity. Shown are median and interquartile range. ***p < 0.0001, ns = not significant, Dunnett's multiple comparisons vs sensor only following one-way ANOVA (p < 0.0001). n = 52, 43, 31, 29, and 18 somata. **(B)** Representative ratio images (mKate2/mKoκ) of the hippocampal neurons (soma and dendrite with spines) expressing BoosterPKA before and after foskolin (FSK). **(C)** PKA activity in Booster-PKA expressing hippocampal neurons. Bar indicates time of FSK application. **(D-E)** Representative ratio images (mKate2/mKoκ) of hippocampal neurons expressing Booster-PKA together with bPAC(wt) **(D)** or PACmn **(E)** before and after being illuminated for 2 s with 1 mW mm^{-2} 470-nm blue light. **(F)** PKA activity in Booster-PKA neurons co-expressing bPAC(wt) or PACmn. Arrow indicates a 2 s blue light pulse. In both **(C)** and **(F)**, the solid lines are from the soma, dashed lines from the dendrites and spines. n (somata): 10 (Booster-PKA), 7 (+bPAC(wt)), 11 (+PACmn); n (dendrites and spines): 10 (Booster-PKA), 18 (+bPAC(wt)), and 14 (+PACmn). Shading indicates SEM. Image and legend from (Yang et al., 2021).

4.1.3 Cyclic AMP-derived silencing optogenetic tools

Manipulating neuronal activity has paved the way for numerous scientific advancements in the field of neuroscience. Controlling if and when specific neurons or circuits are active has been especially useful in revealing the functional roles of network activity in distinct brain areas. While the toolbox of excitatory optogenetic tools is constantly expanding (Gradinaru et al., 2010; Hochbaum et al., 2014; Klapoetke et al., 2014; Mager et al., 2018), the development of tools that silence the activity of neurons has had a slower pace (Wiegert et al., 2017). The current tools available for neuronal silencing require a high expression level and relatively high light intensities which might lead to tissue heating and damage. Furthermore, their activation could lead to paradoxical effects (Mahn et al., 2016, 2018; Malyshev et al., 2017; Raimondo et al., 2012; Wiegert et al., 2016). Light-driven potassium channels could overcome these limitations, given that potassium channels underlie the inherent membrane hyperpolarization process. We took advantage of a recently published cAMP-gated K^+ channel and engineered an uni-molecular light-gated potassium channel consisting of the cAMP-gated K^+ channel SthK from *Spirochaeta thermophila* (Brams et al., 2014; Kesters et al., 2015) fused to bPAC, a bacterial photoactivated adenylyl cyclase (Stierl et al., 2011).

To further develop this initial construct that we published in 2018 (Beck et al., 2018), we lowered its cAMP-binding affinity to avoid activation by resting levels of cAMP, a clear limitation in its usability. Different point mutations were introduced in the cyclic nucleotide binding domain (CNBD) of the SthK channel. Additionally, the C_{term} segment of the CNBD domain was shortened, as to restrict its interaction with cAMP. The final construct that contains a T378V mutation in the CNBD and a 418 amino acid long C_{term} domain, was named KPAC and characterised electrophysiologically in hippocampal neurons (Figure 4.12 A).

A short flash of blue light induced large outward currents in expressing neurons that peaked after 6 seconds and half-decayed in 21 seconds (Figure 4.12 B-C). The currents reversed at -105 mV, the calculated reversal potential for K^+, validating the K^+ conductance of the channels (Figure 4.12 D). Photo-currents were also light dose dependent. By changing the light intensity delivered but keeping the light pulse length the same, an EC_{50} of 0.42 mW mm^{-2} could be calculated (Figure 4.12 E).

To check whether the light-driven K^+ conductance is sufficient to block action potential firing, expressing cells were current-clamped and somatic current injections (700 pA) were

delivered every 5 seconds in order to elicit action potentials. Five light stimulation conditions were tested, by keeping the dose constant but increasing the pulse length (5 ms to 50 seconds) and decreasing the light intensity (10 mW mm^{-2} to 0.001 mW mm^{-2}) (Figure 4.13 A). Light activation of KPAC was able to suppress action potential generation in all tested conditions. On average, the membrane potential hyperpolarized by around -15 mV. Blocking of APs was quick and sustained, starting at around 5 seconds after the light was applied and lasting up to 20-30 seconds (Figure 4.13 B). KPAC activation was able to suppress even high-frequency firing. Somatic current was injected (from 0 pA to 1400 pA) in order to drive spiking. Blue light intensities as low as 0.001 mW mm^{-2} were able to completely block spiking rates up to 100 Hz, demonstrating the efficient inhibition capabilities of KPAC (Figure 4.13 C). Thus, KPAC can be used for chronic silencing by using either repeating short pulses of high intensity blue light (50 ms at 1 mW mm^{-2}, every 30 seconds) or by applying very low intensity light for the whole duration that silencing is wanted (0.001 mW mm^{-2} for 5 minutes).

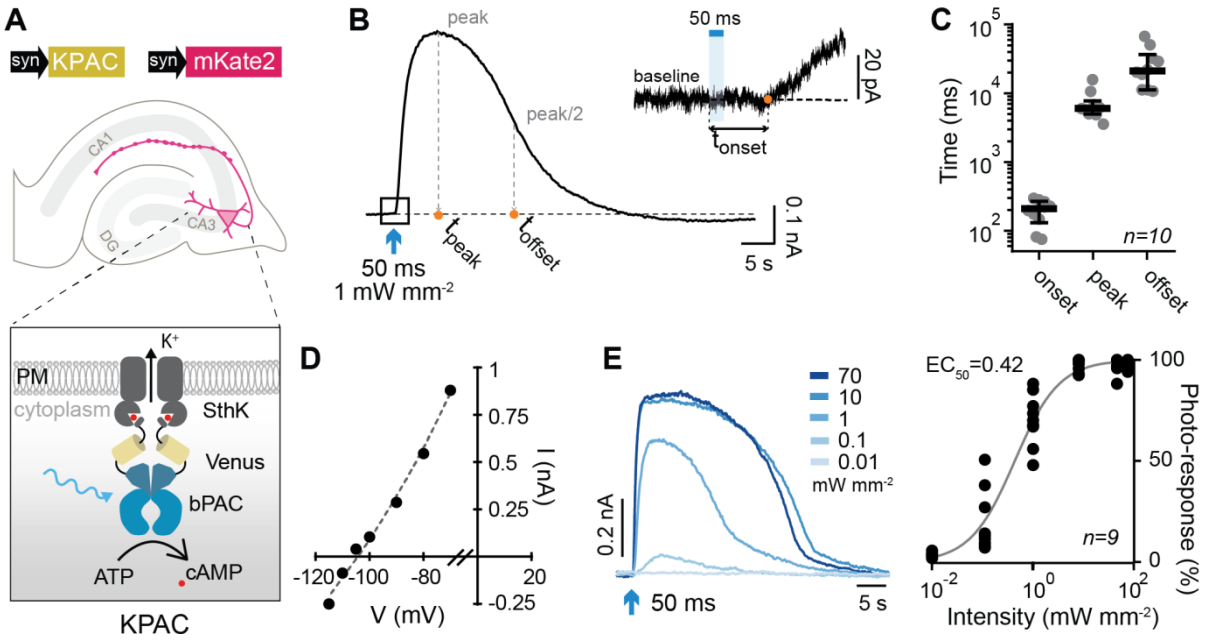

Figure 4.12 Characterization of KPAC photocurrents in hippocampal neurons. (A) Illustration of KPAC design and expression in organotypic hippocampal cultures. **(B)** Sample outward current elicited by a short 470 nm light pulse in neurons expressing KPAC; inset shows a zoom-in on the initial response segment. **(C)** Time characteristics of currents in subpanel (B). **(D)** I-V curve for KPAC photocurrents; a non-linear fit was applied to determine the reversal potential (−105 mV, K+ equilibrium potential -105 mV). **(E)** Sample currents recorded from a KPAC-expressing neuron when stimulated with different intensities of 470 nm light; Light intensity-response relationship fitted with a quadratic equation (normalization was performed to the maximum peak of currents recorded for each neuron).

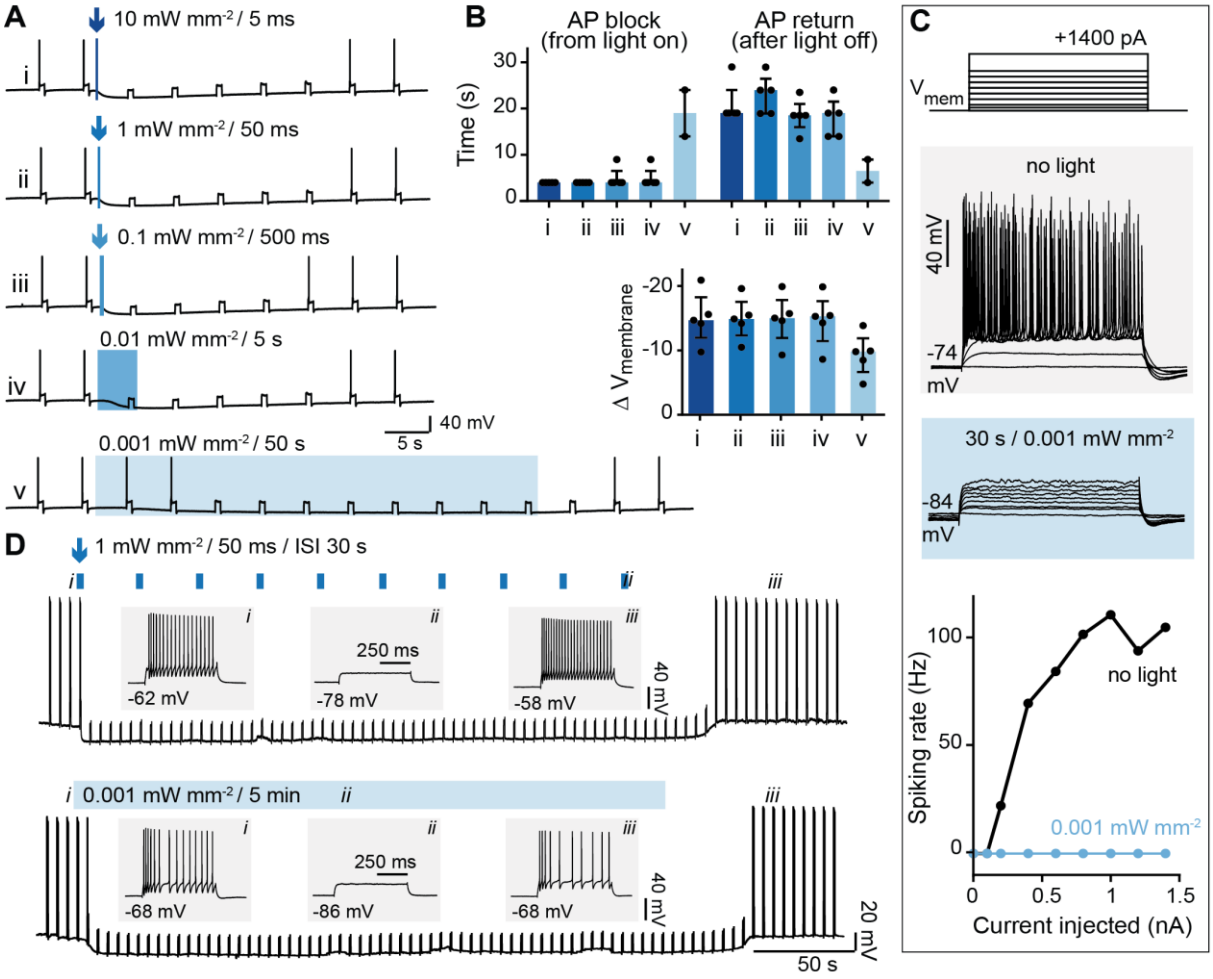

Figure 4.13 KPAC mediated silencing of firing in hippocampal neurons. (A) Example recordings where action potentials generated by somatic current injections (700 pA 600 ms) can be blocked by KPAC activation with extremely low light intensities by increasing the duration of the light pulse. **(B)** Up: Time characteristics of action potential block and return in conditions i-v depicted in subpanel A; Down: membrane potential changes in conditions i-v. **(C)** Light activation of KPAC efficiently blocks high-frequency action potentials generated by somatic current injections (0 to 1400 pA); n = 9 neurons, spiking rate calculated based on the time between the first two APs; graph depicts median spiking rate of all neurons. **(D)** Strategies for long-term block of firing using KPAC: very short, repetitive higher light intensities (upper example) or continuous very low-intensity light (lower example trace); insets show magnification of the responses during the current injection before, during and after light.

An enormous advantage given by bPAC's light-sensing BLUF domain is its insensitivity to wavelengths longer than 520 nm. This property makes possible combining bPAC with other optogenetic tools that are activated by green-red light. An inhibitory tool with this characteristic can be used together with an excitatory opsin to enable push-pull type experiments, where two colors are used to drive excitation and inhibition within the same cell (Figure 4.14 A).

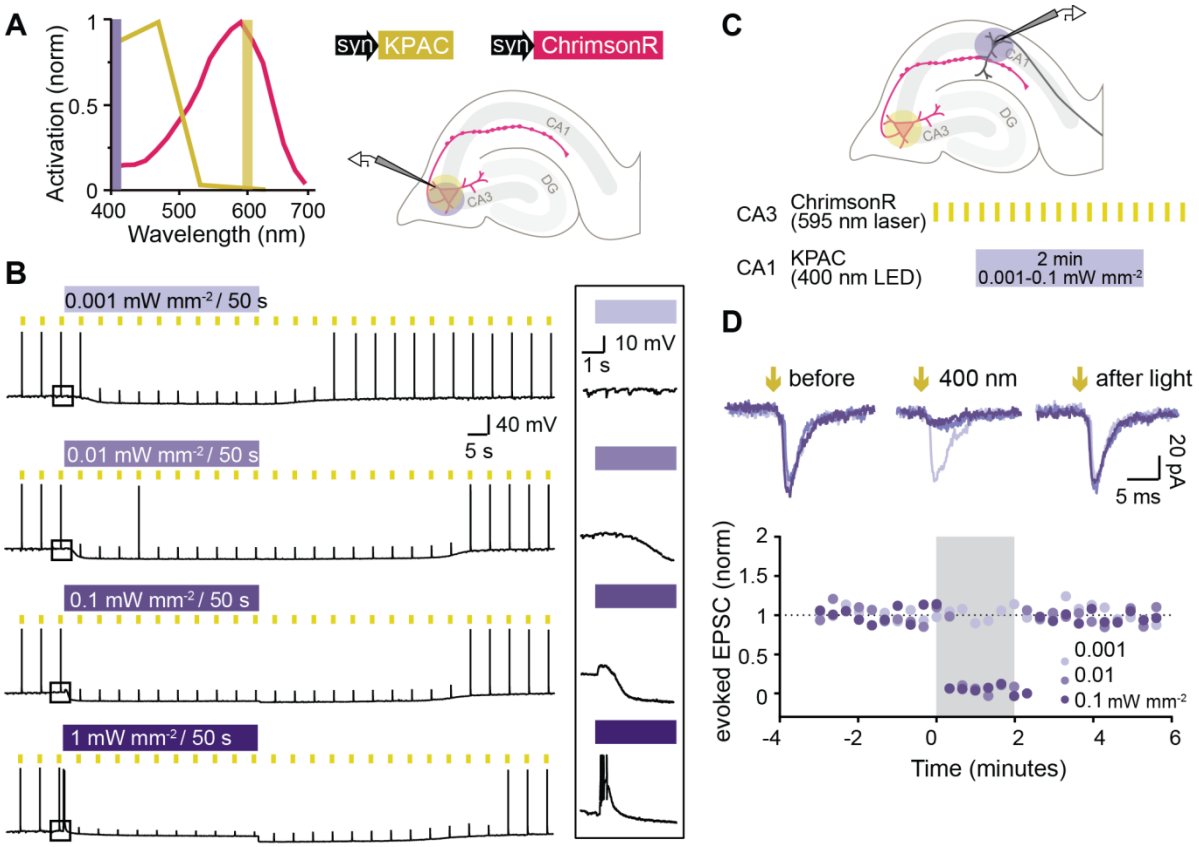

Figure 4.14 KPAC/ChrimsonR pair for dual colour inhibition/excitation. (A) Left: wavelength-dependent activation of KPAC and ChrimsonR, a red-shifted Channelrhodopsin; to minimize cross-activation, the indicated wavelengths were used for activation; Right: Illustration of the experimental design: KPAC and ChrimsonR expressing CA3 neurons were patch-clamped while stimulated with 595 nm laser light and 400 nm LED light. **(B)** AP firing evoked by ChrimsonR activation was blocked by KPAC generated hyperpolarization using medium to very low intensity of 400 nm light. Inset shows the start of KPAC activation and subsequent cross-activation of ChrimsonR at higher violet light intensities. **(C)** Illustration of the experimental design: ChrimsonR evoked EPSCs were recorded in non-transfected CA1 neurons. To block synaptic activity, 400 nm light was shined over the CA1 region (str. pyramidale and str. radiatum). **(D)** KPAC activation at the axon and terminals blocks synaptic currents in area CA1.

To validate the dual color approach, CA3 cells were electroporated with both KPAC and the red-shifted channelrhodopsin ChrimsonR (Klapoetke et al., 2014). Cells were stimulated with a 1 ms long 595 nm laser pulse every 5 seconds in order to elicit ChrimsonR-generated spiking. Because the activation spectrum of ChrimsonR covers a wide range of wavelengths, careful considerations were taken regarding the stimulation conditions of KPAC. To minimize any cross activation of ChrimsonR while attempting to activate KPAC, 400 nm light was used for silencing. Light-activation of KPAC with varying intensities and lengths of light successfully inhibited action potential firing generated by activation of ChrimsonR. The light intensities that were sufficient for

silencing spanned 3 orders of magnitude and were as low as 0.001 mW mm^{-2}. Interestingly, violet light in the 0.1-1 mW mm^{-2} range depolarised the cells at the beginning of the light pulse, indicating that ChrimsonR can get activated even at these low intensities (Figure 4.14 B, zoom-in box). Next, with both ChrimsonR and KPAC expressed presynaptically, I investigated whether KPAC would be able to block synaptic transmission in CA1 generated by presynaptic ChrimsonR currents and spiking (Figure 4.14 C). For this, I patched non-transfected CA1 neurons and recorded yellow-light evoked EPSC. Violet light shined over area CA1 (which will activate KPAC in CA3 axons from *stratum radiatum*) generated a fast and reversible block of synaptic transmission (Figure 4.14 D).

4.2 Assessment of cAMP modulation in hippocampal synaptic transmission

Chemical stimulation of endogenous adenylyl cyclases at the Schaffer collateral synapses increases transmission and induces immediate early gene expression

To examine the contribution of cAMP signaling to synaptic activity and gene expression I stimulated endogenous adenylyl cyclases with the diterpene forskolin, a chemical that has been extensively used to study cAMP signaling in the hippocampus. I confirmed that a forskolin-driven rise in intracellular cAMP increases the frequency (61%) but not amplitude of miniature EPSCs (mEPSCs) at the Schaffer collateral synapse in rat organotypic slice cultures (Renner et al., 2017; Sokolova et al., 2006) (Figure 4.15 A-F). Next, I observed that field excitatory postsynaptic potentials (fEPSPs) in mouse acute hippocampal slices were potentiated for at least one hour after 10 min of forskolin (50 µM) and the phosphodiesterase inhibitor IBMX (75 µM) (Figure 4.15 G-H). In addition, forskolin stimulation lead to expression of the immediate-early gene cFos presumably by activation of the cAMP-PKA-CREB signaling pathway (Figure 4.15 I-J). For this, I confined the analysis to CA1 neurons that 7-9 days previously were electroporated with a plasmid encoding the red fluorescent protein mKate2. An hour after treatment with forskolin, di-deoxy forskolin or DMSO, slices were fixed, stained and the intensity of cFos labelling was measured in mKate2-positive cells. Forskolin-stimulated cAMP induced strong cFos expression, which was not evident when di-deoxy-forskolin or vehicle alone (DMSO) was applied to the rat slice cultures (Figure 4.15 I-J).

Optogenetic Elevation of cAMP Levels in hippocampal neurons

The recently published membrane-targeted photoactivatable adenylyl cyclase, PACmn raises intracellular cAMP and increases PKA activity in neurons (Yang et al., 2021). I confirmed that hippocampal neurons electroporated with plasmids encoding PACmn, PACmn_dV (with a point mutation to decrease Venus fluorescence) or transduced with rAAV2/9 CaMKII-PACmn_dV

produced similar responses to short light stimulation in CA1 neurons also expressing a cAMP preferring CNG channel (Figure 4.16 A-B, G-H). There were not obvious differences in morphology and basic cell properties such as resting membrane potential, action potential threshold, membrane resistance or holding current were not different between the three conditions (Figure 4.16 C-F). Prolonged illumination with blue light (10 minutes 1 mW mm^{-2}) evoked inward currents for the whole duration, indicating a continuous production of cAMP (Figure 4.16 I).

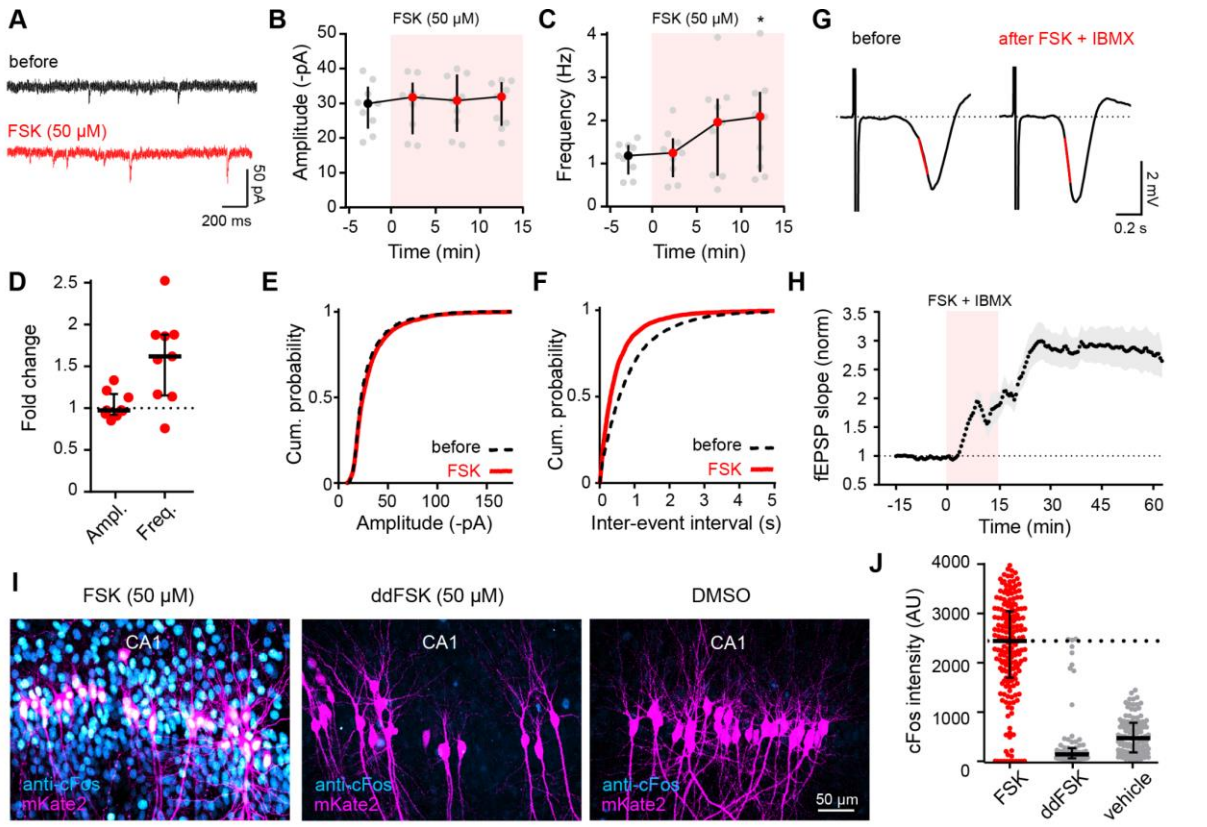

Figure 4.15 Forskolin stimulation of endogenous adenylyl cyclases at the Schaffer collateral synapse increases transmission and induces immediate early gene expression. (A) Miniature excitatory postsynaptic currents (mEPSCs) recorded in a CA1 neuron before and after wash-in of the adenylyl cyclase stimulator forskolin (FSK). **(B)** Forskolin application did not affect the median amplitude of mEPSCs (n = 9 cells). **(C)** Forskolin application induced a significant increase in the frequency of mEPSCs events (n = 9 cells). **(D)** Amplitude and frequency change from baseline 10-15 minutes after wash-in of forskolin solution. **(E)** and **(F)** Cumulative distribution of mEPSC amplitude and inter-event interval before and 10-15 minutes after forskolin. **(G)** Field excitatory postsynaptic potentials evoked by electrical stimulation of Schaffer collaterals from CA1 stratum radiatum of an acute hippocampal slice (mouse) before and 60 min after forskolin/IBMX. Red line indicates slope measured. **(H)** Quantification of experiments as in G. Points and error bars represent mean and SEM. (n = 4 slices). **(I)** Confocal images of hippocampal slice cultures (CA1) stained against cFos after application of forskolin, 1,9-dideoxy-forskolin, or vehicle (DMSO). **(J)** Intensity of cFos signal in nuclei of mKate2-positive CA1 neurons. FSK: n = 188 cells (11 slices); ddFSK: n = 84 cells (7 slices); vehicle: n = 109 cells (7 slices).

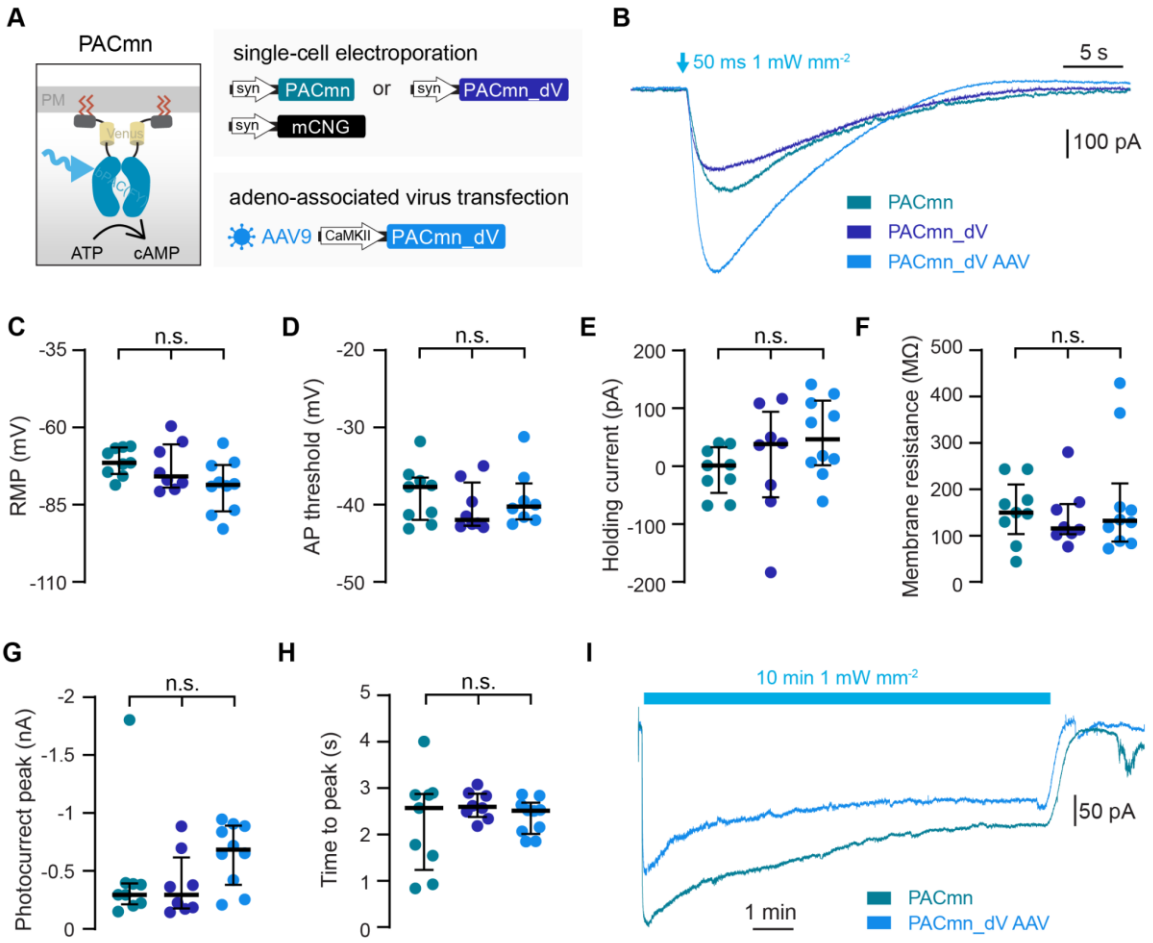

Figure 4.16 Optogenetic elevation of cAMP with photoactivated adenylyl cyclases. (A) PACmn construct design and hippocampal slice culture transfection strategy. **(B)** Representative currents recorded in response to 470 nm light from CA3 hippocampal neurons expressing mCNG together with PACmn, PACmn_dV (single-cell electroporation) or PACmn_dV (virus transfection). **(C-F)** Resting membrane potential **(C)**, action potential threshold **(D)**, holding current **(E)** and membrane resistance of recorded expressing neurons. **(G-H)** Photocurrent amplitude **(G)** and time from stimulation to peak **(H)** in response to 50 ms 470 nm light of 1 mW mm^{-2} intensity. **(I)** Example photocurrents in response to 10 minutes of 470 nm light (1 mW mm^{-2}). Neurons were clamped at -70 mV. Error bars show median and interquartile range. n (neurons) = 9 PACmn, 8 PACmn_dV, 10 PACmn_dV AAV. n.s. = not significant, Dunn's multiple comparisons vs control following Kruskal-Wallis test (p = 0.058).

Pre- and postsynaptic cAMP increase AMPA mEPSCs

My next aim was to determine the site of cAMP-induced changes in miniature excitatory postsynaptic currents (mEPSCs), which are AMPA receptor-mediated currents generated by the spontaneous release of neurotransmitter vesicles. PACmn was expressed using an AAV vector in entire slice cultures or using local injection of AAV either in the CA1 (postsynaptic) or CA3 (presynaptic) neurons (Figure 4.17 A-B). When the AAV was applied on the slice, PACmn was

expressed in all regions whereas after local CA3 or CA1 injection PACmn signal was confined to neurons in the CA3 cell body layer or in CA1, respectively (Figure 4.17 B). As observed using forskolin, light-induced cAMP increased the mEPSC frequency but not amplitude (Figure 4.17 C-D). Interestingly, there were differences depending on the extent of AAV application. When PACmn was expressed everywhere in the slice, the mEPSC frequency increased 2.2 fold (relative to baseline) during the light stimulation and decayed to 1.6 fold after the light was off (Figure 4.17 D-F). When cAMP was raised only in presynaptic CA3 neurons, mEPSC frequency again increased during the light (1.8 fold baseline) and returned to 1.2 fold baseline when the light was off. In contrast, when cAMP was raised only in postsynaptic CA1 neurons, there was a smaller increase in frequency during the light that persisted when the light was off (median fold change during light 1.2, after light 1.3) (Figure 4.17 D-F).

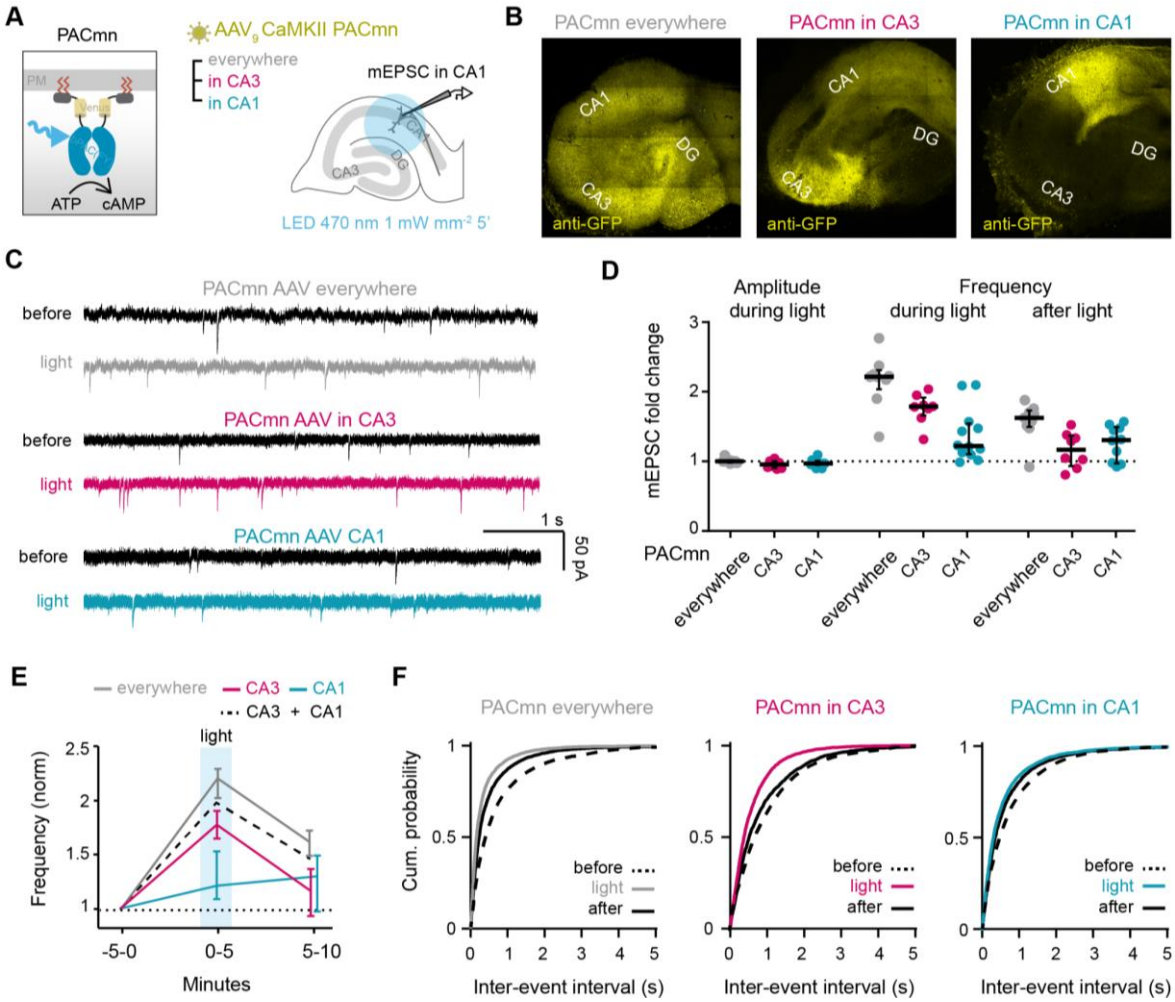

Figure 4.17 Optogenetic elevation of cAMP increased mEPSC frequency at CA3-CA1 synapse. (A) Organotypic hippocampal slice cultures were transfected with an adeno-associated virus (AAV9 serotype, promoter CaMKII) encoding PACmn, a photoactivated adenylyl cyclase. The virus was delivered either on

the whole slice or was locally injected in areas CA1 or CA3. **(B)** Expression of PACmn in areas of interest was confirmed by immunohistochemistry. **(C)** Examples of CA1 miniature recordings in slices where PACmn was expressed everywhere (grey), in CA3 (magenta) or in CA1 (turquoise), before and during its activation with 1 mW mm^{-2} of 470 nm light for 5 minutes. **(D)** Amplitude and frequency change from baseline during and after the light-activation of PACmn. n's = 9, 8, 12 cells, only 1 cell was recorded per slice. **(E)** Timeline of baseline-normalised frequency of mEPSCs in all conditions. **(F)** Cumulative distribution of mEPSC inter-event interval before, during and after light activation of PACmn. All data are shown as median and interquartile range.

Thus, postsynaptic cAMP produces a slowly rising and persistent change in mEPSC frequency whereas presynaptic cAMP rapidly and transiently increases mEPSC frequency. When activated together, the PACmn-induced rise in cAMP has effects on mEPSCs that reflect the addition of pre- and postsynaptic contributions and that closely approximate but are more rapid than the forskolin-induced changes.

Increasing postsynaptic cAMP potentiates CA3-CA1 synapses

I next performed localized injection of PACmn rAAVs into the hippocampus of wildtype mice to achieve expression in all regions (DG, CA3 and CA1) or confined to CA3 (presynaptic) or CA1 (postsynaptic) (Figure 4.18 A-B). In acute slices made from the injected mice, light-driven cAMP had immediate and prolonged effects on CA3-CA1 fEPSPs (Figure 4.18 C-F). Increasing only presynaptic (CA3) cAMP potentiated fEPSPs during the light in most slices (1.27 x baseline) but did not lead to significant LTP of CA3-CA1 synapses (Figure. 4.18 D-F). Due to the high variability of recorded responses, more experiments are needed in this group. A similar rapid and reversible potentiation of release in response to presynaptic cAMP has been reported at hippocampal mossy fibre synapses (Oldani et al., 2021). When PACmn was confined to CA1 or expressed in all regions, the effects on fEPSPs were very similar. fEPSPs were first reduced during the light (0.18 and 0.11 x baseline, respectively) but then LTP lasting at least two hours was apparent (Figure 4.18 C, E-F). The LTP after raising cAMP in CA1 or throughout the slice is similar to forskolin-induced LTP (Figure 4.15 H). The stronger LTP after forskolin suggests that there is a cAMP-dependent contribution to LTP from non-neuronal cell types. All in all, PACmn activation induced strengthening of synapses (short or long lasting) both when expressed exclusively in areas CA1 or CA3, even if cAMP-dependent LTP has long been considered a postsynaptic process at the Schaffer collateral synapse. These results suggest that cAMP can influence synaptic transmission through both pre and postsynaptic mechanisms.

The fEPSP reduction during light when PACmn is expressed in CA1 neurons is most probably due to cAMP-dependent endogenous inward currents that are transiently activated when the light is on (Udwari, 2014). CA1 neurons will thus depolarize, reducing the electrotonic driving force for Na^+ entry through AMPA receptors and therefore decreasing EPSP amplitudes. Increasing cAMP in CA1 neurons evokes endogenous slow inward currents that reverse at a holding potential of -47 mV and that are significantly reduced with inhibitors of the hyperpolarization and cyclic nucleotide-gated (HCN) channel (ZD7288) (Udwari, 2014). Thus, intracellular cAMP leads to HCN channel mediated inward currents at the resting membrane potentials.

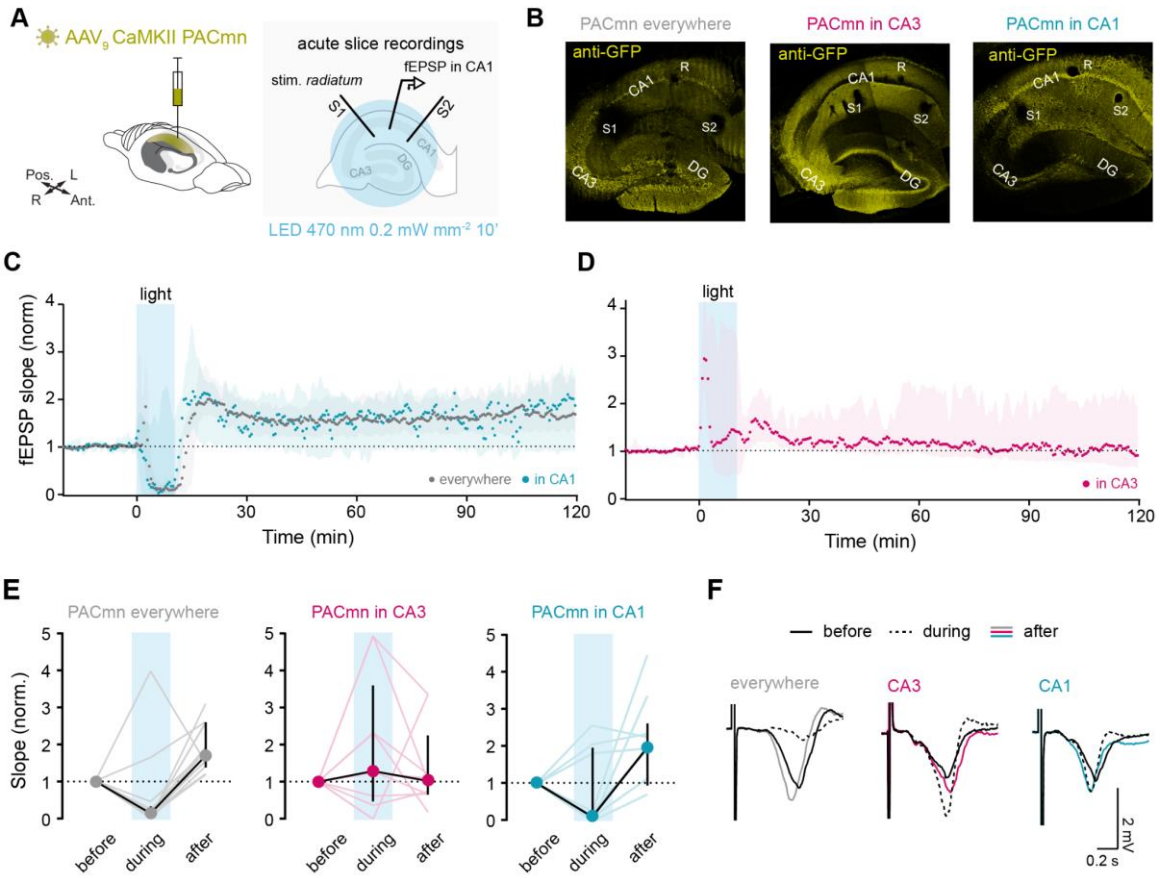

Figure 4.18 Optogenetic elevation of cAMP enhances synaptic transmission between CA3 and CA1 neurons. (A) Experiment design: PACmn-encoding adeno-associated virus was injected in vivo in either CA3, CA1 or in CA3 + CA1 + DG (everywhere). Field recordings in area CA1 were performed in acute slices 7-10 days after injections. **(B)** Expression of PACmn in areas of interest was confirmed by immunohistochemistry. R: recording electrode, S1-S2: stimulating electrodes. **(C)** and **(D)** Timeline of baseline-normalised fEPSP recordings where PACmn was activated with 0.2 mW mm^{-2} of 470 nm light for 10 minutes; n's (recordings, slices, animals) = 14, 7, 2 (everywhere); 9, 6, 2 (CA1); 9, 6, 3 (CA3). **(E)** Change in slope of fEPSPs (relative to baseline) during and 2 hours after PACmn. **(F)** Examples of CA1 field EPSPs responses in slices before, during and 2 hours after light. PACmn was expressed everywhere (grey), in CA3 (magenta) or in CA1 (turquoise). Data shown as median and interquartile range.

Pre and postsynaptic cAMP induces postsynaptic cFos expression

Next, I confirmed that light activation of rAAV-expressed PACmn increases cFos expression in CA1 neurons that were electroporated with mKate2 plasmid on the same day as the rAAV injections (Figure 4.19 A). A week after expression, slice cultures were stimulated with blue light for 10 minutes and 1 hour later fixed and stained against cFos (Figure 4.19 B). Light elevation of cAMP in only pre-, only postsynaptic or throughout the slice induced equally strong cFos expression in mKate-positive CA1 neurons as did forskolin (Figure 4.19 C-D, Figure 4.15 J). Expression of cFos was due to production of cAMP, as slices expressing PACmn but kept in the dark had little cFos expression. Interestingly, the combined effect of simultaneous pre and postsynaptic cAMP was not additive, as I observed with the cAMP effect on mEPSC frequency, but the intensity of cFos labelling was the same regardless of expression pattern. Also different to the effects on fEPSPs both presynaptic and postsynaptic cAMP increased cFos expression.

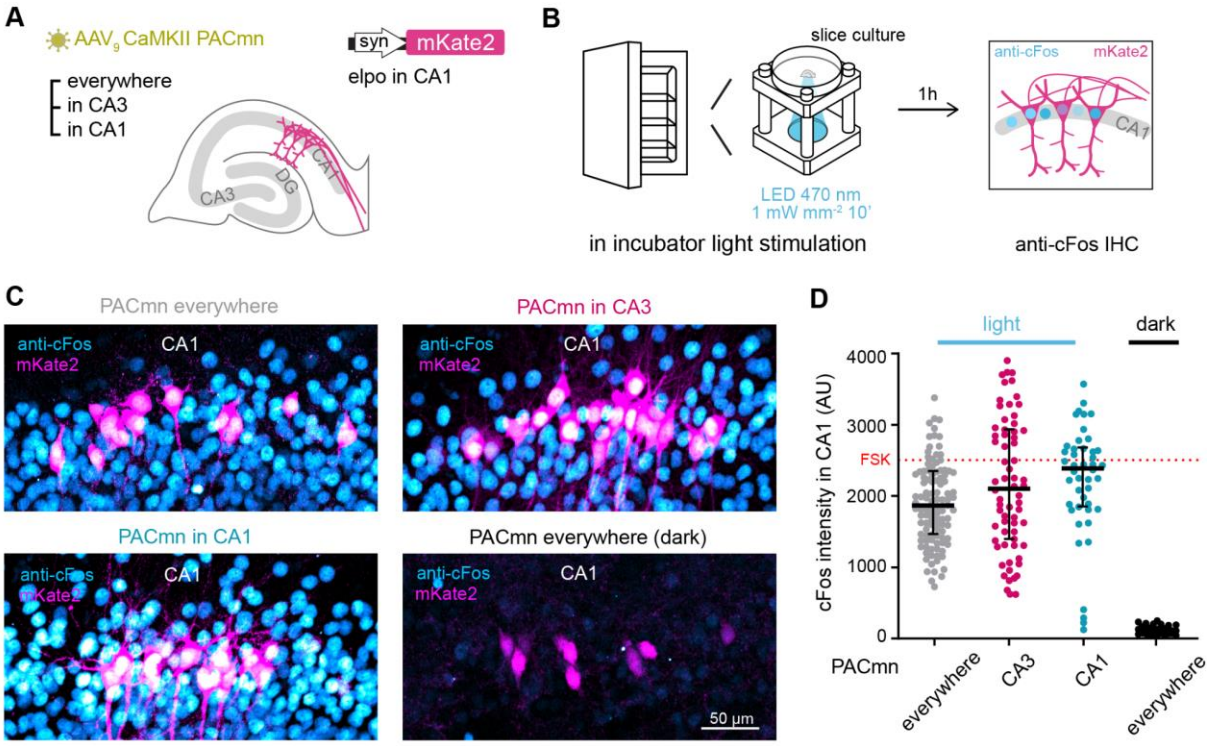

Figure 4.19 Optogenetic elevation of cAMP induces IEG expression in CA1 neurons. (A) Individual CA1 neurons expressed mKate2 (single-cell electroporation) in hippocampal slice cultures that were transduced with AAV to express PACmn in neurons in the entire slice or selectively in CA1 or CA3 regions. **(B)** 5-8 days later PACmn was activated and 1 hour later slices were fixed and stained for cFos. **(C)** Confocal images of CA1 hippocampal neurons stained against cFos after being treated with light or kept in the dark. **(D)** Intensity of cFos signal in nuclei of mKate2+ CA1 neurons. n's (neurons) = 107 (everywhere); 67 (CA3); 45 (CA1); 35 (everywhere dark); Red dotted line represents the median FSK-elicited intensity from Figure 4.15J.

Elevation of cAMP in single postsynaptic neurons does not increase AMPAR currents and is insufficient to induce synaptic strengthening

While there is a vast literature describing the molecular players and mechanisms involved in cAMP-dependent induction of LTP, no studies have achieved single cell resolution. To achieve this, I used single-cell electroporation to express PACmn or soluble bPAC in a few CA1 pyramidal neurons per organotypic slice culture. Given that mEPSC frequency increased when cAMP was elevated with forskolin or PACmn in either pre or postsynaptic neurons, I was surprised that raising cAMP in individual CA1 neurons had no effect on mEPSC amplitude or frequency (Figure 4.20 B-D) (median amplitude fold change after light PACmn 0.91, bPAC 0.94; median frequency change after light PACmn 1.01, bPAC 0.95). Likewise, there was no effect of increasing cAMP on evoked EPSCs when individual CA1 neurons expressed either PACmn or soluble bPAC (Figure 4.20 E-I). This lack of effect was not due to an inability of the patched neurons to exhibit synaptic plasticity as forskolin increased EPSCs. Thus, cAMP-dependent changes in the strength of synaptic transmission require global increases in many neurons. These observations suggest that additional unknown intercellular signaling factors are triggered by cAMP and are required for the functional changes.

cAMP does not induce cFos expression when elevated in single cells

I next investigated whether, as for synaptic function, cAMP raised in individual neurons is also unable to stimulate cFos expression. A week after electroporating up to 20 CA1 neurons, cAMP was increased with light (Figure 4.20 A). Neither PACmn nor bPAC activation led to cFos expression even when phosphodiesterases were inhibited with IBMX (Figure 4.20 J-K). These results further suggest that known downstream effects of cAMP are not mediated by cell autonomous signaling pathways.

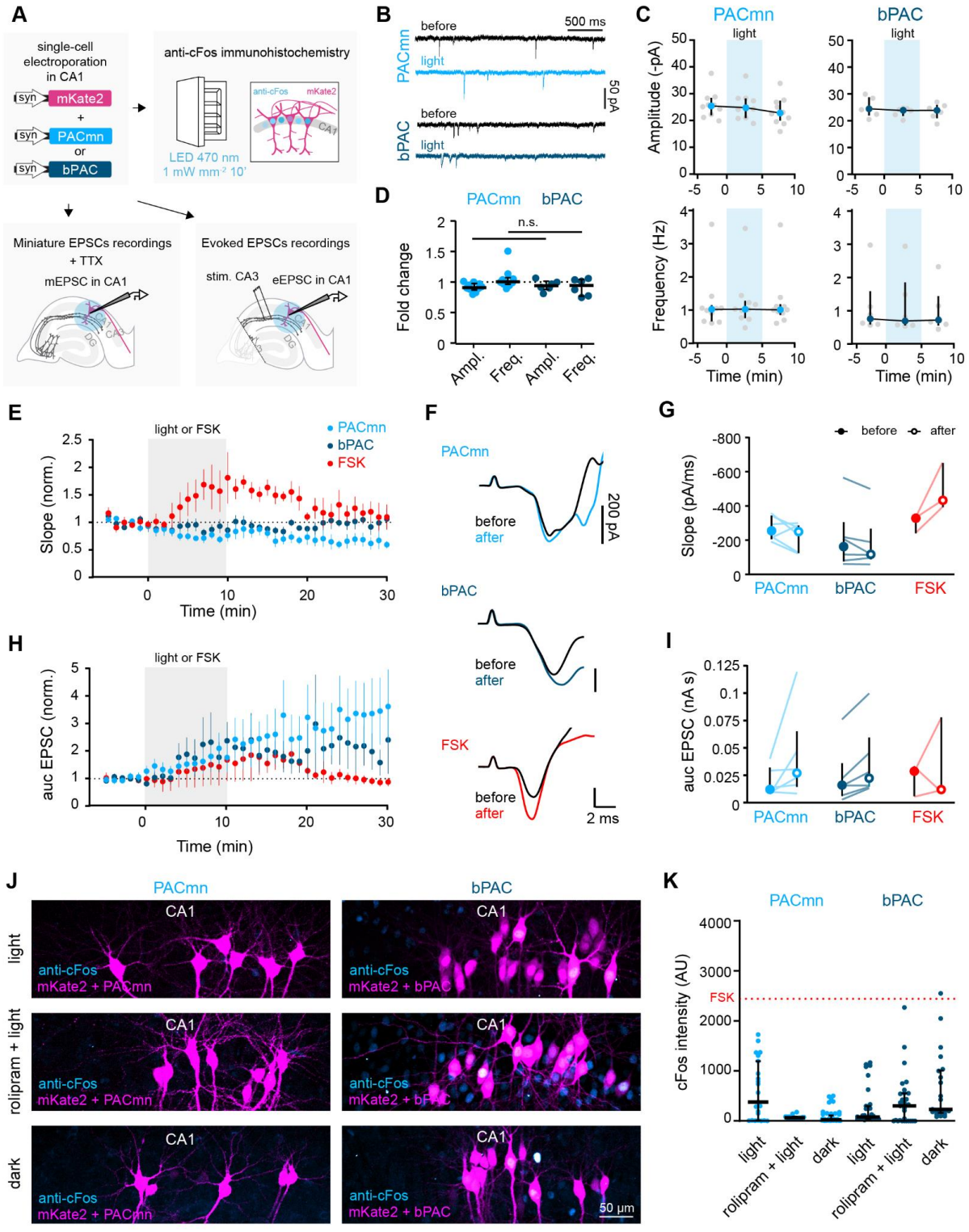

Figure 4.20 Optogenetic elevation of cAMP in single cells does not influence synaptic transmission at CA3-CA1 synapse nor cFos expression. (A) Experimental design: CA1 neurons of organotypic slice cultures were single-cell electroporated with plasmids encoding one of the photo-activatable adenylyl cyclase PACmn or bPAC. After expression, slices were stimulated with blue light and either recorded from

(for miniature EPSCs or evoked EPSCs recordings) or stained against cFos. **(B)** Examples of CA1 miniature recordings in neurons expressing PACmn or bPAC before and during light activation; only 1 cell was recorded per slice. **(C)** The median amplitude and frequency of events detected in 5 minute intervals before, during and after light. Grey points show raw values, n's (neurons) = 11 (PACmn), 7 (bPAC). **(D)** Amplitude and frequency change from baseline 5-10 minutes after the start of the light stimulation. Data shown as median and interquartile range. **(E)** Timeline of baseline-normalised slope of evoked EPSCs recorded in CA1 neurons before and after treatment (10' light stimulation for PACmn or bPAC expressing CA1 neurons and 10' Forskolin for WT CA1 neurons). Light intensity 1 mW mm^{-2} (470 nm), forskolin 50 µM. n's (neurons) = 6 (PACmn), 6 (bPAC), 3 (FSK). Every time point is an average of 3 measurements (ISI 20 s). **(F)** Examples of CA1 evoked EPSC responses before and after treatment. **(G)** Average EPSC slope 5 minutes before and 10-15 minutes after the start of treatment. **(H)** Timeline of baseline-normalised area under curve of evoked EPSCs before and after treatment. Every time point is an average of 3 measurements (ISI 20 s). **(I)** Average area under curve of EPSCs 5 minutes before and 10-15 minutes after the start of treatment. Data shown as median and interquartile range. **(J)** Confocal images of CA1 hippocampal neurons stained against cFos after being treated with light, light + rolipram pre-treatment or kept in the dark. **(K)** Intensity of cFos signal in nuclei of PACmn or bPAC expressing CA1 neurons. n's (from left to right) = 23, 19, 48, 31, 29, 22 neurons. Red dotted line represents the median FSK-elicited intensity from Figure 4.15J. Data shown as median and interquartile range.

cAMP dependent cFos expression is not cell autonomous and requires a synaptically connected network

To examine the signaling downstream of cAMP I focussed on cFos as the readout and applied forskolin to raise cAMP throughout the hippocampal slices. Inhibiting the two main effectors of cAMP (PKA and EPAC) reduced but did not abolish cFos expression (Figure 4.21 A). Interestingly, inhibiting MEK1/2 phosphorylation of ERK (U0126) was more effective, suggesting the ERK rather than PKA activity drives cFos expression (Figure 4.21 A). Surprised that inhibiting PKA and EPAC was not more effective at preventing cFos expression, I tested whether HCN channels might be important. Unexpectedly, inhibiting HCN channels completely abolished cFos expression, indicating that membrane depolarization and activation of an entire network of neurons, and not the classical cAMP-PKA-CREB pathway drives cFos expression (Figure 4.21 A). Indeed, preventing action potentials or fast synaptic transmission were sufficient to completely abolish cFos expression (Figure 4.21 B-D). When light activation of PACmn was used to raise cAMP, action potentials were also required (Figure 4.21 B-D). Together these data suggest that, at least in neurons, the signaling pathways from cAMP leading to changes in synaptic properties or immediate early gene expression are not cell-autonomous. Rather, signaling between neurons, possibly also involving other cell-types such as astrocytes or glia is necessary (Figure 4.22). The transmitters and receptors involved are yet to be identified.

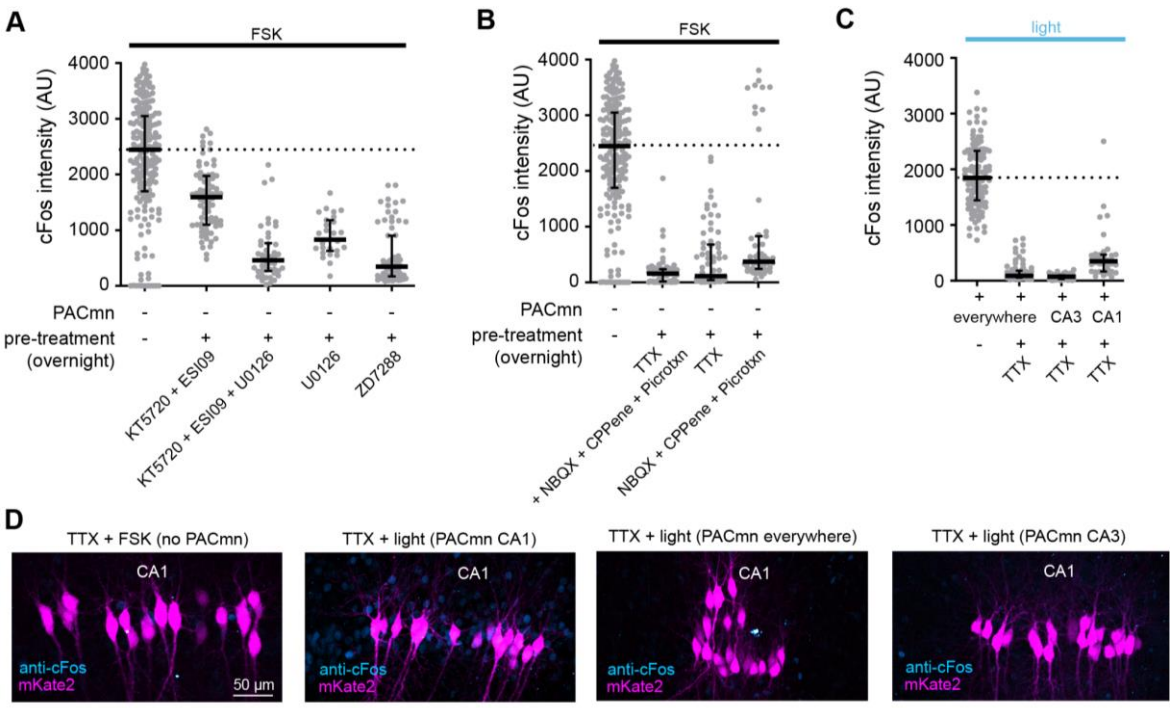

Figure 4.21 Optically induced cAMP-dependent cFos expression is not controlled by the typical cAMP signaling pathway, but by neuronal firing and synaptic transmission. (A) Intensity of cFos signal in nuclei of mKate2-positive CA1 neurons 1 hour after being treated with Forskolin. Slices have been treated overnight with combinations of inhibitors of PKA (KT5720), EPAC (ESI09), MEK1/2 (U0126), HCN channels (ZDF7288). n (neurons) = 188, 74, 46, 27, 70. **(B** cFos intensity in FSK treated CA1 neurons that have been incubated overnight with TTX and/or inhibitors of fast synaptic transmission (NMDAR, AMPAR and GABAR blockers). n (neurons) = 188, 74, 46, 27, 70. **(C)** cFos intensity in light stimulated, PACmn AAV-transduced CA1 neurons (entire slice or selectively in CA1 or CA3) that have been incubated overnight with TTX. n (neurons) = 107, 69, 72, 36. **(D)** Confocal images of CA1 hippocampal neurons expressing mKate2 (alone or together with PACmn via AAV transduction) stained against cFos 1 hour after being treated acutely with light or Forskolin. All conditions were treated overnight with TTX.

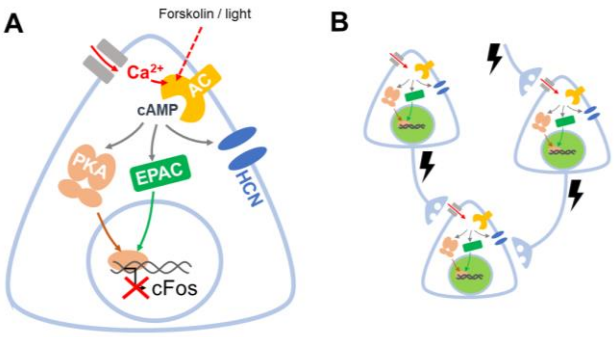

Figure 4.22 Proposed mechanism for cAMP-driven LTP and cFos expression. (A) Artificial elevation of cAMP in single neurons activates the canonical downstream pathways, but is not sufficient to induce cFos expression, and does not change the threshold for synaptic plasticity. **(B)** To induce cFos expression and LTP after cAMP elevation, network activity (spiking) is required.

5. Discussion

5.1 Development of photoactivated tools

In Chapter 4.1 I presented the development and characterization of new photoactivatable tools for modulating cellular activity. These were the rhodopsin guanylyl and adenylyl cyclases CaRhGC and CaRhAC, PACmn a bPAC-based membrane-targeted adenylyl cyclase with no constitutive activity and KPAC, a highly efficient hyperpolarizing tool based on combining bPAC with a cAMP activated potassium channel.

5.1.1 Comparison between PACmn and CaRhAC strategies to optically raise cAMP

Genetically encoded, photo-activated cyclases offer the possibility of precisely manipulating intracellular cAMP with improved spatio-temporal resolution. As stated in previous chapters, the ideal optogenetic tool for cAMP manipulation in mammalian systems should be able to meet the following requirements: fast onset of cyclase activity, encoded by a single gene, small molecular size, insignificant activity in the absence of light, high light sensitivity, high light/dark ratio, narrow activation spectrum, no toxicity when expressed in mammalian cells.

The most popular tool for optical cAMP manipulation has been the soluble adenylyl cyclase bPAC, which meets all requirements with the exception that it exhibits enzymatic activity even in dark conditions. Despite bPAC having one of the lowest dark turnovers (0.057; defined as molecules of cAMP produced by 1 molecule of enzyme per minute) compared with PACs from other species (EuPAC, mPAC), its dark activity is sufficient to activate PKA in hippocampal neurons and to generate changes in *Drosophila* behaviour (Yang et al., 2021). However, its high light sensitivity and thus high light/dark ratio (L/D 1630), made it an ideal candidate for further development and by introducing the F198Y mutation in the substrate binding domain, ATP access was reduced, resulting in a bPAC variant with little to no dark activity (4% of that of bPAC) that still

retains a high L/D ratio (>7000). Incorporating the small anchor peptide from Lyn kinase targeted the expression of the construct to the plasma membrane, resulting in PACmn, a highly light sensitive membrane-targeted adenylyl cyclase with virtually no dark activity. While in neurons PACmn (2xLyn11-Venus-bPAC(198Y)) photocurrents were smaller than that of bPAC, saturating light intensities (around 10 times more for PACmn) generated similar amplitude currents, demonstrating that despite the reduced light activity similar increases in cAMP can be achieved. Furthermore, expression of PACmn does not induce PKA activity, confirming the significant reduction in dark activity.

Another option to optically stimulate cAMP production is using rhodopsin-based cyclases. During my PhD, I contributed to the validation of the photoactivatable guanylyl cyclase from the aquatic fungi *Catenaria anguillulae* as a novel optogenetic tool to increase cGMP (Scheib et al., 2018). Additionally, we generated a rhodopsin adenylyl cyclase by introducing point mutations in the nucleotide binding site that we named CaRhAC. While activation of CaRhAC specifically raises cAMP and not cGMP, quantification of cAMP in oocytes revealed significant residual activity in the absence of light in comparison to control non-injected oocytes (CaRhAC 7.9 pmol cAMP/oocyte; non-injected 3.2 pmol cAMP/oocyte. However, the dark activity measured is lower than that of the first adenylyl cyclase we generated in this study, which was from *Blastocladiella emersonii* (dark turnover YFP-CaRhAC 0.14, YFP-BeRhAC 0.19).

While the dark activity of both PACmn and CaRhAC was measured in oocytes, direct measurements need to be performed in the experimental expression system. When patching neurons expressing both the cyclase and cAMP-sensitive cation channels, a high dark activity should be recorded as lower holding current and membrane resistance. Such differences were not evident in my measurements (Figure 4.9). However, the dark activity of bPAC in neurons was revealed by imaging PKA activity, where just the expression of bPAC increased resting PKA activity. Such measurements are not possible with rhodopsin-based tools (CaRhAC) as their activation spectrum overlaps with the wavelength necessary to image the FRET sensor. This will lead to unwanted CaRhAC activation, defeating the purpose of the experiment. My expectation is that CaRhAC increases PKA activity. Thus, I would recommend PACmn for optogenetic control of adenylyl cyclase.

PACmn is a smaller protein (625 amino acids vs 867 amino acids) and the soluble nature of its main component, bPAC, leaves open the possibility of more specific subcellular targeting. Probably the most important difference is the extremely low dark activity of PACmn in

comparison to CaRhAC. Furthermore, PACmn's light sensing domain is based on BLUF, an extremely light sensitive photoreceptor offering the possibility of using very low doses of light to initiate cyclase activity. Additionally, the BLUF domain is activated by photons in the 400-520 nm visible wavelength range, leaving open a sufficiently wide visible wavelength band (i.e. >530 nm) to combine it with other tools (such as the PKA FRET sensor BoosterPKA or with red-shifted channelrhodopsin). In contrast, the activation wavelengths of CaRhAC occupy most of the visible spectrum, making it hard to use a second tool without inadvertently activating the cyclase. On the other hand, the main advantage of CARhAC over PACmn are the faster kinetics (time from start of light to current onset 20 ms vs 60 ms; time to half decay 1 s vs 6.4 s).

5.1.2 Possible future developments of photo-activated adenylyl cyclases

Although a small and diffusible molecule, cAMP has restricted access to its downstream effectors, leading to compartmentalised cAMP signaling. This is based on the availability of its targets in different cellular compartments, as both PKA and EPAC have been found to exist in multiple isoforms that have a preferred cellular localisation. Similarly, cAMP degradation is accomplished by a large family of phosphodiesterases with affinities ranging from 10-100 nM to more than 10 µM. This implies that although it is a freely diffusing molecule, cyclic AMP's function is regulated by the existence of physical barriers such as cell membranes, the availability of a certain effector molecule (by association to AKAP scaffold complexes) and its uneven degradation by PDEs (Conti et al., 2014). One interesting set of studies looked at differential cAMP concentration within the cell compartments and found that cAMP concentrations at the membrane are insensitive to changes of cytosolic cAMP. This suggests that the two compartments do not equilibrate and that cAMP does not freely diffuse within the cell (Rich et al., 2000, 2001). Multiple studies have since reported similar findings (Agarwal et al., 2016; Richards et al., 2016). For this reason, it would be ideal if one could choose the location of cAMP production in order to determine the roles of subcellular cAMP signaling patterns. To achieve this level of spatial resolution, optogenetic tools can be targeted to subcellular compartments and intracellular organelles by using various targeting sequences. Employing this strategy, bPAC variants were

developed that were targeted to the endosome limiting membrane and the plasma membrane using Hrs and Lyn-derived targeting sequences (Tsvetanova & von Zastrow, 2014). Activation of these constructs in HEK cells revealed the differences in transcriptional signaling based on the origin of cAMP generation. While optogenetic endosomal and cytosolic cAMP elevation induced CREB phosphorylation and transcription of PCK1, a cAMP-regulated enzyme, cAMP generated at the plasma membrane was disconnected from downstream transcription. In a more recent study, bPAC was targeted to synaptic vesicles by fusing it to synaptophysin, a synaptic vesicle protein (Oldani et al., 2021). This new construct, named synaptoPAC, was used to demonstrate light-driven presynaptic potentiation of synaptic connections between dentate gyrus granule cells and CA3 pyramidal neurons in the hippocampus. These experiments show the type of specificity that optogenetic manipulation can provide and highlight the necessity and possibility of subcellular targeting.

Another point of interest for future developments of photoactivatable cyclases is related to their activation spectra. Most naturally-occuring or engineered PACs are based on light-sensing domains that absorb shorter wavelengths of light (BLUF, rhodopsins). This characteristic complicates more complex experimental applications (*in vivo* stimulation), as shorter wavelengths show low tissue penetration and phototoxicity. These issues can be considerably reduced with cyclases that can be activated by light of longer wavelengths. One option for such tools is represented by the engineering of red-shifted photoactivated cyclases. By mutating a key residue (S27A) in the BLUF domain, a bPAC variant with modified absorbance spectra has been developed (Stierl et al., 2014). While its light-modulated enzymatic activity remained unchanged, bPAC-S27A showed a 15 nm shift in its absorption spectra. However, this small spectral change is not sufficient to avoid short-wavelength light challenges and despite efforts, larger shifts in the color tuning of BLUF receptors have not been reported. Another option is the development of phytochrome-based photo-activated cyclases, which can sense light in the red-far red range (600-800 nm). Multiple attempts have been made to engineer such optogenetic tools by fusing the light-sensing domain from several phytochromes to adenylyl cyclase domains (Etzl et al., 2018; Ryu et al., 2014; Stüven et al., 2019). The tools successfully increased cAMP levels and controlled behaviour when expressed in *C. elegans* after red light stimulation. However, the animals exhibited changes in behaviour even in the absence of light, indicating a high enzymatic activity in the dark. While red-light activatable tools can overcome previous shortcomings such as phototoxicity and low penetration of light, there is a clear need to further develop these tools with

regard to their low light activity and high dark activity. Furthermore, the cofactor biliverdin needs to be exogenously added in the case of plant phytochromes as it is not present in animal cells.

5.1.3 Potassium-driven silencing of neurons: advantages, limitations and perspectives

Manipulation of neuronal activity allows us to uncover the function of neurons in relation to a circuit or behaviour. At single cell level, loss-of-function can be achieved either through the block of action potential generation or by the suppression of neurotransmitter release. During the course of my PhD work I contributed to the development of optogenetic silencing tools, SthK-bPAC (Beck et al., 2018) and an improved variant called KPAC (unpublished). The conceptualisation of these optogenetic silencers takes inspiration from the neuron's inherent method of stopping an action potential, namely K^+ conductance. Given that in most neurons the reversal potential of K^+ is even more negative than the resting membrane potential, engineering a light activated K^+ channel would enable efficient block of action potentials.

Over the years there have been a couple of attempts to engineer a light-activatable K^+ channel. The first of such tools designed used a photopharmacogenetic approach, where engineered K^+-selective channels or subunits would open upon binding of a synthetic photoswitchable tethered ligand (Banghart et al., 2004; Fortin et al., 2011; Janovjak et al., 2010). While this strategy offers light-controlled, reversible K^+ conductance, it relies on the continuous presence of the chemical ligand to block the channel's opening. Another remarkable attempt at creating a light-gated K^+ channel is represented by the development of BLINK1 and BLINK2, miniature viral K^+ channels (Kcv) that are fused to a light-activated LOV2 domain (Alberio et al., 2018; Cosentino et al., 2015). These first light-gated K^+ channels did not require additional cofactors and their activation with blue light generated changes in behaviour of *Drosophila* larvae. However, their poor expression in mammalian cells hampered their widespread application by the neuroscience community.

By fusing a cAMP-gated K^+ channel (SthK) to bPAC, we were able to develop a light-activatable K^+ channel that relies on light-driven cAMP production that will then bind and open the channel, allowing K^+ ions to flow outside the cell (Beck et al., 2018). At the same time, a tool

with a similar configuration (SthK and bPAC, unfused; named PAC-K) was developed and characterised in neurons, cardiomyocytes and zebrafish embryos (Bernal Sierra et al., 2018). The original construct we described in (Beck et al., 2018) displayed hyperpolarizing activity even in the absence of light (when measured in oocytes), a clear indication that the SthK channel opens at resting levels of cAMP. To lower the high cAMP affinity of the channel and avoid its activation at resting cAMP, we developed an improved construct that we named KPAC. By introducing the T378V mutation in the cyclic nucleotide binding domain (CNBD) of the SthK channel and shortening the C_{term} segment of the CNBD domain we were able to restrict cAMP binding and thus resting level opening of the channel.

However, the reduction in cAMP binding affinity did not affect photocurrent generation. Indeed, hippocampal neurons displayed cell membrane hyperpolarization of up to 20 mV upon light stimulation. Moreover, due to the high light sensitivity of bPAC, light as little as 0.001 mW mm^{-2} was able to stop action potential generation. The hyperpolarization was so robust that high-frequency firing (100 Hz) generated by somatic current injections of up to 1.5 nA was completely abolished by light intensities as low as 0.001 mW mm^{-2}. This level of silencing efficiency is unprecedented, as all anion-conducting inhibitory optogenetic tools show a shift in the rheobase (minimum current injection necessary to elicit an action potential) of maximum 600 pA upon light stimulation (1-10 mW mm^{-2}), and almost no shift when using low light-intensity pulses (Govorunova et al., 2015; Wietek et al., 2015). In contrast, KPAC is able to shift the action potential threshold by ~700 pA when using only 0.001 mW mm^{-2} blue light and blocks firing completely (maximum current injection 1400 pA) when using 0.01 mW mm^{-2}. One major limitation of KPAC in contrast with anion-conducting rhodopsins, is that due to the slow closing kinetics of bPAC, its activation cannot suppress single action potentials within trains. However, the long-lasting effects of bPAC activation provide the valuable property of long-term sustained silencing with low doses of light. Indeed, prolonged inhibition of spiking can be achieved with KPAC either by using short, repetitive pulses of light, or by prolonging the illumination for the whole duration that inhibition is needed (at lower light intensities).

An enormous advantage given by bPAC's light-sensing BLUF domain is its insensitivity to wavelengths longer than 520 nm, which enables push-pull type experiments, where two colors are used to drive inhibition and excitation within the same cell. However, most red-shifted excitatory opsins (Chrimson, ChrimsonR, ChRmine) retain a significant absorption of 400-470 nm light. For this reason, careful considerations must be taken in order to minimize any cross

activation of the excitatory opsin while activating the silencer. I show that 0.1 mW mm^{-2} of 400 nm light is sufficient to activate co-expressed ChrimsonR and lead to depolarisation, while 1 mW mm^{-2} (a commonly used intensity to activate anion-conducting rhodopsins) generates action potentials. However, due to the high light sensitivity of KPAC, this issue is circumvented by adjusting the light dose parameters (increasing pulse length and lowering its intensity).

The main motivation for silencing neurons is blocking their contribution to circuit activity by inhibiting synaptic transmission. As previously stated, this can be achieved by either blocking action potential generation or by suppression of neurotransmitter release. Due to the higher concentration of chloride at synaptic terminals in comparison to the somatodendritic compartment, the anion-conduction rhodopsins silence action potentials when activated at the soma but increase transmitter release when activated at terminals (Mahn et al., 2016, 2018; Malyshev et al., 2017; Wiegert et al., 2016). While this is not yet tested for KPAC it may be that hyperpolarizing only axon terminals will be effective at blocking transmitter release even when the neuron has fired an action potential.

While KPAC is a highly promising optogenetic tool for silencing neuronal activity, there are two main concerns that could hinder its widespread application. While measurements in KPAC-expressing oocytes did not show any cAMP production in the dark (due to bPAC being fused the the SthK channel), a recent study using PAC-K silencer to study seizures in healthy and epileptic mice showed light-independent effects (generalised seizures and pyramidal cell dispersion in healthy animals) (Kleis et al., 2021). The effects observed in the absence of light might be due to the two component system used, where bPAC is soluble and unattached to the SthK. However, further measurements in KPAC-expressing neurons need to be performed in order to measure the dark activity of KPAC in neurons. Since there are no working cAMP sensors spectrally compatible with KPAC, one can measure PKA activity as a proxy for enzymatic dark activity. Another limitation of KPAC comes from the design of the construct that relies on intracellular cAMP production that will bind and open the SthK channel. This increase in intracellular messenger could trigger cAMP-mediated activation of signaling cascades, affecting molecular pathways and metabolic processes. A more elegant design that could circumvent some of these issues would be the development of cGMP-based silencers using a similar design as KPAC. In neurons, intracellular cyclic GMP concentration is extremely low, indicating that the activation of a cGMP-based silencer by resting cGMP levels could be avoided. Additionally, cGMP signaling is not as complex as that of cAMP, suggesting that cyclic nucleotide signaling side

effects might also be reduced. Recently, such a tool has been developed, where a cGMP-gated K^+ channel (BeCNG1) from *Blastocladiella emersonii* was combined with the photoactivated cyclase BeRhGC (Henß et al., 2021). While the system was capable of small hyperpolarization of body wall muscle in *C. elegans*, its potential to hyperpolarize other cell types is yet to be investigated. Ultimately, a "perfect" K^+-based optogenetic silencer would not need to rely on intracellular cyclic nucleotide synthesis. Long sought for, a naturally-occurring K^+-conducting channelrhodopsin has recently been discovered and characterised in cortical neurons (Govorunova et al., 2021). The question still remains if this new tool is suitable for long range projection silencing of transmitter release.

5.1.4 Advantages and constraints of optogenetic modulators

Since their advent, optogenetic techniques have proven very powerful experimental methods, especially in the field of neuroscience. Their use brought the possibility of dissecting and interrogating neuronal functions with better specificity and temporal resolution. In chapter 4.1 I have presented the development and testing of multiple light-activated modulators. The use of optogenetic modulatory tools (light-activated enzymes) offers several advantages over classical pharmaceutical manipulations, but also carries some limitations and experimental constraints.

Advantages

An important advantage of optogenetic tools when compared with pharmacology is that of effect specificity, as their activation results in effects that are well understood and studied. While a drug can have multiple, unknown binding sites within a cell, activation of a light-gated cyclase will only produce cyclic nucleotides and any other effects observed will be due to cyclic nucleotide signaling. For example, a clear advantage of light-activated cyclases over forskolin is that their activation will only lead to cAMP production, while forskolin binds not only to endogenous cyclases to stimulate their activity, but also exhibits cAMP-independent effects, such as binding to voltage-gated potassium channels or acetylcholine receptors (Allgaier et al., 1990; Hoshi et al., 1988; White, 1988).

Another advantage of optogenetic tools is the high temporal and spatial resolution given by their activation kinetics and targeting possibilities. Actuators (excitatory and inhibitory opsins)

and modulatory tools are activated on a millisecond to second time range, allowing their activation to be timed with the observation of other phenomena (spiking) or even behaviour. Furthermore, by using gene delivery techniques such as single-cell electroporation or virus injections, the engineered protein can be very specifically targeted to particular brain regions and subregions and its activation constrained not only to the expression site but also to the illuminated area. Using optogenetic tools to investigate synaptic connectivity for example, one is able to selectively target either the pre or the postsynaptic compartment, a feature that is unavailable with classic pharmacological manipulation.

Probably the most important advantage of optogenetics is being able to achieve cell type specificity of effects. While drug application will generate effects in all cells regardless of their type, by using cell-specific promoters in the gene delivery design, one is able to target the optogenetic tool's effects to the cell type of interest while keeping the rest unaffected. For instance, when applied on a hippocampal slice, forskolin stimulates cAMP production in all pyramidal neurons, interneurons, microglia and astrocytes. By transfecting tissue with AAVs that encode PACmn under a cell type-specific promoter (GFAP for astrocytes, synapsin for neurons, CaMKII for excitatory neurons), expression and activation of the construct is limited to that particular cell type. This enables more sophisticated experimental designs where one can investigate cell type-specific cAMP-dependent processes without stimulating cAMP production in all other cells, thus avoiding the introduction of signaling "artefacts" originating from other cell types.

Constraints

Perhaps the biggest constraint in successfully using photoactivatable adenylyl cyclases is the activity of the enzyme even in the absence of light. Dark activity has been a limiting factor starting with the earliest discovered light-activated cyclases (EuPAC), which has a measured turnover in the dark of 0.38 (defined as molecules of cAMP produced by 1 molecule of enzyme per minute). Its successor, bPAC (and one of the most widely used modulatory optogenetic tools), has a 7 times lower intrinsic dark activity, with a measured turnover rate in the dark of 0.057. However, even in this low range, the dark activity leads to unstimulated cAMP signaling, as PKA activity in neurons expressing bPAC and kept in the dark was higher than in neurons without bPAC (Figure 4.6). This makes the interpretation of experimental results a very difficult task, as there is no clear

baseline condition before photo-manipulation.

Another important limitation deals with phototoxicity and tissue heating. Albeit more relevant for in-vivo experiments, these issues stem from the need of high-power light sources (such as an implanted light fiber) to activate the expressed optogenetic tool. High intensity or prolonged illumination leads to tissue damage, heating and activation of endogenous light-sensitive proteins, particularly when using highly energetic shorter wavelengths (Godley et al., 2005; Hockberger et al., 1999). One way to reduce these effects is to use longer wavelengths for activation, which will also penetrate tissue better. However, most modulatory tools rely on light between 400 and 530 nm for activation.

Another consideration to keep in mind when designing experiments that rely on optogenetic stimulation is the availability of intracellular factors necessary for activation. In the case of photoactivatable cyclases, the availability of intracellular ATP and GTP is the rate limiting factor of the enzymatic process. Furthermore, microbial rhodopsins (such are the RhGC/AC presented in this thesis) rely on the availability of retinal for light-activation. *All-trans* retinal acts as the chromophore for microbial rhodopsin-based optogenetic tools and while it is produced as part of the vitamin A metabolism in most mammalian tissue (including the brain), lower order organisms that are commonly used in research (*C. elegans, D. melanogaster*) lack *all-trans* retinal and need supplementation through food (Nagel et al., 2005; Schroll et al., 2006).

5.2 Assessment of cAMP modulation of hippocampal synaptic transmission

During my PhD I sought to assess the role of cAMP signaling in hippocampal synaptic transmission by using photo-activated cyclases that offer a more specific spatial and temporal manipulation of cAMP. The questions I sought to answer are: (1) Can synaptic transmission be enhanced at the Schaffer collateral synapse by elevating cAMP optogenetically? (2) Does the locus of cAMP elevation matter? Does cAMP induce synaptic plasticity when elevated presynaptically or postsynaptically? (3) Does intracellular cAMP elevation lead to gene expression, a marker of synaptic plasticity maintenance mechanisms?

Optical LTP induction with photoactivatable cyclases

While the "chemical LTP" protocol has been widely used and enables the study of cAMP-dependent hippocampal plasticity, it suffers from certain limitations, such as drug target specificity (forskolin exhibits cAMP-independent effects, such as binding to voltage-gated potassium channels or acetylcholine receptors (Allgaier et al., 1990; Hoshi et al., 1988; White, 1988)), lack of temporal control due to wash in and wash out, lack of cell-type specificity and spatial resolution. Alternative techniques, such as using transgenic animals with a certain gene (encoding adenylyl cyclase, PKA etc) knocked out or overexpressing produced valuable knowledge on the topic (summarised in chapter 1.3.2) but require the complex and lengthy process of generating transgenic animals.

My results show that global optogenetic elevation of cAMP in excitatory neurons is sufficient on its own to enhance transmission at hippocampal Schaffer collateral synapses. In order to simulate the global elevation in cAMP that is generated with the chemical approach, I used a viral vector containing PACmn_dV under the control of CaMKII promoter to transfect all areas of the hippocampus (dentate gyrus, CA3 and CA1). Light activation of PACmn led to a massive increase in the slope of field EPSPs recorded in area CA1 of hippocampal acute slices, demonstrating that an increase in cAMP is sufficient on its own to enhance synaptic strength at Schaffer collateral synapse, confirming previous studies (Frey et al., 1993; Huang & Kandel, 1994). Furthermore, the enhancement lasted for more than 2 hours, indicating that the effects observed

can be assigned to the late stage of LTP. In contrast to chemical LTP protocols, potentiation of synapses occurs even without blocking the activity of phosphodiesterases, a typical constraint of chemical LTP protocol success (Bolshakov et al., 1997; Duffy & Nguyen, 2003; Frey et al., 1993; Lu & Gean, 1999; Otmakhov et al., 2004). This demonstrates the efficiency of optical cAMP generation in transfected cells and validates optogenetic manipulation of cAMP as an equally effective method for plasticity induction as chemical LTP. Indeed, optical induction of LTP using photoactivatable adenylyl cyclases has been recently reported in other synapses in the hippocampus (medial perforant path to dentate gyrus synapse and mossy fiber-CA3 synapse) (Luyben et al., 2020; Oldani et al., 2021).

Pre versus post debate

The locus of induction and expression of cAMP-dependent LTP is still a matter of debate, mainly due to the difficulty of selectively disrupting signaling pathways only in the pre or the postsynaptic compartments. Using photoactivatable cyclases, one is able to selectively target either the pre or the postsynaptic compartment, a feature that is unavailable with classic pharmacological manipulations. The results I present in chapter 4.2 show that global optogenetic cAMP elevation mimics the effects of the chemical LTP protocol. However, the effects are not restricted to a postsynaptic cAMP increase as a presynaptic cAMP elevation also induces potentiation at the Schaffer collateral synapse, albeit only transiently. Similarly, the frequency of miniature AMPA currents increases upon light activation, with differences depending on the extent of AAV application. The fast but transient increase in the frequency of events when cAMP is elevated presynaptically and the slow, sustained increase when elevated postsynaptically show the existence of parallel signaling mechanisms in the pre and postsynaptic compartment. The summation of these two components closely reflects the effect of stimulating PACmn in all regions (DG, CA3 and CA1). This shows that simultaneous activation of these mechanisms (like in the case of pharmacology) cannot clearly differentiate between pre and postsynaptic mechanisms. These findings fit very well with existing literature, as both pre and postsynaptic cAMP-dependent changes in spontaneous and evoked transmission have been reported (Bolshakov et al., 1997; Carroll et al., 1998; Castillo, 2012; Chavez-Noriega & Stevens, 1994; Duffy & Nguyen, 2003; Otmakhov et al., 2004; Renner et al., 2017; Sokolova et al., 2006). Moreover, a recent study using synaptic vesicle-targeted bPAC to investigate cAMP modulation of mossy fiber-CA3

synaptic transmission showed only a transient increase in transmission that decayed to baseline 30 minutes after light stimulation (Oldani et al., 2021). Albeit a different hippocampal synapse, their finding that presynaptic cAMP induces only a rapid potentiation of release suggests that the timeline of the presynaptic effects I observed at Schaffer collateral-CA1 synapse might not be specific only to this synapse.

Previous studies have mostly relied on electrophysiological measurements of postsynaptic responses as a reporter of synaptic changes, with cAMP-elevating treatments not being restricted to a specific synaptic compartment. The interpretation of results and the conclusions drawn regarding cAMP's locus of action included assumptions about basic synaptic properties that have since been called into question. These assumptions include the constantness of release site number (silent synapses lack functional AMPA receptors but become functional with potentiation), paired pulse ratio as a proxy for release probability (it is also influenced by lateral diffusion or AMPA receptor desensitisation), and a stable AMPA:NMDA ratio as a proxy for presynaptic mechanisms (Heine et al., 2008; Isaac et al., 1995; Liao et al., 1995; Trussell et al., 1993). While the results presented in this thesis are based on similar experimental design, the locus of cAMP elevation is predefined by the expression of the photoactivatable cyclase, thus simplifying the interpretation.

No direct pathway between cAMP and LTP/cFos expression

The results presented in chapter 4.2 show that global optogenetic cAMP elevation mimics the effects of the chemical LTP protocol and induces potentiation at the Schaffer collateral as well as cFos expression in CA1 neurons. However, the results also show that it is not possible to induce cFos expression nor LTP by optogenetically elevating cAMP in individual CA1 pyramidal cells. This was an unexpected finding, as postsynaptic cAMP is thought to be sufficient on its own to induce LTP and gene expression at CA3-CA1 synapses. This implies that the signaling pathway that is activated in the case of global cAMP elevation is more complex than the simplistic cAMP-PKA-CREB. Similar findings were observed by (Udwari, 2014), where a photoactivatable adenylate cyclase (bPAC) was used to investigate cAMP contribution to LTP in individual CA1 neurons for the first time. His work revealed that elevation of cAMP in single neurons is not sufficient to drive synaptic potentiation. Additionally, elevating cAMP postsynaptically could not change the threshold for LTP induction by theta burst stimulation protocol in paired recordings of pre and

postsynaptic neurons. Interestingly, similar results were reported even when using chemical stimulation of adenylyl cyclases. One of the earliest indications that cAMP elevation in multiple neurons does not reflect the changes in single neurons came from (Blitzer et al., 1995). They observed no change in the EPSP when postsynaptic neurons were patched with the cAMP analogue Sp-cAMPS in the intracellular solution, in contrast to when the analogue was applied on the whole slice (Frey et al., 1993).

Similarly surprising was the fact that, while forskolin and global optogenetic cAMP elevation induces cFos expression, cAMP increases in single CA1 neurons does not. These results, together with the fact that PACmn activation leads to cAMP downstream effector activation (Figure 4.11 E-F), indicate that pathways leading from cAMP via PKA/EPAC to CREB activation and immediate early gene expression are not functional in resting neurons. This was further confirmed by the fact that forskolin-driven cFos expression could not be blocked by PKA inhibitors or EPAC inhibitors, the main cAMP effectors. What is absolutely required for cAMP-driven cFos induction is action potential firing and synaptic transmission, suggesting that CRE-CREB activating pathways may only become functional if intracellular calcium levels are elevated. The finding that induction of LTP by chemical agents cannot be attributed directly to the activation of cAMP-dependent signaling pathways has been previously reported in hippocampal acute slices (Otmakhov et al., 2004). They reported that forskolin-driven potentiation of synapses is a NMDA-dependent process and that it requires presynaptic activity and NMDA receptor activation. In my work I could show similar findings, as TTX or blockers of fast synaptic transmission blocked the expression of cFos both when cAMP was elevated chemically or optogenetically. Furthermore, as cAMP activates a depolarizing current in neurons via activation of HCN channels and blocking them hindered cFos expression, it is even possible that global cAMP-driven LTP and cFos expression are simply a consequence of synchronized firing.

Consideration of limitations

The approach used in this study revealed new insights about the mechanisms of cAMP signaling in plasticity-related processes. However, the surprising result of a lack of LTP and cFos expression when PACmn was expressed and activated in single-cells, obliges us to consider the possible limitations of the experimental approach. One first concern is that due to the long exposure time, forskolin is able to stimulate a more robust increase in cAMP than the optogenetic

tools used. However, I have shown that PACmn, when co-expressed with the cAMP-sensitive CNG channels, generated photocurrents that obscured forskolin-generated drop in holding current (Figure 4.10 E). Furthemore, even when illuminated for 10 minutes (the same stimulation protocol used in synaptic plasticity experiments), PACmn generates stable photocurrents, a clear indication of continuous cAMP production (Figure 4.16 I). Another limitation could come from the dilution of intracellular contents that is associated with whole-cell patch clamp electrophysiology, a phenomenon that might affect the normal functioning of intracellular signaling. While this is a valid concern, the lack of LTP was not due to an inability of the patched neurons to exhibit synaptic plasticity, as forskolin increased EPSCs. Furthermore, a previous attempt at optogenetic LTP in single cells using bPAC has used sharp recordings to avoid dilution of intracellular contents, with similar results to mine (Udwari, 2014).

Prospects for future work

It is becoming more apparent that cAMP is insufficient on its own to induce synaptic transmission or cFos expression, even if effector proteins such as PKA are activated. I hypothesise that synchronised firing due to HCN channel activation is the cause for cAMP-dependent potentiation, not the activation of cAMP-PKA-CREB pathway in the same cell. However, while the inhibition of cFos expression when using HCN channel blockers points in this direction, direct measurements of high neuronal activity must be performed. A direct measurement of increased activity could be achieved by imaging postsynaptic calcium. As HCN channels are also permeable to calcium, I would expect an increase in intracellular calcium during light activation. However, my results also suggest that retrograde signaling molecules might be involved in this process, as global postsynaptic cAMP-dependent LTP and cFos expression do not occur when firing and synaptic connectivity are blocked. So far I have not tested any candidate, but one can start by rounding up the usual suspects: nitric oxide, as its synthesis by nitric oxide synthase is a calcium-dependent process (Arancio et al., 1996; Huang, 1997; Pigott & Garthwaite, 2016; Schuman & Madison, 1991); BDNF, as its expression is CREB-dependent and presynaptic TrkB receptor activation by BDNF leads to an increase in neurotransmitter release (Lin et al., 2018; Tao et al., 1998; Zakharenko et al., 2003).

Furthermore, in the light of the new findings, some established hallmarks of cAMP elevation should be reassessed. For example, activation of cAMP signaling pathways has been

associated with changes in dendritic spine density. While an acute activation of PKA activity can increase spine density, chronic PKA stimulation reduces it in apical dendrites of CA1 neurons (Lu et al., 2011). These findings are based on chemical activation or block of PKA activity. An interesting experiment would be to assess spine morphology and density changes by using either a global or a single-cell optogenetic elevation of cAMP and evaluate if any potential changes are due to cell-autonomous mechanisms or if, similar to my findings, they rely on global activation of synaptic connections.

By using a global approach to elevate cAMP I was able to validate previous studies that reported LTP upon chemical stimulation of adenylyl cyclases. However, non-neuronal cAMP signaling effects cannot be ruled out, as pharmacology cannot differentiate between neurons and glia. Additional cAMP-dependent mechanisms in non-neuronal cells that can influence synaptic transmission efficiency can coexist with reported neuronal pathways. A recent study evaluated the effect of astrocytic cAMP signaling on synaptic transmission (Zhou et al., 2021). Using a bPAC transgenic mouse line, optogenetic elevation of astrocytic cAMP was sufficient to induce synaptic plasticity at CA3-CA1 synapse, cFos expression and to modulate memory and behaviour. These new findings demonstrate that cAMP signaling and its role in synaptic plasticity is not as simple as previously thought and that multiple mechanisms can coexist. With the development of more specific methods of manipulating cAMP signaling pathways, we are able to understand its complex role in synaptic transmission and plasticity.

6. Summary

English

The second messenger cAMP is an ubiquitously important molecule that controls an impressive number of intracellular functions, from cell division, motility, metabolism and gene expression. In the hippocampus, cAMP is thought to induce long term-potentiation of synaptic connections, a process considered to represent the cellular correlate of learning and memory storage. At the Schaffer collateral CA1 synapse, cAMP-dependent induction of LTP is thought to be a postsynaptic process, characterised by an increase in glutamate receptor number and conductance, as well as expression of immediate-early genes. However, due to the lack of spatial and temporal resolution of classical pharmacology, it cannot be differentiated between pre and postsynaptic cAMP sites of action, nor can individual cell contributions be evaluated.

For this reason, during my PhD I have worked on the development of photoactivatable adenylyl cyclases that can be expressed and activated in cell types of interest and specific synaptic compartments, ensuring a higher spatial resolution of cAMP manipulation. In this work I present the development and characterisation of multiple optogenetic tools with which one can optogenetically elevate intracellular cAMP with high spatial and temporal resolution (PACmn, RhAC).

To establish if optogenetic elevation of cAMP in excitatory neurons is sufficient on its own to enhance transmission at hippocampal Schaffer collateral synapse, I expressed PACmn in population and single cells. While global optogenetic cAMP elevation mimics the effects of pharmacological treatment, the effects are not restricted to postsynaptic cAMP, as presynaptic cAMP elevation also induces transient potentiation at the Schaffer collateral. Furthermore, global optogenetic cAMP induces cFos expression in CA1 neurons, regardless if elevated pre or postsynaptically. However, it is not possible to induce cFos expression or LTP in individual CA1 pyramidal cells, indicating that the pathways leading from cAMP via PKA/EPAC to CREB activation and immediate early gene expression are not functional in resting neurons and that action potential firing and synaptic transmission are required.

Deutsch

Der Second Messenger cAMP steuert eine beeindruckende Anzahl intrazellulärer Funktionen, von Zellteilung und Motilität über Stoffwechsel bis zu Genexpression. Es wird angenommen, dass cAMP im Hippocampus die langfristige Potenzierung synaptischer Verbindungen (LTP) induziert, ein Prozess, der als zelluläres Korrelat von Lernen und Gedächtnis angesehen wird. An den Synapsen zwischen CA3- und CA1-Pyramidenzellen (Schaffer Kollaterale) wird die cAMP-abhängige Induktion von LTP als postsynaptischer Prozess angesehen, der durch eine Zunahme der Anzahl und Leitfähigkeit von Glutamat-Rezeptoren sowie durch Expression von Immediate-Early-Genen gekennzeichnet ist. Aufgrund der breitbandigen Wirkung klassischer Pharmakologie besteht jedoch Unsicherheit, ob cAMP prä- oder postsynaptisch wirkt, und eine eventuelle Beteiligung nicht-neuronaler Zellen (Astrozyten, Microglia) kann ebenfalls nicht ausgeschlossen werden.

Um die Mechanismen cAMP-abhängiger Plastizität besser untersuchen zu können, habe ich während meiner Promotion an der Entwicklung photoaktivierbarer Adenylylzyklasen gearbeitet, die in genetisch definierten Zelltypen und spezifischen synaptischen Kompartimenten exprimiert und aktiviert werden können, um zellspezifische und zeitlich präzise cAMP-Manipulation zu ermöglichen. In dieser Arbeit präsentiere ich die Entwicklung und Charakterisierung mehrerer optogenetischer Werkzeuge, mit denen man intrazelluläres cAMP mit hoher räumlicher und zeitlicher Auflösung optogenetisch erhöhen kann (PACmn, RhAC). Darüber hinaus war ich an der Entwicklung eines neuartigen Werkzeugs zur neuronalen Hemmung beteiligt, in dem eine photoaktivierbare Cyclase mit einem zyklischen Nukleotid-gesteuerten Kaliumkanal kombiniert ist.

Um festzustellen, ob die optogenetische Erhöhung von cAMP in exzitatorischen Neuronen allein ausreicht, um die Übertragung an der hippocampalen Schaffer-Kollateral-synapse zu potenzieren, exprimierte ich PACmn in einzelnen Zellen oder viral in größeren Zellgruppen. Obwohl globale optogenetische cAMP-Erhöhung ähnliche Konsequenzen wie die pharmakologische cAMP-Erhöhung hatte, ist die Wirkungen nicht durch postsynaptisches cAMP zu erklären, da eine cAMP-Erhöhung in den präsynaptischen Zellen (CA3) auch eine transiente Potenzierung der Schaffer-Kollateralsynapse induzierte. Expression von cFos in CA1-Neuronen war unabhängig davon, ob cAMP prä- oder postsynaptisch erhöht wurde. Es ist jedoch nicht möglich, cFos-Expression oder LTP in einzelnen CA1-Pyramidenzellen zu induzieren, was darauf hindeutet, dass die klassischen zellautonomen Signalwege, die von cAMP über PKA/EPAC zur CREB-Aktivierung und Expression von Immediate-Early-Genen führen, cAMP-induzierte synaptische Plastizität nicht erklären können. Meine Arbeit legt nahe, dass die konzertierte Aktivität vieler Neuronen und Glutamat-Freisetzung für die Aktivierung von CREB notwendig sind.

7. References

Abraham, W. C., & Williams, J. M. (2003). Properties and mechanisms of LTP maintenance. *The Neuroscientist: A Review Journal Bringing Neurobiology, Neurology and Psychiatry*, *9*(6), 463–474.

Abreu, N., & Levitz, J. (2020). Optogenetic Techniques for Manipulating and Sensing G Protein-Coupled Receptor Signaling. *Methods in Molecular Biology* , *2173*, 21–51.

Agarwal, S. R., Clancy, C. E., & Harvey, R. D. (2016). Mechanisms Restricting Diffusion of Intracellular cAMP. *Scientific Reports*, *6*.

Agnetta, L., Kauk, M., Canizal, M. C. A., Messerer, R., Holzgrabe, U., Hoffmann, C., & Decker, M. (2017). A Photoswitchable Dualsteric Ligand Controlling Receptor Efficacy. *Angewandte Chemie* , *56*(25).

Airan, R. D., Thompson, K. R., Fenno, L. E., Bernstein, H., & Deisseroth, K. (2009). Temporally precise in vivo control of intracellular signalling. *Nature*, *458*(7241).

Alasbahi, R. H., & Melzig, M. F. (2010a). Plectranthus barbatus: a review of phytochemistry, ethnobotanical uses and pharmacology - Part 1. *Planta Medica*, *76*(7), 653–661.

Alasbahi, R. H., & Melzig, M. F. (2010b). Plectranthus barbatus: a review of phytochemistry, ethnobotanical uses and pharmacology - part 2. *Planta Medica*, *76*(8), 753–765.

Alasbahi, R. H., & Melzig, M. F. (2012). Forskolin and derivatives as tools for studying the role of cAMP. *Die Pharmazie*, *67*(1), 5–13.

Alberio, L., Locarno, A., Saponaro, A., Romano, E., Bercier, V., Albadri, S., Simeoni, F., Moleri, S., Pelucchi, S., Porro, A., & Others. (2018). A light-gated potassium channel for sustained neuronal inhibition. *Nature Methods*, *15*(11), 969–976.

Allgaier, C., Choi, B. K., & Hertting, G. (1990). Forskolin modulates acetylcholine release in the hippocampus independently of adenylate cyclase activation. In *European Journal of Pharmacology* (Vol. 181, Issue 3, pp. 279–282).

Altarejos, J. Y., & Montminy, M. (2011). CREB and the CRTC co-activators: sensors for hormonal and metabolic signals. *Nature Reviews. Molecular Cell Biology*, *12*(3), 141–151.

Amaral, D. G., Scharfman, H. E., & Lavenex, P. (2007). The dentate gyrus: fundamental neuroanatomical organization (dentate gyrus for dummies). *Progress in Brain Research*, *163*, 3–22.

Andersen, P., Morris, R., Amaral, D., Bliss, T., & O'Keefe, J. (2006). *The Hippocampus Book*. Oxford University Press.

Arancio, O., Kiebler, M., Lee, C. J., Lev-Ram, V., Tsien, R. Y., Kandel, E. R., & Hawkins, R. D. (1996). Nitric Oxide Acts Directly in the Presynaptic Neuron to Produce Long-Term Potentiationin Cultured Hippocampal Neurons. *Cell*, *87*(6), 1025–1035.

Avelar, G. M., Schumacher, R. I., Zaini, P. A., Leonard, G., Richards, T. A., & Gomes, S. L. (2014a). A Rhodopsin-Guanylyl Cyclase Gene Fusion Functions in Visual Perception in a Fungus. In *Current Biology* (Vol. 24,

Issue 11, pp. 1234–1240).

Avelar, G. M., Schumacher, R. I., Zaini, P. A., Leonard, G., Richards, T. A., & Gomes, S. L. (2014b). A rhodopsin-guanylyl cyclase gene fusion functions in visual perception in a fungus. *Current Biology: CB*, *24*(11), 1234–1240.

Bailes, H. J., Zhuang, L.-Y., & Lucas, R. J. (2012). Reproducible and sustained regulation of Gαs signalling using a metazoan opsin as an optogenetic tool. *PloS One*, *7*(1), e30774.

Banghart, M., Borges, K., Isacoff, E., Trauner, D., & Kramer, R. H. (2004). Light-activated ion channels for remote control of neuronal firing. *Nature Neuroscience*, *7*(12), 1381–1386.

Barco, A., Alarcon, J. M., & Kandel, E. R. (2002). Expression of constitutively active CREB protein facilitates the late phase of long-term potentiation by enhancing synaptic capture. *Cell*, *108*(5), 689–703.

Basu, J., & Siegelbaum, S. A. (2015). The Corticohippocampal Circuit, Synaptic Plasticity, and Memory. *Cold Spring Harbor Perspectives in Biology*, *7*(11).

Beaulieu, J.-M., & Gainetdinov, R. R. (2011). The physiology, signaling, and pharmacology of dopamine receptors. *Pharmacological Reviews*, *63*(1), 182–217.

Beck, S., Yu-Strzelczyk, J., Pauls, D., Constantin, O. M., Gee, C. E., Ehmann, N., Kittel, R. J., Nagel, G., & Gao, S. (2018). Synthetic Light-Activated Ion Channels for Optogenetic Activation and Inhibition. *Frontiers in Neuroscience*, *12*, 643.

Beharry, A. A., & Woolley, G. A. (2011). Azobenzene photoswitches for biomolecules. *Chemical Society Reviews*, *40*(8), 4422–4437.

Bender, A. T., & Beavo, J. A. (2006). Cyclic nucleotide phosphodiesterases: molecular regulation to clinical use. *Pharmacological Reviews*, *58*(3), 488–520.

Bernal Sierra, Y. A., Rost, B. R., Pofahl, M., Fernandes, A. M., Kopton, R. A., Moser, S., Holtkamp, D., Masala, N., Beed, P., Tukker, J. J., Oldani, S., Bönigk, W., Kohl, P., Baier, H., Schneider-Warme, F., Hegemann, P., Beck, H., Seifert, R., & Schmitz, D. (2018). Potassium channel-based optogenetic silencing. *Nature Communications*, *9*(1), 4611.

Berthet, J., Sutherland, E. W., & Rall, T. W. (1957). The assay of glucagon and epinephrine with use of liver homogenates. *The Journal of Biological Chemistry*, *229*(1), 351–361.

Biel, M. (2009). Cyclic nucleotide-regulated cation channels. *The Journal of Biological Chemistry*, *284*(14), 9017–9021.

Biel, M., & Michalakis, S. (2007). Function and dysfunction of CNG channels: insights from channelopathies and mouse models. *Molecular Neurobiology*, *35*(3), 266–277.

Biel, M., Wahl-Schott, C., Michalakis, S., & Zong, X. (2009). Hyperpolarization-activated cation channels: from genes to function. *Physiological Reviews*, *89*(3), 847–885.

Blain-Hartung, M., Rockwell, N. C., Moreno, M. V., Martin, S. S., Gan, F., Bryant, D. A., & Lagarias, J. C. (2018). Cyanobacteriochrome-based photoswitchable adenylyl cyclases (cPACs) for broad spectrum light regulation of cAMP levels in cells. *The Journal of Biological Chemistry*, *293*(22), 8473–8483.

Bliss, T. V., & Collingridge, G. L. (1993). A synaptic model of memory: long-term potentiation in the hippocampus. *Nature*, *361*(6407), 31–39.

Bliss, T. V., & Lomo, T. (1973). Long-lasting potentiation of synaptic transmission in the dentate area of the anaesthetized rabbit following stimulation of the perforant path. *The Journal of Physiology*, *232*(2), 331–356.

Bliss, T. V. P., & Collingridge, G. L. (2013). Expression of NMDA receptor-dependent LTP in the hippocampus: bridging the divide. *Molecular Brain*, *6*, 5.

Bliss, T. V. P., Collingridge, G. L., Morris, R. G. M., & Reymann, K. G. (2018). Long-term potentiation in the hippocampus: discovery, mechanisms and function. In *Neuroforum* (Vol. 24, Issue 3, pp. A103–A120).

Blitzer, R. D., Wong, T., Nouranifar, R., Iyengar, R., & Landau, E. M. (1995). Postsynaptic cAMP pathway gates early LTP in hippocampal CA1 region. *Neuron*, *15*(6), 1403–1414.

Blumenthal, S. A. (2012). Earl Sutherland (1915-1975) and the Discovery of Cyclic AMP. In *Perspectives in Biology and Medicine* (Vol. 55, Issue 2, pp. 236–249).

Bockaert, J., Claeysen, S., Bécamel, C., Dumuis, A., & Marin, P. (2006). Neuronal 5-HT metabotropic receptors: fine-tuning of their structure, signaling, and roles in synaptic modulation. In *Cell and Tissue Research* (Vol. 326, Issue 2, pp. 553–572).

Bolshakov, V. Y., Golan, H., Kandel, E. R., & Siegelbaum, S. A. (1997). Recruitment of new sites of synaptic transmission during the cAMP-dependent late phase of LTP at CA3-CA1 synapses in the hippocampus. *Neuron*, *19*(3), 635–651.

Bonni, A. (1999). Cell Survival Promoted by the Ras-MAPK Signaling Pathway by Transcription-Dependent and -Independent Mechanisms. In *Science* (Vol. 286, Issue 5443, pp. 1358–1362).

Bos, J. L. (2006). Epac proteins: multi-purpose cAMP targets. *Trends in Biochemical Sciences*, *31*(12), 680–686.

Bradley, J., Zhang, Y., Bakin, R., Lester, H. A., Ronnett, G. V., & Zinn, K. (1997). Functional Expression of the Heteromeric "Olfactory" Cyclic Nucleotide-Gated Channel in the Hippocampus: A Potential Effector of Synaptic Plasticity in Brain Neurons. In *The Journal of Neuroscience* (Vol. 17, Issue 6, pp. 1993–2005).

Brams, M., Kusch, J., Spurny, R., Benndorf, K., & Ulens, C. (2014). Family of prokaryote cyclic nucleotide-modulated ion channels. *Proceedings of the National Academy of Sciences of the United States of America*, *111*(21), 7855–7860.

Bredt, D. S., & Nicoll, R. A. (2003). AMPA Receptor Trafficking at Excitatory Synapses. In *Neuron* (Vol. 40, Issue 2, pp. 361–379).

Brown, G. P., Blitzer, R. D., Connor, J. H., Wong, T., Shenolikar, S., Iyengar, R., & Landau, E. M. (2000). Long-term potentiation induced by theta frequency stimulation is regulated by a protein phosphatase-1-operated gate. *The Journal of Neuroscience: The Official Journal of the Society for Neuroscience*, *20*(21), 7880–7887.

Brown, S., & Sharpey-Schäfer, S. E. A. (1889). *An Investigation Into the Functions of the Occipital & Temporal Lobes of the Monkey's Brain*.

Burwell, R. D., Witter, M. P., & Amaral, D. G. (1995). Perirhinal and postrhinal cortices of the rat: a review of the neuroanatomical literature and comparison with findings from the monkey brain. *Hippocampus*, *5*(5), 390–408.

Carroll, R. C., Nicoll, R. A., & Malenka, R. C. (1998). Effects of PKA and PKC on miniature excitatory postsynaptic currents in CA1 pyramidal cells. *Journal of Neurophysiology*, *80*(5), 2797–2800.

Castillo, P. E. (2012). Presynaptic LTP and LTD of excitatory and inhibitory synapses. *Cold Spring Harbor Perspectives in Biology*, *4*(2).

Castillo, P. E., Janz, R., Südhof, T. C., Tzounopoulos, T., Malenka, R. C., & Nicoll, R. A. (1997). Rab3A is essential for mossy fibre long-term potentiation in the hippocampus. *Nature*, *388*(6642), 590–593.

Castillo, P. E., Schoch, S., Schmitz, F., Südhof, T. C., & Malenka, R. C. (2002). RIM1α is required for presynaptic long-term potentiation. In *Nature* (Vol. 415, Issue 6869, pp. 327–330).

Chavez-Noriega, L. E., & Stevens, C. F. (1994). Increased transmitter release at excitatory synapses produced by direct activation of adenylate cyclase in rat hippocampal slices. In *The Journal of Neuroscience* (Vol. 14, Issue 1, pp. 310–317).

Cheng, X., Ji, Z., Tsalkova, T., & Mei, F. (2008). Epac and PKA: a tale of two intracellular cAMP receptors. In *Acta Biochimica et Biophysica Sinica* (Vol. 40, Issue 7, pp. 651–662).

Chen, Y., & Sabatini, B. L. (2021). The Kinase Specificity of Protein Kinase Inhibitor Peptide. *Frontiers in Pharmacology*, *12*, 632815.

Chevaleyre, V., Heifets, B. D., Kaeser, P. S., Südhof, T. C., & Castillo, P. E. (2007). Endocannabinoid-mediated long-term plasticity requires cAMP/PKA signaling and RIM1alpha. *Neuron*, *54*(5), 801–812.

Citri, A., & Malenka, R. C. (2008). Synaptic Plasticity: Multiple Forms, Functions, and Mechanisms. In *Neuropsychopharmacology* (Vol. 33, Issue 1, pp. 18–41).

Conti, M., & Beavo, J. (2007). Biochemistry and Physiology of Cyclic Nucleotide Phosphodiesterases: Essential Components in Cyclic Nucleotide Signaling. In *Annual Review of Biochemistry* (Vol. 76, Issue 1, pp. 481–511).

Conti, M., Mika, D., & Richter, W. (2014). Cyclic AMP compartments and signaling specificity: Role of cyclic nucleotide phosphodiesterases. In *Journal of General Physiology* (Vol. 143, Issue 1, pp. 29–38).

Cook, W. H., Lipkin, D., & Markham, R. (1957). THE FORMATION OF A CYCLIC DIANHYDRODIADENYLIC ACID (I) BY THE ALKALINE DEGRADATION OF ADENOSINE-5'-TRIPHOSPHORIC ACID (II)1. In *Journal of the American Chemical Society* (Vol. 79, Issue 13, pp. 3607–3608).

Cooper, D. M. F., & Crossthwaite, A. J. (2006). Higher-order organization and regulation of adenylyl cyclases. *Trends in Pharmacological Sciences*, *27*(8), 426–431.

Corradetti, R., Ballerini, L., Pugliese, A. M., & Pepeu, G. (1992). Serotonin blocks the long-term potentiation induced by primed burst stimulation in the CA1 region of rat hippocampal slices. *Neuroscience*, *46*(3), 511–518.

Cosentino, C., Alberio, L., Gazzarrini, S., Aquila, M., Romano, E., Cermenati, S., Zuccolini, P., Petersen, J., Beltrame,

M., Van Etten, J. L., Christie, J. M., Thiel, G., & Moroni, A. (2015). Optogenetics. Engineering of a light-gated potassium channel. *Science*, *348*(6235), 707–710.

Dalton, G. D., & Dewey, W. L. (2006). Protein kinase inhibitor peptide (PKI): a family of endogenous neuropeptides that modulate neuronal cAMP-dependent protein kinase function. *Neuropeptides*, *40*(1), 23–34.

Dannenberg, H., Young, K., & Hasselmo, M. (2017). Modulation of Hippocampal Circuits by Muscarinic and Nicotinic Receptors. *Frontiers in Neural Circuits*, *11*, 102.

Dasari, S., & Gulledge, A. T. (2011). M1 and M4 receptors modulate hippocampal pyramidal neurons. *Journal of Neurophysiology*, *105*(2), 779–792.

Davies, S. P., Reddy, H., Caivano, M., & Cohen, P. (2000). Specificity and mechanism of action of some commonly used protein kinase inhibitors. *Biochemical Journal*, *351*(Pt 1), 95–105.

Deisseroth, K., Bito, H., & Tsien, R. W. (1996). Signaling from synapse to nucleus: postsynaptic CREB phosphorylation during multiple forms of hippocampal synaptic plasticity. *Neuron*, *16*(1), 89–101.

Descarries, L., Gisiger, V., & Steriade, M. (1997). Diffuse transmission by acetylcholine in the CNS. *Progress in Neurobiology*, *53*(5), 603–625.

Dessauer, C. W. (2009). Adenylyl Cyclase–A-kinase Anchoring Protein Complexes: The Next Dimension in cAMP Signaling. In *Molecular Pharmacology* (Vol. 76, Issue 5, pp. 935–941).

Dessauer, C. W., Watts, V. J., Ostrom, R. S., Conti, M., Dove, S., & Seifert, R. (2017). International Union of Basic and Clinical Pharmacology. CI. Structures and Small Molecule Modulators of Mammalian Adenylyl Cyclases. *Pharmacological Reviews*, *69*(2), 93–139.

de Wit, R. J., Hekstra, D., Jastorff, B., Stec, W. J., Baraniak, J., Van Driel, R., & Van Haastert, P. J. (1984). Inhibitory action of certain cyclophosphate derivatives of cAMP on cAMP-dependent protein kinases. *European Journal of Biochemistry / FEBS*, *142*(2), 255–260.

Diering, G. H., Heo, S., Hussain, N. K., Liu, B., & Huganir, R. L. (2016). Extensive phosphorylation of AMPA receptors in neurons. *Proceedings of the National Academy of Sciences of the United States of America*, *113*(33), E4920–E4927.

Ding, C., Potter, E. D., Qiu, W., Coon, S. L., Levine, M. A., & Guggino, S. E. (1997). Cloning and widespread distribution of the rat rod-type cyclic nucleotide-gated cation channel. *The American Journal of Physiology*, *272*(4 Pt 1), C1335–C1344.

Dodge-Kafka, K. L., Langeberg, L., & Scott, J. D. (2006). Compartmentation of cyclic nucleotide signaling in the heart: the role of A-kinase anchoring proteins. *Circulation Research*, *98*(8), 993–1001.

Dudek, S. M., Alexander, G. M., & Farris, S. (2016). Rediscovering area CA2: unique properties and functions. *Nature Reviews. Neuroscience*, *17*(2), 89–102.

Duffy, S. N., & Nguyen, P. V. (2003). Postsynaptic Application of a Peptide Inhibitor of cAMP-Dependent Protein Kinase Blocks Expression of Long-Lasting Synaptic Potentiation in Hippocampal Neurons. In *The Journal of Neuroscience* (Vol. 23, Issue 4, pp. 1142–1150).

Edelmann, E., & Lessmann, V. (2018). Dopaminergic innervation and modulation of hippocampal networks. *Cell and Tissue Research*, *373*(3), 711–727.

Emptage, N. J., Reid, C. A., Fine, A., & Bliss, T. V. P. (2003). Optical quantal analysis reveals a presynaptic component of LTP at hippocampal Schaffer-associational synapses. *Neuron*, *38*(5), 797–804.

Espadas, I., Ortiz, O., García-Sanz, P., Sanz-Magro, A., Alberquilla, S., Solis, O., Delgado-García, J. M., Gruart, A., & Moratalla, R. (2021). Dopamine D2R is Required for Hippocampal-dependent Memory and Plasticity at the CA3-CA1 Synapse. In *Cerebral Cortex* (Vol. 31, Issue 4, pp. 2187–2204).

Esteban, J. A., Shi, S.-H., Wilson, C., Nuriya, M., Huganir, R. L., & Malinow, R. (2003). PKA phosphorylation of AMPA receptor subunits controls synaptic trafficking underlying plasticity. *Nature Neuroscience*, *6*(2), 136–143.

Etzl, S., Lindner, R., Nelson, M. D., & Winkler, A. (2018). Structure-guided design and functional characterization of an artificial red light-regulated guanylate/adenylate cyclase for optogenetic applications. *The Journal of Biological Chemistry*, *293*(23), 9078–9089.

Fortin, D. L., Dunn, T. W., Fedorchak, A., Allen, D., Montpetit, R., Banghart, M. R., Trauner, D., Adelman, J. P., & Kramer, R. H. (2011). Optogenetic photochemical control of designer K+ channels in mammalian neurons. *Journal of Neurophysiology*, *106*(1), 488–496.

Fourcaudot, E., Gambino, F., Humeau, Y., Casassus, G., Shaban, H., Poulain, B., & Lüthi, A. (2008). cAMP/PKA signaling and RIM1alpha mediate presynaptic LTP in the lateral amygdala. *Proceedings of the National Academy of Sciences of the United States of America*, *105*(39), 15130–15135.

Francis, S. H., Conti, M., & Houslay, M. D. (2011). *Phosphodiesterases as Drug Targets*. Springer Science & Business Media.

Frey, U., Huang, Y. Y., & Kandel, E. R. (1993). Effects of cAMP simulate a late stage of LTP in hippocampal CA1 neurons. *Science*, *260*(5114), 1661–1664.

Frey, U., Schroeder, H., & Matthies, H. (1990). Dopaminergic antagonists prevent long-term maintenance of posttetanic LTP in the CA1 region of rat hippocampal slices. *Brain Research*, *522*(1), 69–75.

Fritz-Laylin, L. K., Prochnik, S. E., Ginger, M. L., Dacks, J. B., Carpenter, M. L., Field, M. C., Kuo, A., Paredez, A., Chapman, J., Pham, J., Shu, S., Neupane, R., Cipriano, M., Mancuso, J., Tu, H., Salamov, A., Lindquist, E., Shapiro, H., Lucas, S., … Dawson, S. C. (2010). The genome of Naegleria gruberi illuminates early eukaryotic versatility. *Cell*, *140*(5), 631–642.

Ganesan, S., Ameer-Beg, S. M., Ng, T. T. C., Vojnovic, B., & Wouters, F. S. (2006). A dark yellow fluorescent protein (YFP)-based Resonance Energy-Accepting Chromoprotein (REACh) for Förster resonance energy transfer with GFP. *Proceedings of the National Academy of Sciences of the United States of America*, *103*(11), 4089–4094.

Gao, S., Nagpal, J., Schneider, M. W., Kozjak-Pavlovic, V., Nagel, G., & Gottschalk, A. (2015). Optogenetic manipulation of cGMP in cells and animals by the tightly light-regulated guanylyl-cyclase opsin CyclOp. *Nature Communications*, *6*, 8046.

Gasbarri, A., Sulli, A., & Packard, M. G. (1997). The dopaminergic mesencephalic projections to the hippocampal formation in the rat. *Progress in Neuro-Psychopharmacology & Biological Psychiatry*, *21*(1), 1–22.

Gasser, C., Taiber, S., Yeh, C.-M., Wittig, C. H., Hegemann, P., Ryu, S., Wunder, F., & Möglich, A. (2014). Engineering of a red-light-activated human cAMP/cGMP-specific phosphodiesterase. *Proceedings of the National Academy of Sciences of the United States of America*, *111*(24), 8803–8808.

Gee, C. E., Ohmert, I., Wiegert, J. S., & Oertner, T. G. (2017). Preparation of Slice Cultures from Rodent Hippocampus. *Cold Spring Harbor Protocols*, *2017*(2).

Gelinas, J. N., & Nguyen, P. V. (2005). Beta-adrenergic receptor activation facilitates induction of a protein synthesis-dependent late phase of long-term potentiation. *The Journal of Neuroscience: The Official Journal of the Society for Neuroscience*, *25*(13), 3294–3303.

Gilbert, P. E., & Brushfield, A. M. (2009). The role of the CA3 hippocampal subregion in spatial memory: a process oriented behavioral assessment. *Progress in Neuro-Psychopharmacology & Biological Psychiatry*, *33*(5), 774–781.

Godley, B. F., Shamsi, F. A., Liang, F.-Q., Jarrett, S. G., Davies, S., & Boulton, M. (2005). Blue light induces mitochondrial DNA damage and free radical production in epithelial cells. *The Journal of Biological Chemistry*, *280*(22), 21061–21066.

Gonzalez, G. A., & Montminy, M. R. (1989). Cyclic AMP stimulates somatostatin gene transcription by phosphorylation of CREB at serine 133. In *Cell* (Vol. 59, Issue 4, pp. 675–680).

Govorunova, E. G., Gou, Y., Sineshchekov, O. A., & Li, H. (2021). Kalium rhodopsins: Natural light-gated potassium channels. *bioRxiv*.

Govorunova, E. G., Sineshchekov, O. A., Janz, R., Liu, X., & Spudich, J. L. (2015). NEUROSCIENCE. Natural light-gated anion channels: A family of microbial rhodopsins for advanced optogenetics. *Science*, *349*(6248), 647–650.

Gradinaru, V., Zhang, F., Ramakrishnan, C., Mattis, J., Prakash, R., Diester, I., Goshen, I., Thompson, K. R., & Deisseroth, K. (2010). Molecular and cellular approaches for diversifying and extending optogenetics. *Cell*, *141*(1), 154–165.

Greengard, P., Jen, J., Nairn, A. C., & Stevens, C. F. (1991). Enhancement of the glutamate response by cAMP-dependent protein kinase in hippocampal neurons. *Science*, *253*(5024), 1135–1138.

Guo, N.-N., & Li, B.-M. (2007). Cellular and subcellular distributions of beta1- and beta2-adrenoceptors in the CA1 and CA3 regions of the rat hippocampus. *Neuroscience*, *146*(1), 298–305.

Hagiwara, M., Brindle, P., Harootunian, A., Armstrong, R., Rivier, J., Vale, W., Tsien, R., & Montminy, M. R. (1993). Coupling of hormonal stimulation and transcription via the cyclic AMP-responsive factor CREB is rate limited by nuclear entry of protein kinase A. *Molecular and Cellular Biology*, *13*(8), 4852–4859.

Halls, M. L., & Cooper, D. M. F. (2017). Adenylyl cyclase signalling complexes - Pharmacological challenges and opportunities. *Pharmacology & Therapeutics*, *172*, 171–180.

Hansen, N. (2017). The Longevity of Hippocampus-Dependent Memory Is Orchestrated by the Locus Coeruleus-Noradrenergic System. *Neural Plasticity*, *2017*, 2727602.

Harada, K., Ito, M., Wang, X., Tanaka, M., Wongso, D., Konno, A., Hirai, H., Hirase, H., Tsuboi, T., & Kitaguchi, T. (2017). Red fluorescent protein-based cAMP indicator applicable to optogenetics and in vivo imaging. *Scientific Reports*, *7*(1), 7351.

Hasselmo, M. E., & Giocomo, L. M. (2006). Cholinergic modulation of cortical function. *Journal of Molecular Neuroscience: MN*, *30*(1-2), 133–135.

Hebb, D. O. (2005). *The Organization of Behavior: A Neuropsychological Theory*. Psychology Press.

Heine, M., Groc, L., Frischknecht, R., Béïque, J.-C., Lounis, B., Rumbaugh, G., Huganir, R. L., Cognet, L., & Choquet, D. (2008). Surface mobility of postsynaptic AMPARs tunes synaptic transmission. *Science*, *320*(5873), 201–205.

Henß, T., Nagpal, J., Gao, S., Scheib, U., Pieragnolo, A., Hirschhäuser, A., Schneider-Warme, F., Hegemann, P., Nagel, G., & Gottschalk, A. (2021). Optogenetic tools for manipulation of cyclic nucleotides functionally coupled to cyclic nucleotide-gated channels. *British Journal of Pharmacology*.

Hochbaum, D. R., Zhao, Y., Farhi, S. L., Klapoetke, N., Werley, C. A., Kapoor, V., Zou, P., Kralj, J. M., Maclaurin, D., Smedemark-Margulies, N., Saulnier, J. L., Boulting, G. L., Straub, C., Cho, Y. K., Melkonian, M., Wong, G. K.-S., Harrison, D. J., Murthy, V. N., Sabatini, B. L., … Cohen, A. E. (2014). All-optical electrophysiology in mammalian neurons using engineered microbial rhodopsins. *Nature Methods*, *11*(8), 825–833.

Hockberger, P. E., Skimina, T. A., Centonze, V. E., Lavin, C., Chu, S., Dadras, S., Reddy, J. K., & White, J. G. (1999). Activation of flavin-containing oxidases underlies light-induced production of H2O2 in mammalian cells. *Proceedings of the National Academy of Sciences of the United States of America*, *96*(11), 6255–6260.

Hofmann, F., Biel, M., & Kaupp, U. B. (2005). International Union of Pharmacology. LI. Nomenclature and structure-function relationships of cyclic nucleotide-regulated channels. *Pharmacological Reviews*, *57*(4), 455–462.

Hoshi, T., Garber, S. S., & Aldrich, R. W. (1988). Effect of forskolin on voltage-gated K+ channels is independent of adenylate cyclase activation. *Science*, *240*(4859), 1652–1655.

Houslay, M. D. (2010). Underpinning compartmentalised cAMP signalling through targeted cAMP breakdown. *Trends in Biochemical Sciences*, *35*(2), 91–100.

Howe, A. K. (2004). Regulation of actin-based cell migration by cAMP/PKA. *Biochimica et Biophysica Acta*, *1692*(2-3), 159–174.

Huang, E. P. (1997). Synaptic plasticity: a role for nitric oxide in LTP. *Current Biology: CB*, *7*(3), R141–R143.

Huang, Y. Y., & Kandel, E. R. (1994). Recruitment of long-lasting and protein kinase A-dependent long-term potentiation in the CA1 region of hippocampus requires repeated tetanization. *Learning & Memory* , *1*(1), 74–82.

Huang, Y. Y., Kandel, E. R., Varshavsky, L., Brandon, E. P., Qi, M., Idzerda, R. L., McKnight, G. S., & Bourtchouladze,

R. (1995). A genetic test of the effects of mutations in PKA on mossy fiber LTP and its relation to spatial and contextual learning. *Cell*, *83*(7), 1211–1222.

Hussain, L. S., Reddy, V., & Maani, C. V. (2021). Physiology, Noradrenergic Synapse. In *StatPearls*. StatPearls Publishing.

Isaac, J. T., Nicoll, R. A., & Malenka, R. C. (1995). Evidence for silent synapses: implications for the expression of LTP. *Neuron*, *15*(2), 427–434.

Iseki, M., Matsunaga, S., Murakami, A., Ohno, K., Shiga, K., Yoshida, K., Sugai, M., Takahashi, T., Hori, T., & Watanabe, M. (2002). A blue-light-activated adenylyl cyclase mediates photoavoidance in Euglena gracilis. In *Nature* (Vol. 415, Issue 6875, pp. 1047–1051).

Iseki, M., & Park, S.-Y. (2021). Photoactivated Adenylyl Cyclases: Fundamental Properties and Applications. In *Advances in Experimental Medicine and Biology* (pp. 129–139).

Ito, S., Murakami, A., Sato, K., Nishina, Y., Shiga, K., Takahashi, T., Higashi, S., Iseki, M., & Watanabe, M. (2005). Photocycle features of heterologously expressed and assembled eukaryotic flavin-binding BLUF domains of photoactivated adenylyl cyclase (PAC), a blue-light receptor in Euglena gracilis. In *Photochemical & Photobiological Sciences* (Vol. 4, Issue 9, p. 762).

Izquierdo, I., Medina, J. H., Izquierdo, L. A., Barros, D. M., de Souza, M. M., & Souza, T. M. e. (1998). Short- and Long-Term Memory Are Differentially Regulated by Monoaminergic Systems in the Rat Brain. In *Neurobiology of Learning and Memory* (Vol. 69, Issue 3, pp. 219–224).

Janovjak, H., Trauner, D., & Isacoff, E. Y. (2010). A Light-Gated, Potassium-Selective Glutamate Receptor for the Optical Inhibition of Neuronal Firing. In *Biophysical Journal* (Vol. 98, Issue 3, p. 223a).

Johnstone, T. B., Agarwal, S. R., Harvey, R. D., & Ostrom, R. S. (2018). cAMP Signaling Compartmentation: Adenylyl Cyclases as Anchors of Dynamic Signaling Complexes. *Molecular Pharmacology*, *93*(4), 270–276.

Joiner, M.-L. A., Lisé, M.-F., Yuen, E. Y., Kam, A. Y. F., Zhang, M., Hall, D. D., Malik, Z. A., Qian, H., Chen, Y., Ulrich, J. D., Burette, A. C., Weinberg, R. J., Law, P.-Y., El-Husseini, A., Yan, Z., & Hell, J. W. (2010). Assembly of a beta2-adrenergic receptor--GluR1 signalling complex for localized cAMP signalling. *The EMBO Journal*, *29*(2), 482–495.

Kaeser, P. S., Kwon, H.-B., Blundell, J., Chevaleyre, V., Morishita, W., Malenka, R. C., Powell, C. M., Castillo, P. E., & Sudhof, T. C. (2008). RIM1 phosphorylation at serine-413 by protein kinase A is not required for presynaptic long-term plasticity or learning. In *Proceedings of the National Academy of Sciences* (Vol. 105, Issue 38, pp. 14680–14685).

Kaeser-Woo, Y. J., Younts, T. J., Yang, X., Zhou, P., Wu, D., Castillo, P. E., & Südhof, T. C. (2013). Synaptotagmin-12 phosphorylation by cAMP-dependent protein kinase is essential for hippocampal mossy fiber LTP. *The Journal of Neuroscience: The Official Journal of the Society for Neuroscience*, *33*(23), 9769–9780.

Kalappa, B. I., Gusev, A. G., & Uteshev, V. V. (2010). Activation of functional α7-containing nAChRs in hippocampal CA1 pyramidal neurons by physiological levels of choline in the presence of PNU-120596.

PloS One, *5*(11), e13964.

Kandel, E. (2013). *Principles of Neural Science, Fifth Edition*. McGraw Hill Professional.

Kandel, E. R. (2001). The molecular biology of memory storage: a dialog between genes and synapses. *Bioscience Reports*, *21*(5), 565–611.

Kapiloff, M. S., Rigatti, M., & Dodge-Kafka, K. L. (2014). Architectural and functional roles of A kinase-anchoring proteins in cAMP microdomains. *The Journal of General Physiology*, *143*(1), 9–15.

Kasahara, K., Nakayama, Y., Ikeda, K., Fukushima, Y., Matsuda, D., Horimoto, S., & Yamaguchi, N. (2004). Trafficking of Lyn through the Golgi caveolin involves the charged residues on αE and αI helices in the kinase domain. In *Journal of Cell Biology* (Vol. 165, Issue 5, pp. 641–652).

Kato, H. E. (2021). Structure-Function Relationship of Channelrhodopsins. *Advances in Experimental Medicine and Biology*, *1293*, 35–53.

Kauer, J. A., & Malenka, R. C. (2007). Synaptic plasticity and addiction. *Nature Reviews. Neuroscience*, *8*(11), 844–858.

Kaupp, U. B., Benjamin Kaupp, U., & Seifert, R. (2001). Molecular Diversity of Pacemaker Ion Channels. In *Annual Review of Physiology* (Vol. 63, Issue 1, pp. 235–257).

Kaupp, U. B., Benjamin Kaupp, U., & Seifert, R. (2002). Cyclic Nucleotide-Gated Ion Channels. In *Physiological Reviews* (Vol. 82, Issue 3, pp. 769–824).

Kawasaki, H., Springett, G. M., Mochizuki, N., Toki, S., Nakaya, M., Matsuda, M., Housman, D. E., & Graybiel, A. M. (1998). A family of cAMP-binding proteins that directly activate Rap1. *Science*, *282*(5397), 2275–2279.

Kerchner, G. A., & Nicoll, R. A. (2008). Silent synapses and the emergence of a postsynaptic mechanism for LTP. *Nature Reviews. Neuroscience*, *9*(11), 813–825.

Kesters, D., Brams, M., Nys, M., Wijckmans, E., Spurny, R., Voets, T., Tytgat, J., Kusch, J., & Ulens, C. (2015). Structure of the SthK carboxy-terminal region reveals a gating mechanism for cyclic nucleotide-modulated ion channels. *PloS One*, *10*(1), e0116369.

Kim, J.-M., Hwa, J., Garriga, P., Reeves, P. J., RajBhandary, U. L., & Khorana, H. G. (2005). Light-driven activation of beta 2-adrenergic receptor signaling by a chimeric rhodopsin containing the beta 2-adrenergic receptor cytoplasmic loops. *Biochemistry*, *44*(7), 2284–2292.

Kingston, P. A., Zufall, F., & Barnstable, C. J. (1996). Rat hippocampal neurons express genes for both rod retinal and olfactory cyclic nucleotide-gated channels: novel targets for cAMP/cGMP function. *Proceedings of the National Academy of Sciences of the United States of America*, *93*(19), 10440–10445.

Klapoetke, N. C., Murata, Y., Kim, S. S., Pulver, S. R., Birdsey-Benson, A., Cho, Y. K., Morimoto, T. K., Chuong, A. S., Carpenter, E. J., Tian, Z., Wang, J., Xie, Y., Yan, Z., Zhang, Y., Chow, B. Y., Surek, B., Melkonian, M., Jayaraman, V., Constantine-Paton, M., … Boyden, E. S. (2014). Independent optical excitation of distinct neural populations. *Nature Methods*, *11*(3), 338–346.

Kleinlogel, S. (2016). Optogenetic user s guide to Opto-GPCRs. In *Frontiers in Bioscience* (Vol. 21, Issue 4, pp.

794–805).

Kleis, P., Paschen, E., Haeussler, U., Sierra, Y. A. B., & Haas, C. A. (2021). In vivo characterization and application of a novel potassium channel-based optogenetic silencer in the healthy and epileptic mouse hippocampus. *bioRxiv*.

Knighton, D. R., Zheng, J. H., Ten Eyck, L. F., Ashford, V. A., Xuong, N. H., Taylor, S. S., & Sowadski, J. M. (1991). Crystal structure of the catalytic subunit of cyclic adenosine monophosphate-dependent protein kinase [Review of *Crystal structure of the catalytic subunit of cyclic adenosine monophosphate-dependent protein kinase*]. *Science*, *253*(5018), 407–414.

Komagiri, Y., & Kitamura, N. (2007). Comparison of effects of PKA catalytic subunit on Ih and calcium channel currents in rat dorsal root ganglion cells. In *Biomedical Research* (Vol. 28, Issue 4, pp. 177–189).

Konorski, J. (1948). Conditioned reflexes and neuron organization. In *New York: Cambridge University Press*.

Levey, A. I., Edmunds, S. M., Koliatsos, V., Wiley, R. G., & Heilman, C. J. (1995). Expression of m1-m4 muscarinic acetylcholine receptor proteins in rat hippocampus and regulation by cholinergic innervation. *The Journal of Neuroscience: The Official Journal of the Society for Neuroscience*, *15*(5 Pt 2), 4077–4092.

Liao, D., Hessler, N. A., & Malinow, R. (1995). Activation of postsynaptically silent synapses during pairing-induced LTP in CA1 region of hippocampal slice. *Nature*, *375*(6530), 400–404.

Limbutara, K., Kelleher, A., Yang, C.-R., Raghuram, V., & Knepper, M. A. (2019). Phosphorylation Changes in Response to Kinase Inhibitor H89 in PKA-Null Cells. *Scientific Reports*, *9*(1), 2814.

Lindner, R. (2019). *Blue-Light-Regulated Adenylyl Cyclases - Optogenetic Tools and Model Systems for Inter-domain Communication*.

Lin, P.-Y., Kavalali, E. T., & Monteggia, L. M. (2018). Genetic Dissection of Presynaptic and Postsynaptic BDNF-TrkB Signaling in Synaptic Efficacy of CA3-CA1 Synapses. *Cell Reports*, *24*(6), 1550–1561.

Li, P., Rial, D., Canas, P. M., Yoo, J.-H., Li, W., Zhou, X., Wang, Y., van Westen, G. J. P., Payen, M.-P., Augusto, E., Gonçalves, N., Tomé, A. R., Li, Z., Wu, Z., Hou, X., Zhou, Y., PIJzerman, A., Boyden, E. S., Cunha, R. A., … Chen, J.-F. (2015). Optogenetic activation of intracellular adenosine A2A receptor signaling in the hippocampus is sufficient to trigger CREB phosphorylation and impair memory. *Molecular Psychiatry*, *20*(11), 1481.

Lisman, J. E. (2009). The pre/post LTP debate [Review of *The pre/post LTP debate*]. *Neuron*, *63*(3), 281–284.

Lisman, J. E., & Grace, A. A. (2005). The hippocampal-VTA loop: controlling the entry of information into long-term memory. *Neuron*, *46*(5), 703–713.

Lisman, J. E., Raghavachari, S., & Tsien, R. W. (2007). The sequence of events that underlie quantal transmission at central glutamatergic synapses. *Nature Reviews. Neuroscience*, *8*(8), 597–609.

Lisman, J., Lichtman, J. W., & Sanes, J. R. (2003). LTP: perils and progress. *Nature Reviews. Neuroscience*, *4*(11), 926–929.

Lisman, J., Schulman, H., & Cline, H. (2002). The molecular basis of CaMKII function in synaptic and behavioural memory. *Nature Reviews. Neuroscience*, *3*(3), 175–190.

Liu, C., Ke, P., Zhang, J., Zhang, X., & Chen, X. (2020). Protein Kinase Inhibitor Peptide as a Tool to Specifically

Inhibit Protein Kinase A. *Frontiers in Physiology*, *11*, 574030.

Lonart, G., Schoch, S., Kaeser, P. S., Jenny Larkin, C., Südhof, T. C., & Linden, D. J. (2003). Phosphorylation of RIM1α by PKA Triggers Presynaptic Long-Term Potentiation at Cerebellar Parallel Fiber Synapses. In *Cell* (Vol. 115, Issue 1, pp. 49–60).

Lu, K. T., & Gean, P. W. (1999). Masking of forskolin-induced long-term potentiation by adenosine accumulation in area CA1 of the rat hippocampus. *Neuroscience*, *88*(1), 69–78.

Lüscher, C., & Malenka, R. C. (2012). NMDA receptor-dependent long-term potentiation and long-term depression (LTP/LTD). *Cold Spring Harbor Perspectives in Biology*, *4*(6).

Luyben, T. T., Rai, J., Li, H., Georgiou, J., Avila, A., Zhen, M., Collingridge, G. L., Tominaga, T., & Okamoto, K. (2020). Optogenetic Manipulation of Postsynaptic cAMP Using a Novel Transgenic Mouse Line Enables Synaptic Plasticity and Enhances Depolarization Following Tetanic Stimulation in the Hippocampal Dentate Gyrus. *Frontiers in Neural Circuits*, *14*, 24.

Lu, Y., Zha, X.-M., Kim, E. Y., Schachtele, S., Dailey, M. E., Hall, D. D., Strack, S., Green, S. H., Hoffman, D. A., & Hell, J. W. (2011). A kinase anchor protein 150 (AKAP150)-associated protein kinase A limits dendritic spine density. *The Journal of Biological Chemistry*, *286*(30), 26496–26506.

Mager, T., Lopez de la Morena, D., Senn, V., Schlotte, J., D Errico, A., Feldbauer, K., Wrobel, C., Jung, S., Bodensiek, K., Rankovic, V., Browne, L., Huet, A., Jüttner, J., Wood, P. G., Letzkus, J. J., Moser, T., & Bamberg, E. (2018). High frequency neural spiking and auditory signaling by ultrafast red-shifted optogenetics. *Nature Communications*, *9*(1), 1750.

Mahn, M., Gibor, L., Patil, P., Cohen-Kashi Malina, K., Oring, S., Printz, Y., Levy, R., Lampl, I., & Yizhar, O. (2018). High-efficiency optogenetic silencing with soma-targeted anion-conducting channelrhodopsins. *Nature Communications*, *9*(1), 4125.

Mahn, M., Prigge, M., Ron, S., Levy, R., & Yizhar, O. (2016). Biophysical constraints of optogenetic inhibition at presynaptic terminals. *Nature Neuroscience*, *19*(4), 554–556.

Makino, Y., Johnson, R. C., Yu, Y., Takamiya, K., & Huganir, R. L. (2011). Enhanced synaptic plasticity in mice with phosphomimetic mutation of the GluA1 AMPA receptor. *Proceedings of the National Academy of Sciences of the United States of America*, *108*(20), 8450–8455.

Malenka, R. C. (2003). The long-term potential of LTP. *Nature Reviews. Neuroscience*, *4*(11), 923–926.

Malenka, R. C., & Bear, M. F. (2004). LTP and LTD: an embarrassment of riches. *Neuron*, *44*(1), 5–21.

Malenka, R. C., & Nicoll, R. A. (1999). Long-term potentiation--a decade of progress? *Science*, *285*(5435), 1870–1874.

Malyshev, A. Y., Roshchin, M. V., Smirnova, G. R., Dolgikh, D. A., Balaban, P. M., & Ostrovsky, M. A. (2017). Chloride conducting light activated channel GtACR2 can produce both cessation of firing and generation of action potentials in cortical neurons in response to light. *Neuroscience Letters*, *640*, 76–80.

Manganiello, V. C., Murata, T., Taira, M., Belfrage, P., & Degerman, E. (1995). Diversity in cyclic nucleotide phosphodiesterase isoenzyme families. *Archives of Biochemistry and Biophysics*, *322*(1), 1–13.

Matsuzaki, M., Honkura, N., Ellis-Davies, G. C. R., & Kasai, H. (2004). Structural basis of long-term potentiation in single dendritic spines. *Nature*, *429*(6993), 761–766.

Matthies, H., Becker, A., Schröeder, H., Kraus, J., Höllt, V., & Krug, M. (1997). Dopamine D1-deficient mutant mice do not express the late phase of hippocampal long-term potentiation. In *NeuroReport* (Vol. 8, Issue 16, pp. 3533–3535).

Matt, L., Michalakis, S., Hofmann, F., Hammelmann, V., Ludwig, A., Biel, M., & Kleppisch, T. (2011). HCN2 channels in local inhibitory interneurons constrain LTP in the hippocampal direct perforant path. *Cellular and Molecular Life Sciences: CMLS*, *68*(1), 125–137.

Mayr, B., & Montminy, M. (2001). Transcriptional regulation by the phosphorylation-dependent factor CREB. In *Nature Reviews Molecular Cell Biology* (Vol. 2, Issue 8, pp. 599–609).

McNamara, C. G., Tejero-Cantero, Á., Trouche, S., Campo-Urriza, N., & Dupret, D. (2014). Dopaminergic neurons promote hippocampal reactivation and spatial memory persistence. In *Nature Neuroscience* (Vol. 17, Issue 12, pp. 1658–1660).

Michalakis, S., Kleppisch, T., Polta, S. A., Wotjak, C. T., Koch, S., Rammes, G., Matt, L., Becirovic, E., & Biel, M. (2011). Altered synaptic plasticity and behavioral abnormalities in CNGA3-deficient mice. *Genes, Brain, and Behavior*, *10*(2), 137–148.

Mockett, B. G., Brooks, W. M., Tate, W. P., & Abraham, W. C. (2004). Dopamine D1/D5 receptor activation fails to initiate an activity-independent late-phase LTP in rat hippocampus. *Brain Research*, *1021*(1), 92–100.

Monday, H. R., Younts, T. J., & Castillo, P. E. (2018). Long-Term Plasticity of Neurotransmitter Release: Emerging Mechanisms and Contributions to Brain Function and Disease. *Annual Review of Neuroscience*, *41*, 299–322.

Moore, R. Y., & Halaris, A. E. (1975). Hippocampal innervation by serotonin neurons of the midbrain raphe in the rat. In *The Journal of Comparative Neurology* (Vol. 164, Issue 2, pp. 171–183). Morris, R. G. M. (2013). NMDA receptors and memory encoding. In *Neuropharmacology* (Vol. 74, pp. 32–40).

Murchison, C. F., Zhang, X.-Y., Zhang, W.-P., Ouyang, M., Lee, A., & Thomas, S. A. (2004). A distinct role for norepinephrine in memory retrieval. *Cell*, *117*(1), 131–143.

Murphy, J. A., Stein, I. S., Geoffrey Lau, C., Peixoto, R. T., Aman, T. K., Kaneko, N., Aromolaran, K., Saulnier, J. L., Popescu, G. K., Sabatini, B. L., Hell, J. W., & Suzanne Zukin, R. (2014). Phosphorylation of Ser1166 on GluN2B by PKA Is Critical to Synaptic NMDA Receptor Function and Ca 2 Signaling in Spines. In *The Journal of Neuroscience* (Vol. 34, Issue 3, pp. 869–879).

Murphy, J. A., Stein, I. S., Lau, C. G., Peixoto, R. T., Aman, T. K., Kaneko, N., Aromolaran, K., Saulnier, J. L., Popescu, G. K., Sabatini, B. L., Hell, J. W., & Zukin, R. S. (2014). Phosphorylation of Ser1166 on GluN2B by PKA is critical to synaptic NMDA receptor function and Ca2+ signaling in spines. *The Journal of Neuroscience: The Official Journal of the Society for Neuroscience*, *34*(3), 869–879.

Murphy, J. G., & Dell'Acqua, M. L. (2014). AKAP79/150-Anchored CaN and PKA Regulate Neuronal L-Type Calcium Channel Activity and NFAT Transcriptional Signaling. In *Biophysical Journal* (Vol. 106, Issue 2, p.

137a). 1

Murray, A. J. (2008). Pharmacological PKA Inhibition: All May Not Be What It Seems. In *Science Signaling* (Vol. 1, Issue 22, pp. re4–re4).

Nagahama, T., Suzuki, T., Yoshikawa, S., & Iseki, M. (2007). Functional transplant of photoactivated adenylyl cyclase (PAC) into Aplysia sensory neurons. *Neuroscience Research*, *59*(1), 81–88.

Nagel, G., Brauner, M., Liewald, J. F., Adeishvili, N., Bamberg, E., & Gottschalk, A. (2005). Light activation of channelrhodopsin-2 in excitable cells of Caenorhabditis elegans triggers rapid behavioral responses. *Current Biology: CB*, *15*(24), 2279–2284.

Nam, Y.-W., Kong, D., Wang, D., Orfali, R., Sherpa, R. T., Totonchy, J., Nauli, S. M., & Zhang, M. (2021). Differential modulation of SK channel subtypes by phosphorylation. *Cell Calcium*, *94*, 102346.

Nguyen, P. V., & Connor, S. A. (2019). Noradrenergic Regulation of Hippocampus-Dependent Memory. In *Central Nervous System Agents in Medicinal Chemistry* (Vol. 19, Issue 3, pp. 187–196).

Nguyen, P. V., & Gelinas, J. N. (2018). Noradrenergic gating of long-lasting synaptic potentiation in the hippocampus: from neurobiology to translational biomedicine. *Journal of Neurogenetics*, *32*(3), 171–182.

Nicoll, R. A., & Schmitz, D. (2005). Synaptic plasticity at hippocampal mossy fibre synapses. *Nature Reviews. Neuroscience*, *6*(11), 863–876.

Nolan, M. F., Malleret, G., Dudman, J. T., Buhl, D. L., Santoro, B., Gibbs, E., Vronskaya, S., Buzsáki, G., Siegelbaum, S. A., Kandel, E. R., & Morozov, A. (2004). A behavioral role for dendritic integration: HCN1 channels constrain spatial memory and plasticity at inputs to distal dendrites of CA1 pyramidal neurons. *Cell*, *119*(5), 719–732.

Ntefidou, M., Iseki, M., Watanabe, M., Lebert, M., & Häder, D.-P. (2003). Photoactivated adenylyl cyclase controls phototaxis in the flagellate Euglena gracilis. *Plant Physiology*, *133*(4), 1517–1521.

O'Banion, C. P., Priestman, M. A., Hughes, R. M., Herring, L. E., Capuzzi, S. J., & Lawrence, D. S. (2018). Design and Profiling of a Subcellular Targeted Optogenetic cAMP-Dependent Protein Kinase. *Cell Chemical Biology*, *25*(1), 100–109.e8.

O'Dell, T. J., Connor, S. A., Guglietta, R., & Nguyen, P. V. (2015). β-Adrenergic receptor signaling and modulation of long-term potentiation in the mammalian hippocampus. In *Learning & Memory* (Vol. 22, Issue 9, pp. 461–471).

Oh, E., Maejima, T., Liu, C., Deneris, E., & Herlitze, S. (2010). Substitution of 5-HT1A receptor signaling by a light-activated G protein-coupled receptor. *The Journal of Biological Chemistry*, *285*(40), 30825–30836.

Ohki, M., Sugiyama, K., Kawai, F., Tanaka, H., Nihei, Y., Unzai, S., Takebe, M., Matsunaga, S., Adachi, S.-I., Shibayama, N., Zhou, Z., Koyama, R., Ikegaya, Y., Takahashi, T., Tame, J. R. H., Iseki, M., & Park, S.-Y. (2016). Structural insight into photoactivation of an adenylate cyclase from a photosynthetic cyanobacterium. *Proceedings of the National Academy of Sciences of the United States of America*, *113*(24), 6659–6664.

Ohta, Y., Furuta, T., Nagai, T., & Horikawa, K. (2018). Red fluorescent cAMP indicator with increased affinity and expanded dynamic range. *Scientific Reports*, *8*(1), 1866.

Oldani, S., Moreno-Velasquez, L., Faiss, L., Stumpf, A., Rosenmund, C., Schmitz, D., & Rost, B. R. (2021). SynaptoPAC, an optogenetic tool for induction of presynaptic plasticity. *Journal of Neurochemistry*, *156*(3), 324–336.

Orlando, M., Dvorzhak, A., Bruentgens, F., Maglione, M., Rost, B. R., Sigrist, S. J., Breustedt, J., & Schmitz, D. (2021). Recruitment of release sites underlies chemical presynaptic potentiation at hippocampal mossy fiber boutons. *PLoS Biology*, *19*(6), e3001149.

Otmakhova, N. A., & Lisman, J. E. (2006). Dopamine, Serotonin, and Noradrenaline Strongly Inhibit the Direct Perforant Path-CA1 Synaptic Input, but Have Little Effect on the Schaffer Collateral Input. In *Annals of the New York Academy of Sciences* (Vol. 911, Issue 1, pp. 462–464).

Otmakhov, N., Khibnik, L., Otmakhova, N., Carpenter, S., Riahi, S., Asrican, B., & Lisman, J. (2004). Forskolin-induced LTP in the CA1 hippocampal region is NMDA receptor dependent. *Journal of Neurophysiology*, *91*(5), 1955–1962.

Palacios-Filardo, J., & Mellor, J. R. (2019). Neuromodulation of hippocampal long-term synaptic plasticity. *Current Opinion in Neurobiology*, *54*, 37–43.

Papouin, T., Dunphy, J. M., Tolman, M., Dineley, K. T., & Haydon, P. G. (2017). Septal Cholinergic Neuromodulation Tunes the Astrocyte-Dependent Gating of Hippocampal NMDA Receptors to Wakefulness. *Neuron*, *94*(4), 840–854.e7.

Parent, A., Schrader, K., Munger, S. D., Reed, R. R., Linden, D. J., & Ronnett, G. V. (1998). Synaptic transmission and hippocampal long-term potentiation in olfactory cyclic nucleotide-gated channel type 1 null mouse. *Journal of Neurophysiology*, *79*(6), 3295–3301.

Park, P., Georgiou, J., Sanderson, T. M., Ko, K.-H., Kang, H., Kim, J.-I., Bradley, C. A., Bortolotto, Z. A., Zhuo, M., Kaang, B.-K., & Collingridge, G. L. (2021). PKA drives an increase in AMPA receptor unitary conductance during LTP in the hippocampus. *Nature Communications*, *12*(1), 413.

Pedarzani, P., & Storm, J. F. (1995). Protein kinase A-independent modulation of ion channels in the brain by cyclic AMP. *Proceedings of the National Academy of Sciences of the United States of America*, *92*(25), 11716–11720.

Peng, T., Qi, B., He, J., Ke, H., & Shi, J. (2020). Advances in the Development of Phosphodiesterase-4 Inhibitors. In *Journal of Medicinal Chemistry* (Vol. 63, Issue 19, pp. 10594–10617).

Penzkofer, A., Tanwar, M., Veetil, S. K., & Kateriya, S. (2015). Photo-dynamics of photoactivated adenylyl cyclase TpPAC from the spirochete bacterium Turneriella parva strain H(T). *Journal of Photochemistry and Photobiology. B, Biology*, *153*, 90–102.

Penzkofer, A., Tanwar, M., Veetil, S. K., Kateriya, S., Stierl, M., & Hegemann, P. (2014). Photo-dynamics of BLUF domain containing adenylyl cyclase NgPAC3 from the amoeboflagellate Naegleria gruberi NEG-M strain. In *Journal of Photochemistry and Photobiology A: Chemistry* (Vol. 287, pp. 19–29).

Pierre, S., Eschenhagen, T., Geisslinger, G., & Scholich, K. (2009). Capturing adenylyl cyclases as potential drug targets. *Nature Reviews. Drug Discovery*, *8*(4), 321–335. 10.1038/nrd2827

Pigott, B. M. (2012). *Nitric Oxide Signalling in Hippocampal Synaptic Plasticity*.

Pigott, B. M., & Garthwaite, J. (2016). Nitric Oxide Is Required for L-Type Ca(2+) Channel-Dependent Long-Term Potentiation in the Hippocampus. *Frontiers in Synaptic Neuroscience*, *8*, 17.

Pinto, C., Papa, D., Hübner, M., Mou, T.-C., Lushington, G. H., & Seifert, R. (2008). Activation and inhibition of adenylyl cyclase isoforms by forskolin analogs. *The Journal of Pharmacology and Experimental Therapeutics*, *325*(1), 27–36.

Podda, M. V., & Grassi, C. (2014). New perspectives in cyclic nucleotide-mediated functions in the CNS: the emerging role of cyclic nucleotide-gated (CNG) channels. *Pflugers Archiv: European Journal of Physiology*, *466*(7), 1241–1257.

Purkey, A. M., & Dell'Acqua, M. L. (2020). Phosphorylation-Dependent Regulation of Ca-Permeable AMPA Receptors During Hippocampal Synaptic Plasticity. *Frontiers in Synaptic Neuroscience*, *12*, 8.

Qian, H., Matt, L., Zhang, M., Nguyen, M., Patriarchi, T., Koval, O. M., Anderson, M. E., He, K., Lee, H.-K., & Hell, J. W. (2012). β2-Adrenergic receptor supports prolonged theta tetanus-induced LTP. *Journal of Neurophysiology*, *107*(10), 2703–2712.

Qi, X.-L., Zhu, B., Zhang, X.-H., & Li, B.-M. (2008). Are beta-adrenergic receptors in the hippocampal CA1 region required for retrieval of contextual fear memory? *Biochemical and Biophysical Research Communications*, *368*(2), 186–191.

Raffelberg, S., Wang, L., Gao, S., Losi, A., Gärtner, W., & Nagel, G. (2013). A LOV-domain-mediated blue-light-activated adenylate (adenylyl) cyclase from the cyanobacterium Microcoleus chthonoplastes PCC 7420. *Biochemical Journal*, *455*(3), 359–365.

Raimondo, J. V., Kay, L., Ellender, T. J., & Akerman, C. J. (2012). Optogenetic silencing strategies differ in their effects on inhibitory synaptic transmission. *Nature Neuroscience*, *15*(8), 1102–1104.

Ramón y Cajal, S. (1909). *Histologie du système nerveux de l'homme & des vertébrés*. Renner, M. C., Albers, E. H., Gutierrez-Castellanos, N., Reinders, N. R., van Huijstee, A. N., Xiong, H., Lodder, T. R., & Kessels, H. W. (2017). Synaptic plasticity through activation of GluA3-containing AMPA-receptors. *eLife*, *6*.

Renström, E., Eliasson, L., & Rorsman, P. (1997). Protein kinase A-dependent and -independent stimulation of exocytosis by cAMP in mouse pancreatic B-cells. *The Journal of Physiology*, *502 (Pt 1)*, 105–118.

Riccio, A. (1999). Mediation by a CREB Family Transcription Factor of NGF-Dependent Survival of Sympathetic Neurons. In *Science* (Vol. 286, Issue 5448, pp. 2358–2361).

Richards, M., Lomas, O., Jalink, K., Ford, K. L., Vaughan-Jones, R. D., Lefkimmiatis, K., & Swietach, P. (2016). Intracellular tortuosity underlies slow cAMP diffusion in adult ventricular myocytes. *Cardiovascular Research*, *110*(3), 395–407.

Rich, T. C., Fagan, K. A., Nakata, H., Schaack, J., Cooper, D. M., & Karpen, J. W. (2000). Cyclic nucleotide-gated channels colocalize with adenylyl cyclase in regions of restricted cAMP diffusion. *The Journal of General Physiology*, *116*(2), 147–161.

Rich, T. C., Fagan, K. A., Tse, T. E., Schaack, J., Cooper, D. M., & Karpen, J. W. (2001). A uniform extracellular

stimulus triggers distinct cAMP signals in different compartments of a simple cell. *Proceedings of the National Academy of Sciences of the United States of America*, *98*(23), 13049–13054.

Rich, T. C., Tse, T. E., Rohan, J. G., Schaack, J., & Karpen, J. W. (2001). In Vivo Assessment of Local Phosphodiesterase Activity Using Tailored Cyclic Nucleotide–Gated Channels as Camp Sensors. In *Journal of General Physiology* (Vol. 118, Issue 1, pp. 63–78).

Richter, W., Day, P., Agrawal, R., Bruss, M. D., Granier, S., Wang, Y. L., Rasmussen, S. G. F., Horner, K., Wang, P., Lei, T., Patterson, A. J., Kobilka, B., & Conti, M. (2008). Signaling from beta1- and beta2-adrenergic receptors is defined by differential interactions with PDE4. *The EMBO Journal*, *27*(2), 384–393.

Roscioni, S. S., Elzinga, C. R. S., & Schmidt, M. (2008). Epac: effectors and biological functions. *Naunyn-Schmiedeberg's Archives of Pharmacology*, *377*(4-6), 345–357.

Rosen, Z. B., Cheung, S., & Siegelbaum, S. A. (2015). Midbrain dopamine neurons bidirectionally regulate CA3-CA1 synaptic drive. *Nature Neuroscience*, *18*(12), 1763–1771.

Roskoski, R., Jr. (2015). A historical overview of protein kinases and their targeted small molecule inhibitors. *Pharmacological Research: The Official Journal of the Italian Pharmacological Society*, *100*, 1–23.

Rudy, J. W. (2008). Is there a baby in the bathwater? Maybe: Some methodological issues for the de novo protein synthesis hypothesis. In *Neurobiology of Learning and Memory* (Vol. 89, Issue 3, pp. 219–224).

Ryu, M.-H., Kang, I.-H., Nelson, M. D., Jensen, T. M., Lyuksyutova, A. I., Siltberg-Liberles, J., Raizen, D. M., & Gomelsky, M. (2014). Engineering adenylate cyclases regulated by near-infrared window light. *Proceedings of the National Academy of Sciences of the United States of America*, *111*(28), 10167–10172.

Ryu, M.-H., Moskvin, O. V., Siltberg-Liberles, J., & Gomelsky, M. (2010). Natural and engineered photoactivated nucleotidyl cyclases for optogenetic applications. *The Journal of Biological Chemistry*, *285*(53), 41501–41508.

Sanabra, C., & Mengod, G. (2011). Neuroanatomical distribution and neurochemical characterization of cells expressing adenylyl cyclase isoforms in mouse and rat brain. *Journal of Chemical Neuroanatomy*, *41*(1), 43–54.

Sanes, J. R., & Lichtman, J. W. (1999). Can molecules explain long-term potentiation? In *Nature Neuroscience* (Vol. 2, Issue 7, pp. 597–604).

Sassone-Corsi, P. (2012). The cyclic AMP pathway. *Cold Spring Harbor Perspectives in Biology*, *4*(12).

Scatton, B., Simon, H., Le Moal, M., & Bischoff, S. (1980). Origin of dopaminergic innervation of the rat hippocampal formation. In *Neuroscience Letters* (Vol. 18, Issue 2, pp. 125–131).

Scheib, U., Broser, M., Constantin, O. M., Yang, S., Gao, S., Mukherjee, S., Stehfest, K., Nagel, G., Gee, C. E., & Hegemann, P. (2018). Rhodopsin-cyclases for photocontrol of cGMP/cAMP and 2.3 Å structure of the adenylyl cyclase domain. *Nature Communications*, *9*(1), 2046.

Scheib, U., Stehfest, K., Gee, C. E., Körschen, H. G., Fudim, R., Oertner, T. G., & Hegemann, P. (2015). The rhodopsin-guanylyl cyclase of the aquatic fungus Blastocladiella emersonii enables fast optical control of cGMP signaling. *Science Signaling*, *8*(389), rs8.

Schönberger, M., & Trauner, D. (2014). A photochromic agonist for μ-opioid receptors. *Angewandte Chemie* , *53*(12), 3264–3267.

Schröder-Lang, S., Schwärzel, M., Seifert, R., Strünker, T., Kateriya, S., Looser, J., Watanabe, M., Kaupp, U. B., Hegemann, P., & Nagel, G. (2007). Fast manipulation of cellular cAMP level by light in vivo. *Nature Methods*, *4*(1), 39–42.

Schroll, C., Riemensperger, T., Bucher, D., Ehmer, J., Völler, T., Erbguth, K., Gerber, B., Hendel, T., Nagel, G., Buchner, E., & Fiala, A. (2006). Light-induced activation of distinct modulatory neurons triggers appetitive or aversive learning in Drosophila larvae. *Current Biology: CB*, *16*(17), 1741–1747.

Schuman, E. M., & Madison, D. V. (1991). A requirement for the intercellular messenger nitric oxide in long-term potentiation. *Science*, *254*(5037), 1503–1506.

Scoville, W. B., & Milner, B. (1957). Loss of recent memory after bilateral hippocampal lesions. *Journal of Neurology, Neurosurgery, and Psychiatry*, *20*(1), 11–21.

Sengupta, S., & Mehta, G. (2018). Natural products as modulators of the cyclic-AMP pathway: evaluation and synthesis of lead compounds. *Organic & Biomolecular Chemistry*, *16*(35), 6372–6390.

Seo, H., Seol, M.-J., & Lee, K. (2015). Differential expression of hyperpolarization-activated cyclic nucleotide-gated channel subunits during hippocampal development in the mouse. *Molecular Brain*, *8*, 13.

Sette, C., & Conti, M. (1996). Phosphorylation and activation of a cAMP-specific phosphodiesterase by the cAMP-dependent protein kinase. Involvement of serine 54 in the enzyme activation. *The Journal of Biological Chemistry*, *271*(28), 16526–16534. 1

Shintani, Y., & Marunaka, Y. (1996). Regulation of chloride channel trafficking by cyclic AMP via protein kinase A-independent pathway in A6 renal epithelial cells. *Biochemical and Biophysical Research Communications*, *223*(2), 234–239.

Shirey, J. K., Xiang, Z., Orton, D., Brady, A. E., Johnson, K. A., Williams, R., Ayala, J. E., Rodriguez, A. L., Wess, J., Weaver, D., Niswender, C. M., & Conn, P. J. (2008). An allosteric potentiator of M4 mAChR modulates hippocampal synaptic transmission. *Nature Chemical Biology*, *4*(1), 42–50.

Silva, A. J., Kogan, J. H., Frankland, P. W., & Kida, S. (1998). CREB and memory. *Annual Review of Neuroscience*, *21*, 127–148.

Siuda, E. R., Copits, B. A., Schmidt, M. J., Baird, M. A., Al-Hasani, R., Planer, W. J., Funderburk, S. C., McCall, J. G., Gereau, R. W., 4th, & Bruchas, M. R. (2015). Spatiotemporal control of opioid signaling and behavior. *Neuron*, *86*(4), 923–935.

Siuda, E. R., McCall, J. G., Al-Hasani, R., Shin, G., Il Park, S., Schmidt, M. J., Anderson, S. L., Planer, W. J., Rogers, J. A., & Bruchas, M. R. (2015). Optodynamic simulation of β-adrenergic receptor signalling. *Nature Communications*, *6*, 8480.

Søberg, K., & Skålhegg, B. S. (2018). The Molecular Basis for Specificity at the Level of the Protein Kinase a Catalytic Subunit. In *Frontiers in Endocrinology* (Vol. 9).

Sohn, H. W., Tolar, P., & Pierce, S. K. (2008). Membrane heterogeneities in the formation of B cell receptor-Lyn

kinase microclusters and the immune synapse. *The Journal of Cell Biology*, *182*(2), 367–379.

Sokolova, I. V., Lester, H. A., & Davidson, N. (2006). Postsynaptic mechanisms are essential for forskolin-induced potentiation of synaptic transmission. *Journal of Neurophysiology*, *95*(4), 2570–2579.

Song, I., & Huganir, R. L. (2002). Regulation of AMPA receptors during synaptic plasticity. In *Trends in Neurosciences* (Vol. 25, Issue 11, pp. 578–588).

Spangler, S. M., & Bruchas, M. R. (2017). Optogenetic approaches for dissecting neuromodulation and GPCR signaling in neural circuits. *Current Opinion in Pharmacology*, *32*, 56–70.

Spoida, K., Masseck, O. A., Deneris, E. S., & Herlitze, S. (2014). Gq/5-HT2c receptor signals activate a local GABAergic inhibitory feedback circuit to modulate serotonergic firing and anxiety in mice. *Proceedings of the National Academy of Sciences of the United States of America*, *111*(17), 6479–6484.

Stabel, R., Stüven, B., Hansen, J. N., Körschen, H. G., Wachten, D., & Möglich, A. (2019). Revisiting and Redesigning Light-Activated Cyclic-Mononucleotide Phosphodiesterases. *Journal of Molecular Biology*, *431*(17), 3029–3045.

Staubli, U., & Xu, F. B. (1995). Effects of 5-HT3 receptor antagonism on hippocampal theta rhythm, memory, and LTP induction in the freely moving rat. In *The Journal of Neuroscience* (Vol. 15, Issue 3, pp. 2445–2452).

Steegborn, C. (2014). Structure, mechanism, and regulation of soluble adenylyl cyclases – similarities and differences to transmembrane adenylyl cyclases. In *Biochimica et Biophysica Acta (BBA) - Molecular Basis of Disease* (Vol. 1842, Issue 12, pp. 2535–2547).

Stierl, M., Penzkofer, A., Kennis, J. T. M., Hegemann, P., & Mathes, T. (2014). Key residues for the light regulation of the blue light-activated adenylyl cyclase from Beggiatoa sp. *Biochemistry*, *53*(31), 5121–5130.

Stierl, M., Stumpf, P., Udwari, D., Gueta, R., Hagedorn, R., Losi, A., Gärtner, W., Petereit, L., Efetova, M., Schwarzel, M., Oertner, T. G., Nagel, G., & Hegemann, P. (2011). Light Modulation of Cellular cAMP by a Small Bacterial Photoactivated Adenylyl Cyclase, bPAC, of the Soil Bacterium Beggiatoa. In *Journal of Biological Chemistry* (Vol. 286, Issue 2, pp. 1181–1188).

Storm, D. R., Hansel, C., Hacker, B., Parent, A., & Linden, D. J. (1998). Impaired Cerebellar Long-Term Potentiation in Type I Adenylyl Cyclase Mutant Mice. In *Neuron* (Vol. 20, Issue 6, pp. 1199–1210).

Strijbos, P. J., Pratt, G. D., Khan, S., Charles, I. G., & Garthwaite, J. (1999). Molecular characterization and in situ localization of a full-length cyclic nucleotide-gated channel in rat brain. *The European Journal of Neuroscience*, *11*(12), 4463–4467.

Stüven, B., Stabel, R., Ohlendorf, R., Beck, J., Schubert, R., & Möglich, A. (2019). Characterization and engineering of photoactivated adenylyl cyclases. *Biological Chemistry*, *400*(3), 429–441.

Suter, B. (2010). Ephus: multipurpose data acquisition software for neuroscience experiments. In *Frontiers in Neural Circuits* (Vol. 4).

Sutherland, E. W., & Rall, T. W. (1958). Fractionation and characterization of a cyclic adenine ribonucleotide formed by tissue particles. *The Journal of Biological Chemistry*, *232*(2), 1077–1091.

Sutherland, E. W., Rall, T. W., & Menon, T. (1962). Adenyl cylase. I. Distribution, preparation, and properties. *The Journal of Biological Chemistry*, *237*, 1220–1227.

Sweatt, J. D. (1999). Toward a molecular explanation for long-term potentiation. *Learning & Memory* , *6*(5), 399–416.

Sweatt, J. D. (2004). Mitogen-activated protein kinases in synaptic plasticity and memory. In *Current Opinion in Neurobiology* (Vol. 14, Issue 3, pp. 311–317).

Takács, V. T., Cserép, C., Schlingloff, D., Pósfai, B., Szőnyi, A., Sos, K. E., Környei, Z., Dénes, Á., Gulyás, A. I., Freund, T. F., & Nyiri, G. (2018). Co-transmission of acetylcholine and GABA regulates hippocampal states. *Nature Communications*, *9*(1), 2848.

Tanwar, M., Sharma, K., Moar, P., & Kateriya, S. (2018). Biochemical Characterization of the Engineered Soluble Photoactivated Guanylate Cyclases from Microbes Expands Optogenetic Tools. *Applied Biochemistry and Biotechnology*, *185*(4), 1014–1028.

Tao, X., Finkbeiner, S., Arnold, D. B., Shaywitz, A. J., & Greenberg, M. E. (1998). Ca2+ influx regulates BDNF transcription by a CREB family transcription factor-dependent mechanism. *Neuron*, *20*(4), 709–726.

Tenorio, G., Connor, S. A., Guevremont, D., Abraham, W. C., Williams, J., O'Dell, T. J., & Nguyen, P. V. (2010). "Silent" priming of translation-dependent LTP by -adrenergic receptors involves phosphorylation and recruitment of AMPA receptors. In *Learning & Memory* (Vol. 17, Issue 12, pp. 627–638).

Thevenaz, P., Ruttimann, U. E., & Unser, M. (1998). A pyramid approach to subpixel registration based on intensity. In *IEEE Transactions on Image Processing* (Vol. 7, Issue 1, pp. 27–41).

Thomas, G. M., & Huganir, R. L. (2004). MAPK cascade signalling and synaptic plasticity. In *Nature Reviews Neuroscience* (Vol. 5, Issue 3, pp. 173–183).

Tian, Y., Yang, S., & Gao, S. (2020). Advances, Perspectives and Potential Engineering Strategies of Light-Gated Phosphodiesterases for Optogenetic Applications. *International Journal of Molecular Sciences*, *21*(20).

Tichy, A.-M., Gerrard, E. J., Sexton, P. M., & Janovjak, H. (2019). Light-activated chimeric GPCRs: limitations and opportunities. *Current Opinion in Structural Biology*, *57*, 196–203.

Tresguerres, M., Levin, L. R., & Buck, J. (2011). Intracellular cAMP signaling by soluble adenylyl cyclase. In *Kidney International* (Vol. 79, Issue 12, pp. 1277–1288).

Trieu, M. M., Devine, E. L., Lamarche, L. B., Ammerman, A. E., Greco, J. A., Birge, R. R., Theobald, D. L., & Oprian, D. D. (2017). Expression, purification, and spectral tuning of RhoGC, a retinylidene/guanylyl cyclase fusion protein and optogenetics tool from the aquatic fungus. *The Journal of Biological Chemistry*, *292*(25), 10379–10389.

Trussell, L. O., Zhang, S., & Raman, I. M. (1993). Desensitization of AMPA receptors upon multiquantal neurotransmitter release. *Neuron*, *10*(6), 1185–1196.

Tsvetanova, N. G., & von Zastrow, M. (2014). Spatial encoding of cyclic AMP signaling specificity by GPCR endocytosis. *Nature Chemical Biology*, *10*(12), 1061–1065.

Twarkowski, H., Hagena, H., & Manahan-Vaughan, D. (2016). The 5-hydroxytryptamine 4 receptor enables differentiation of informational content and encoding in the hippocampus. In *Hippocampus* (Vol. 26, Issue 7, pp. 875–891).

Udwari, D. (2014). *A Photoactivated Adenylyl Cyclase as an Optogenetic Tool to Manipulate Neuronal Signaling and Synaptic Plasticity*.

van Wyk, M., Pielecka-Fortuna, J., Löwel, S., & Kleinlogel, S. (2015). Restoring the ON Switch in Blind Retinas: Opto-mGluR6, a Next-Generation, Cell-Tailored Optogenetic Tool. *PLoS Biology*, *13*(5), e1002143.

Varga, V., Losonczy, A., Zemelman, B. V., Borhegyi, Z., Nyiri, G., Domonkos, A., Hangya, B., Holderith, N., Magee, J. C., & Freund, T. F. (2009). Fast synaptic subcortical control of hippocampal circuits. *Science*, *326*(5951), 449–453.

Villacres, E. C., Wong, S. T., Chavkin, C., & Storm, D. R. (1998). Type I Adenylyl Cyclase Mutant Mice Have Impaired Mossy Fiber Long-Term Potentiation. In *The Journal of Neuroscience* (Vol. 18, Issue 9, pp. 3186–3194).

Villers, A., Godaux, E., & Ris, L. (2012). Long-lasting LTP requires neither repeated trains for its induction nor protein synthesis for its development. *PloS One*, *7*(7), e40823.

Walsh, D. A., Perkins, J. P., & Krebs, E. G. (1968). An adenosine 3',5'-monophosphate-dependant protein kinase from rabbit skeletal muscle. *The Journal of Biological Chemistry*, *243*(13), 3763–3765.

Wang, H., Ferguson, G. D., Pineda, V. V., Cundiff, P. E., & Storm, D. R. (2004). Overexpression of type-1 adenylyl cyclase in mouse forebrain enhances recognition memory and LTP. *Nature Neuroscience*, *7*(6), 635–642.

Wang, H., Pineda, V. V., Chan, G. C. K., Wong, S. T., Muglia, L. J., & Storm, D. R. (2003). Type 8 adenylyl cyclase is targeted to excitatory synapses and required for mossy fiber long-term potentiation. *The Journal of Neuroscience: The Official Journal of the Society for Neuroscience*, *23*(30), 9710–9718.

Wang, L. Y., Salter, M. W., & MacDonald, J. F. (1991). Regulation of kainate receptors by cAMP-dependent protein kinase and phosphatases. *Science*, *253*(5024), 1132–1135.

Wang, Z., Phan, T., & Storm, D. R. (2011). The type 3 adenylyl cyclase is required for novel object learning and extinction of contextual memory: role of cAMP signaling in primary cilia. *The Journal of Neuroscience: The Official Journal of the Society for Neuroscience*, *31*(15), 5557–5561.

Watabe, T., Terai, K., Sumiyama, K., & Matsuda, M. (2020). Booster, a Red-Shifted Genetically Encoded Förster Resonance Energy Transfer (FRET) Biosensor Compatible with Cyan Fluorescent Protein/Yellow Fluorescent Protein-Based FRET Biosensors and Blue Light-Responsive Optogenetic Tools. *ACS Sensors*, *5*(3), 719–730.

Weisskopf, M. G., Castillo, P. E., Zalutsky, R. A., & Nicoll, R. A. (1994). Mediation of hippocampal mossy fiber long-term potentiation by cyclic AMP. *Science*, *265*(5180), 1878–1882.

Wess, J. (2003). Novel insights into muscarinic acetylcholine receptor function using gene targeting technology. In *Trends in Pharmacological Sciences* (Vol. 24, Issue 8, pp. 414–420).

Westphal, M. V., Schafroth, M. A., Sarott, R. C., Imhof, M. A., Bold, C. P., Leippe, P., Dhopeshwarkar, A., Grandner, J. M., Katritch, V., Mackie, K., Trauner, D., Carreira, E. M., & Frank, J. A. (2017). Synthesis of Photoswitchable Δ-Tetrahydrocannabinol Derivatives Enables Optical Control of Cannabinoid Receptor 1 Signaling. *Journal of the American Chemical Society*, *139*(50), 18206–18212.

West, P. J., Marcy, V. R., Marino, M. J., & Schaffhauser, H. (2009). Activation of the 5-HT6 receptor attenuates long-term potentiation and facilitates GABAergic neurotransmission in rat hippocampus. In *Neuroscience* (Vol. 164, Issue 2, pp. 692–701).

White, M. M. (1988). Forskolin alters acetylcholine receptor gating by a mechanism independent of adenylate cyclase activation. *Molecular Pharmacology*, *34*(4), 427–430.

Wieczorek, L., Majumdar, D., Wills, T. A., Hu, L., Winder, D. G., Webb, D. J., & Muglia, L. J. (2012). Absence of Ca2 -stimulated adenylyl cyclases leads to reduced synaptic plasticity and impaired experience-dependent fear memory. In *Translational Psychiatry* (Vol. 2, Issue 5, pp. e126–e126).

Wiegert, J. S., Simon Wiegert, J., Gee, C. E., & Oertner, T. G. (2017a). Single-Cell Electroporation of Neurons. In *Cold Spring Harbor Protocols* (Vol. 2017, Issue 2, p. db.prot094904).

Wiegert, J. S., Simon Wiegert, J., Gee, C. E., & Oertner, T. G. (2017b). Viral Vector-Based Transduction of Slice Cultures. In *Cold Spring Harbor Protocols* (Vol. 2017, Issue 2, p. db.prot094896).

Wiegert, J. S., Simon Wiegert, J., Mahn, M., Prigge, M., Printz, Y., & Yizhar, O. (2017). Silencing Neurons: Tools, Applications, and Experimental Constraints. In *Neuron* (Vol. 95, Issue 3, pp. 504–529).

Wiegert, J. S., Simon Wiegert, J., & Oertner, T. G. (2016). How (not) to silence long-range projections with light. In *Nature Neuroscience* (Vol. 19, Issue 4, pp. 527–528).

Wietek, J., Beltramo, R., Scanziani, M., Hegemann, P., Oertner, T. G., & Wiegert, J. S. (2015). An improved chloride-conducting channelrhodopsin for light-induced inhibition of neuronal activity in vivo. *Scientific Reports*, *5*, 14807.

Willoughby, D., & Cooper, D. M. F. (2007). Organization and Ca2+ regulation of adenylyl cyclases in cAMP microdomains. *Physiological Reviews*, *87*(3), 965–1010.

Wolfgang, W. J., Roberts, I. J., Quan, F., O'Kane, C., & Forte, M. (1996). Activation of protein kinase A-independent pathways by Gs alpha in Drosophila. *Proceedings of the National Academy of Sciences of the United States of America*, *93*(25), 14542–14547.

Wong, S. T., Athos, J., Figueroa, X. A., Pineda, V. V., Schaefer, M. L., Chavkin, C. C., Muglia, L. J., & Storm, D. R. (1999). Calcium-stimulated adenylyl cyclase activity is critical for hippocampus-dependent long-term memory and late phase LTP. *Neuron*, *23*(4), 787–798.

Wong, W., & Scott, J. D. (2004). AKAP signalling complexes: focal points in space and time. *Nature Reviews. Molecular Cell Biology*, *5*(12), 959–970.

Woolfrey, K. M., & Dell'Acqua, M. L. (2015). Coordination of Protein Phosphorylation and Dephosphorylation in Synaptic Plasticity. *The Journal of Biological Chemistry*, *290*(48), 28604–28612.

Wu, Z. L., Thomas, S. A., Villacres, E. C., Xia, Z., Simmons, M. L., Chavkin, C., Palmiter, R. D., & Storm, D. R. (1995).

Altered behavior and long-term potentiation in type I adenylyl cyclase mutant mice. In *Proceedings of the National Academy of Sciences* (Vol. 92, Issue 1, pp. 220–224).

Xu, Y., Zhang, H.-T., & O'Donnell, J. M. (2011). Phosphodiesterases in the Central Nervous System: Implications in Mood and Cognitive Disorders. In *Phosphodiesterases as Drug Targets* (pp. 447–485).

Yang, S., Constantin, O. M., Sachidanandan, D., Hofmann, H., Kunz, T. C., Kozjak-Pavlovic, V., Oertner, T. G., Nagel, G., Kittel, R. J., Gee, C. E., & Gao, S. (2021). PACmn for improved optogenetic control of intracellular cAMP. *BMC Biology*, *19*(1), 227.

Yang, Y., & Calakos, N. (2013). Presynaptic long-term plasticity. *Frontiers in Synaptic Neuroscience*, *5*, 8.

Yan, K., Gao, L.-N., Cui, Y.-L., Zhang, Y., & Zhou, X. (2016). The cyclic AMP signaling pathway: Exploring targets for successful drug discovery (Review). *Molecular Medicine Reports*, *13*(5), 3715–3723.

Yasuda, H., Barth, A. L., Stellwagen, D., & Malenka, R. C. (2003). A developmental switch in the signaling cascades for LTP induction. *Nature Neuroscience*, *6*(1), 15–16.

Yasukawa, H., Sato, A., Kita, A., Kodaira, K.-I., Iseki, M., Takahashi, T., Shibusawa, M., Watanabe, M., & Yagita, K. (2013). Identification of photoactivated adenylyl cyclases in Naegleria australiensis and BLUF-containing protein in Naegleria fowleri. *The Journal of General and Applied Microbiology*, *59*(5), 361–369.

Yuste, R., & Bonhoeffer, T. (2001). Morphological Changes in Dendritic Spines Associated with Long-Term Synaptic Plasticity. In *Annual Review of Neuroscience* (Vol. 24, Issue 1, pp. 1071–1089).

Yu, X., Chen, X.-W., Zhou, P., Yao, L., Liu, T., Zhang, B., Li, Y., Zheng, H., Zheng, L.-H., Zhang, C. X., Bruce, I., Ge, J.-B., Wang, S.-Q., Hu, Z.-A., Yu, H.-G., & Zhou, Z. (2007). Calcium influx through If channels in rat ventricular myocytes. In *American Journal of Physiology-Cell Physiology* (Vol. 292, Issue 3, pp. C1147–C1155).

Zakharenko, S. S., Patterson, S. L., Dragatsis, I., Zeitlin, S. O., Siegelbaum, S. A., Kandel, E. R., & Morozov, A. (2003). Presynaptic BDNF Required for a Presynaptic but Not Postsynaptic Component of LTP at Hippocampal CA1-CA3 Synapses. In *Neuron* (Vol. 39, Issue 6, pp. 975–990).

Zhang, M., & Wang, H. (2013). Mice overexpressing type 1 adenylyl cyclase show enhanced spatial memory flexibility in the absence of intact synaptic long-term depression. *Learning & Memory* , *20*(7), 352–357.

Zhou, Z., Okamoto, K., Onodera, J., Hiragi, T., Andoh, M., Ikawa, M., Tanaka, K. F., Ikegaya, Y., & Koyama, R. (2021). Astrocytic cAMP modulates memory via synaptic plasticity. *Proceedings of the National Academy of Sciences of the United States of America*, *118*(3).

Zhou, Z., Tanaka, K. F., Matsunaga, S., Iseki, M., Watanabe, M., Matsuki, N., Ikegaya, Y., & Koyama, R. (2016). Photoactivated adenylyl cyclase (PAC) reveals novel mechanisms underlying cAMP-dependent axonal morphogenesis. *Scientific Reports*, *5*, 19679.

8. Appendix

8.1 List of figures

8.2 List of tables

8.3 List of abbreviations

5' AMP	adenosine 5'-monophosphate
5-HT	serotonin
AAV	adeno-associated virus
AC	adenylyl cyclase
ACh	acetylcholine
AKAP	A-kinase anchoring proteins
AMPA(R)	α-amino-3-hydroxy-5-methyl-4-isoxazolepropionic acid (receptor)
AP	action potential
AR	adrenergic receptor
ATP	adenosine-5'-triphosphate
BDNF	brain-derived neurotrophic factor
BLUF	Blue Light sensor Using FAD
bPAC	photoactivated cyclase from Beggiatoa sp.
CA(1-4)	*cornu ammonis*(1-4)
CaMKII	Ca^{2+}/calmodulin-dependent protein kinase II
cAMP	cyclic AMP; 3',5'-cyclic adenosine monophosphate
cGMP	cyclic GMP; 3',5'-cyclic guanosine monophosphate

CNBD	cyclic nucleotide-binding domain
CNG	cyclic nucleotide-gated channel
CRE	cAMP-responsive element
CREB	cAMP response element-binding protein
DG	dentate gyrus
EC	entorhinal cortex
EPAC	exchange protein directly activated by cAMP
EPSC	excitatory postsynaptic current
EPSP	excitatory postsynaptic potential
ERK	extracellular signal-regulated kinases; also MAPK
fEPSP	field excitatory postsynaptic potentials
FRET	Förster resonance energy transfer
FSK	forskolin
GC	guanylyl cyclase
GDP	guanosine 5′-diphosphate
GEF	guanine nucleotide exchange factor
GPCR	G protein-coupled receptor
GTP	guanosine-5'-triphosphate
HCN	hyperpolarization-activated, cyclic nucleotide-gated channel
Ihold	holding current
LTD	long-term depression
LTP	long-term potentiation
MAPK	mitogen-activated protein kinase; also ERK
mEPSC	miniature excitatory postsynaptic current
NE	norepinephrine
NMDA(R)	N-Methyl-D-aspartate (receptor)
NO	nitric oxide
optoXR	chimeric GPCR
PAC	photo-activated cyclase
PDE	phosphodiesterase
PKA	protein kinase A
PKC	protein kinase C
PKG	protein kinase G
PKI	protein kinase inhibitor
PLC	phospholipase C

PP	protein phosphatase
RM	membrane resistance
RMP	resting membrane potential
Rs	series resistance
sAC	soluble adenylyl cyclase
tmAC	transmembrane adenylyl cyclase

8.4 Acknowledgements

First and foremost, I want to thank my research supervisors Prof. Dr. Thomas Oertner and Dr. Christine Gee for their guidance and support. I am infinitely grateful for your supervision and for giving me the opportunity to grow as a scientist through your advice and support. Thank you for being very cool bosses that have set a high standard for my future employers. Thomas, you are an immense source of knowledge and your never-ending curiosity and fascination with nature was a continuous source of inspiration. Chris, you have been the best teacher and mentor I could have hoped for. Your continuous curiosity, your amazing knowledge and general cool attitude pushed me to be a better scientist.

Immense gratitude for the people who, through their dedication and hard work, keep the lab going and without whom we would all be lost: Heike Pehlke, Iris Ohmert, Jan Schröder and Sabine Graff. Particular thank yous go out to Iris, Jan and Sabine for excellent technical support and for providing us with reliable slice cultures week after week. Likewise, I deeply thank all the actual and former members of the ISP for their continuous support, good spirits and easy-goingness. You are all brilliant people and scientists and I am thankful to have learned from and alongside you. I would like to express my gratitude to my thesis committee members, Prof. Dr. Viacheslav Nikolaev and Prof. Dr. Christian Lohr and to the Promotionsbüro at the UKE, particularly to Dr. Kathrin Lempahn and Ruth Bahlman for their guidance and support. I would like to thank the group of Prof. Dr. Georg Nagel, particularly to Shiqiang and Shang, for our fruitful collaboration over the years. I would also like to thank the SfB1328 for the financial support and incredible development offer, as well as the DAAD for offering me the opportunity to come to Germany and start this academic adventure.

Lastly, I would like to thank my friends and my family for their continuous support and for always being there to take me on a new adventure and to show me that there is a rich and meaningful life to be lived outside the lab. Mama, îți mulțumesc că mi-ai oferit dintotdeauna tot ce ai avut și că te-ai oferit pe tine ca exemplu de femeie inteligentă, puternică și curajoasă. Datorită ție și a încurajărilor tale am reușit să îmi îndeplinesc visele. Paul, e greu sa exprim cât de mult te prețuiesc și cât de mult înseamnă pentru mine prezența ta în viața mea. Îți mulțumesc că ai decis sa devii un refugiat academic alături de mine și că am reușit să ne construim împreună un univers așa de frumos, încât oricât de fascinante sunt zilele în laborator alături de misterele naturii, tu reușești cumva să le faci și mai interesante. Mulțumesc că mă faci un om mai bun.

8.5 *Curriculum Vitae*

Lebenslauf wurde aus datenschutzrechtlichen Gründen entfernt.

9. Eidesstattliche Erklärung

Ich versichere ausdrücklich, dass ich die Arbeit selbständig und ohne fremde Hilfe verfasst, andere als die von mir angegebenen Quellen und Hilfsmittel nicht benutzt und die aus den benutzten Werken wörtlich oder inhaltlich entnommenen Stellen einzeln nach Ausgabe (Auflage und Jahr des Erscheinens), Band und Seite des benutzten Werkes kenntlich gemacht habe.

Ferner versichere ich, dass ich die Dissertation bisher nicht einem Fachvertreter an einer anderen Hochschule zur Überprüfung vorgelegt oder mich anderweitig um Zulassung zur Promotion beworben habe.

Ich erkläre mich einverstanden, dass meine Dissertation vom Dekanat der Medizinischen Fakultät mit einer gängigen Software zur Erkennung von Plagiaten überprüft werden kann.

Unterschrift: